Hacettepe Journal of Mathematics and Statistics
Volume 33 (2004), 1 – 10

BASIC COMPRESSIBLE FLOW OVER A ROTATING DISK

M. Türkyılmazoğlu* and N. Uygun*

Received 02 : 01 : 2003 : Accepted 09 : 08 : 2004

Abstract

In this work the basic flow field is investigated for the compressible boundary layer flow over a rotating disk. Making use of self-consistent assumptions within boundary layer theory, the governing basic equations of motion are derived leading to a generalized steady compressible Von Karman flow. A Runge-Kutta integration method accurate to the fourth order is then employed for the solution of the resulting equations. Finally the velocity and temperature distributions corresponding to the various parameters are calculated numerically and presented.

Keywords: Compressible flow, Rotating-disk boundary layer, Runge-Kutta integrator.
2000 AMS Classification: 46 F 10

1. Introduction

The boundary layer flow due to a rotating disk has received substantial interest, in particular during the last two decades, since it constitutes a prototype for the flow over modern aircraft wings. Its significance lies in the fact that owing to the resemblance of the mean velocity profiles in cross flow directions, most of the fluid dynamical properties of the flow over a rotating disk and a swept-back wing almost coincide as far as the nature of instabilities is concerned. To be more precise, both flows are subject to cross flow vortices leading to convective or absolute instabilities.

A series of studies have been conducted to understand the reasons behind the instability mechanisms in three-dimensional boundary layer flows. Among these, the theoretical works of Gregory, Stuart and Walker [7], Malik [15], Malik, Wilkinson and Orszag [17], Mack [14], Hall [8], Bassom and Gajjar [3], Balakumar and Malik [2], Lingwood [11] and Turkyilmazoglu [21] have highlighted the inevitable instabilities caused by the stationary or, in some circumstances, travelling disturbances. In particular, the latest two works have demonstrated that unlike the convective instability mechanism which arises in most three-dimensional boundary layer flows, the rotating disk boundary layer flow is subjected to absolute instability. Although the earlier experiments by Gregory, Stuart

*Mathematics Department, University of Hacettepe, 06532-Beytepe, Ankara, Turkey.
E-mail : turkyilm@hotmail.com

and Walker [7], Wilkinson and Malik [23], and Kohama [10] were only able to detect convective type instability, the more recent experiment carried out by Lingwood [12] has given an apparent support for the existence of absolute instability over a rotating disk.

The aforementioned stability studies require genuine basic velocity profiles, which, for the incompressible flow case, is the well known Von Karman's basic steady flow. On the other hand, the compressible basic flow is much more complicated to evaluate. This is because, as pointed out by Stewartson [20] and others, there are several parameters involved in the compressible flow case, such as the Prandtl number and the second coefficient of viscosity which are not even constants as they are in the incompressible case. Our motivation here is, therefore, to devise an approach which will involve a series of approximation to obtain the basic compressible equations for the three dimensional rotating disk boundary layer flow that we will call the generalized Von Karman's flow. The ultimate goal of the research is to investigate the character of the instabilities existing in this generalized Von Karman's flow, which is currently under investigation and will be reported elsewhere.

The present study is organized in the following manner. The governing equations of motion and the derivation of the mean flow equations are presented in section 2. Next, the numerical scheme and the results corresponding to several parameters are given in section 3. Conclusions are finally drawn in section 4.

2. Derivation of the Mean Flow Equations

Here, we deal with the compressible three-dimensional boundary layer flow over a rigid disk rotating about its axis with a constant angular velocity Ω in the cylindrical coordinates (r, θ, z), having been made dimensionless with respect to a reference length scale l which can be taken to be the local radius of the disk. Velocities are non-dimensionalized by $l\Omega$, while the pressure is by $l^2\Omega^2$. Moreover, the density and the temperature of the fluid are non-dimensionalized with respect to their free-stream values. As a consequence, the corresponding unsteady Navier-Stokes equations governing the motion can be expressed in the form

$$\frac{\partial \rho}{\partial t} + \nabla \cdot (\rho \mathbf{u}) = 0, \tag{2.1}$$

$$\rho\big[\frac{\partial \mathbf{u}}{\partial t} + (\mathbf{u}\cdot\nabla)\mathrm{u} + 2(\hat{k}\times\mathbf{u}) - \mathrm{r}\hat{r}\big] = -\nabla p + \frac{1}{Re}\big[\nabla(\lambda\nabla\cdot\mathbf{u}) + \nabla(\mu e_{ij})\big], \tag{2.2}$$

$$\gamma M_\infty^2 p = \rho T, \tag{2.3}$$

$$\begin{aligned}\rho\big[\tfrac{\partial T}{\partial t} \quad &+(\mathbf{u}\cdot\nabla)T\big] = M_\infty^2(\gamma-1)\big[\tfrac{\partial p}{\partial t} + (\mathbf{u}\cdot\nabla)p\big] + \tfrac{1}{Re}\big[\nabla\cdot(k\nabla T)\\ &+\tfrac{\gamma-1}{Re}M_\infty^2\big[\tfrac{1}{2}\mu(e_{11}^2+e_{22}^2+e_{33}^2+2e_{12}^2+2e_{13}^2+2e_{23}^2)+\lambda(\nabla\cdot\mathbf{u})^2\big].\end{aligned} \tag{2.4}$$

It should be remarked that the viscous, Coriolis and streamline curvature effects are all included in equations (2.1-2.4). Equation (2.1) is the continuity equation, equation (2.2) is the momentum equation in vector form, Equation (2.3) is the equation of state and Equation (2.4) the energy equation, respectively. Together with these equations, the appropriate boundary conditions are the usual no-slip condition on the wall except the azimuthal velocity in the θ direction (though, the extra r term appearing in equation (2.2) allows the azimuthal velocity to disappear on the wall as well), and the vanishing quantities at the far-field apart from the uniform temperature. The several parameters appearing in equations (2.1-2.4) are defined as follows; ρ the density, $\mathbf{u}$ the velocity

vector, ∇ the usual gradient operator in cylindrical coordinates, p the pressure, T the temperature. Moreover, the strain tensors are defined by

$$e_{11} = 2\frac{\partial u}{\partial r}, \qquad e_{12} = e_{21} = r\frac{\partial}{\partial r}(\frac{v}{r}) + \frac{1}{r}\frac{\partial u}{\partial \theta}, \qquad e_{13} = e_{31} = \frac{\partial u}{\partial z} + \frac{\partial w}{\partial r},$$
$$e_{22} = 2(\frac{1}{r}\frac{\partial v}{\partial \theta} + \frac{u}{r}), \qquad e_{23} = e_{32} = \frac{1}{r}\frac{\partial w}{\partial \theta} + \frac{\partial v}{\partial z}, \qquad e_{33} = 2\frac{\partial w}{\partial z}.$$

Furthermore, μ is the dynamical viscosity, λ the second coefficient of viscosity related to the bulk viscosity, γ the ratio of the specific heats, M_∞ the free stream Mach number, Re the Reynolds number characterizing the flow defined by $Re = \frac{\Omega l^2}{\nu}$, and finally k is the parameter associated with the Prandtl number σ. The Reynolds number is taken to be large in the following analysis.

The basic flow of the incompressible case, also called the Von Karman's steady state flow, is well known since the work of Kármán [9]. The steady compressible flow, hereafter to be termed the generalized Von Karman's flow, will be considered here using a series of approximations in line with the boundary layer flow assumption. First of all, the basic flow is assumed to evolve alongside the boundary layer coordinate $\xi = Re^{1/2}z$, which is of order unity. The flow being axisymmetric about the axis of rotation entails all derivatives with respect to θ to vanish. Taking these into account, if we substitute the basic flow velocities $(u_B, v_B, Re^{-1/2}w_B)$ and the other quantities into the governing equations (2.1-2.4), and also neglect terms of $O(Re^{-1})$, the mean flow quantities are determined from the subsequent equations and boundary conditions:

$$\rho_B(\frac{\partial u_B}{\partial r} + \frac{\partial w_B}{\partial \xi}) + u_B\frac{\partial \rho_B}{\partial r} + w_B\frac{\partial \rho_B}{\partial \xi} + \frac{\rho_B u_B}{r} = 0, \tag{2.5}$$

$$\rho_B(u_B\frac{\partial u_B}{\partial r} + w_B\frac{\partial u_B}{\partial \xi} - \frac{v_B^2}{r} - 2v_B - r) = -\frac{\partial p_B}{\partial r} + \frac{\partial}{\partial \xi}(\mu_B\frac{\partial u_B}{\partial \xi}), \tag{2.6}$$

$$\rho_B(u_B\frac{\partial v_B}{\partial r} + w_B\frac{\partial v_B}{\partial \xi} + \frac{u_B v_B}{r} + 2u_B) = \frac{\partial}{\partial \xi}(\mu_B\frac{\partial v_B}{\partial \xi}), \tag{2.7}$$

$$\frac{\partial p_B}{\partial \xi} = 0, \tag{2.8}$$

$$\gamma M_\infty^2 p_B = \rho_B T_B, \tag{2.9}$$

$$\rho_B(u_B\frac{\partial T_B}{\partial r} + w_B\frac{\partial T_B}{\partial \xi}) = M_\infty^2(\gamma - 1)\{u_B\frac{\partial p_B}{\partial r} + w_B\frac{\partial p_B}{\partial \xi} + \mu_B[(\frac{\partial u_B}{\partial \xi})^2 + (\frac{\partial v_B}{\partial \xi})^2]\} + \frac{\partial}{\partial \xi}(k_B\frac{\partial T_B}{\partial \xi}), \tag{2.10}$$

$$u_B = v_B = w_B = 0 \text{ at } \xi = 0,$$
$$u_B \to 0,\ v_B \to -r \text{ as } \xi \to \infty, \tag{2.11}$$
$$\rho_B,\ T_B,\ \mu_B \to 1,\ p_B \to \frac{1}{\gamma M_\infty^2} \text{ as } \xi \to \infty.$$

In contrast to the case of incompressible flow, it should be noticed that since we consider the fluid to be a perfect gas in the state equation (2.9), and further, since the fluid is stationary everywhere outside the boundary layer, it is straightforward to deduce from equations (2.8-2.9) and (2.11) that p_B is constant and equal to $(\gamma M_\infty^2)^{-1}$. Secondly, we will assume the Chapman's viscosity law, that is, $\mu = CT$ for some constant C. Such an approximation is particularly shown to be useful for low Mach numbers, see for instance Stewartson [20] and Papageourgiou [18]. Furthermore, despite the fact that the bulk viscosity does not enter into the following analysis, having been cancelled out by the large Reynolds number limit, experimental researches prove that viscosity coefficients can be taken as a function of temperature only, and for a monatomic gas $\lambda = -\frac{2}{3}\mu$ is

generally a good choice, see for instance Rosenhead [19]. Thirdly, to remove the density terms from the mean flow equations (2.5-2.11), we make use of the Dorotonitsyn-Howarth transformation, that is, $y = C^{-1/2}\int_0^\xi \rho_B d\xi$ as given in Stewartson [20]. In the light of the previous assumptions and taking into consideration the strategies of the incompressible Von Karman's flow, the form of the generalized Von Karman's flow may be written as

$$u_B = (u_B, v_B, w_B, p_B) = (r\bar{u}(y), r\bar{v}(y), \bar{w}(y), \frac{1}{\gamma M_\infty^2}).$$

Eventually, making use of the stream function formulae automatically satisfying Equation (2.5), that is,

$$\bar{u} = \frac{d\psi}{dy} = \psi'(y), \quad \bar{w} = -C^{1/2}T_B(2\psi + r\psi'\frac{\partial y}{\partial r}),$$

will greatly simplify the form of Equations (2.5-2.11).

Keeping in mind all the above assumptions and doing the necessary substitutions into equations (2.5-2.11), the subsequent equations and boundary conditions will result in respectively

$$\psi''' = \psi'^2 - 2\psi\psi'' - (\bar{v}+1)^2, \tag{2.12}$$

$$\bar{v}'' = 2(\bar{v}+1)\psi' - 2\psi\bar{v}', \tag{2.13}$$

$$\frac{\partial^2 T_B}{\partial y^2} + 2\sigma\psi\frac{\partial T_B}{\partial y} - r\sigma\psi'\frac{\partial T_B}{\partial r} + (\gamma-1)\sigma r^2 M_\infty^2(\psi''^2 + \bar{v}'^2) = 0, \tag{2.14}$$

$$\psi(0) = \psi'(0) = \psi(\infty) = \bar{v}(0) = \bar{v}(\infty) + 1 = T_B(\infty) - 1 = 0. \tag{2.15}$$

The system (2.12-2.15) is called the generalized Von Karman's equations for the compressible flow for short. Although the Karman equations (2.12-2.13) are well known to exhibit infinite degrees of non-uniqueness, the solution that we have obtained in the coming section under the constraints (2.15) are physically expected ones because they absolutely match with the experimentally determined profiles, see for instance Lingwood [13], which have been used for several instability investigations, amongst these being Malik [15], Hall [8] and Balakumar and Malik [2]. In addition to this, it can be easily seen that the influence of the compressibility comes into effect owing to the temperature field given in (2.14), which significantly alters the flow field from the incompressible case. Now supposing that the temperature field in (2.14) can be written in terms of a viscous dissipation term f and a heat conducting term q, it is possible to express it in the form

$$T_B = \frac{1}{\rho_B} = 1 - \frac{\gamma-1}{2}M_r^2 f(y) + (T_w - 1)q(y), \tag{2.16}$$

which allows the splitting of the energy equation into two ordinary differential equations

$$\begin{aligned} &f'' + 2\sigma\psi f' - 2\sigma\psi' f = 2\sigma(\psi''^2 + \bar{v}'^2), \\ &q'' + 2\sigma\psi q' = 0. \end{aligned} \tag{2.17}$$

The parameter M_r appearing in equation (2.16) is the local Mach number defined by $M_r = rM_\infty$. Moreover, taking into account the far-field uniform temperature in (2.11), $f = q = 0$ as $y \to \infty$. However, for an insulated disk, $\frac{\partial T}{\partial y}(0) = 0$ requiring $f'(0) = q'(0) = 0$, leading to $q \equiv 0$. Taking into consideration the heat transfer on the wall, that is $T(0) = T_w$, we have $f(0) = q(0) - 1 = 0$. Additionally, the heat conducting term q in (2.17) can be solved analytically as $q = \int_y^\infty e^{-2\sigma\int_0^y \psi dy} dy / \int_0^\infty e^{-2\sigma\int_0^y \psi dy} dy$ for any prescribed σ, whereas the function f cannot be solved analytically from equation (2.17), therefore, it needs to be treated numerically apart from the perfect fluid case $\sigma = 1$, for which the insulated disk results in $f = \psi'^2 + \bar{v}^2 - 1$ and heat transfer gives rise to $f = \psi'^2 + \bar{v} + \bar{v}^2$.

A further thing worthy of mentioning is the boundary layer thickness. Having obtained the temperature distributions from (2.16), the physically dimensionless quantity z can be recovered as

$$(2.18)\quad z = C^{1/2}Re^{-1/2}\int_0^y T_B dy = C^{1/2}Re^{-1/2}\{y - \frac{\gamma-1}{2}M_r^2\int_0^y f dy + (T_w - 1)\int_0^y q dy\}.$$

Equation (2.18) clearly indicates the stretching effect of the compressibility. It can also be deduced from (2.18) that the distance from the disk surface at which the same value of the azimuthal velocity is attained differ for compressible and incompressible fluids not only by a term proportional to M_r^2, which in turn depends on the radial distance, but also by the wall temperature values.

3. Numerical Scheme, Results and Discussions

In this section, the numerical procedure used to solve equations (2.12-2.17) will be briefly presented first, followed by the numerical results. A fourth-order accurate Runge-Kutta scheme is employed in conjunction with a shooting technique to match the variables at infinity. Such a technique has been successfully applied to many boundary layer flow problems, for example see Cebeci [6] and Canuto, Hussaini, Quarteroni and Zang [5]; and to hydrodynamic stability calculations, see for example Arnal [1] and Turkyilmazoglu, Gajjar and Ruban [22]. The incompressible steady boundary layer flow over a rotating disk was obtained in Lingwood [12, 13] by means of this method and in Turkyilmazoglu [21] using a Spectral Chebyshev collocation scheme. Based on our experience, the Runge-Kutta method is more straightforward to implement than other methods. To check out the accuracy of the numerical scheme, as well as to validate the code, we first solved as a test case the well known Blasius boundary layer flow over a flat plate, which is governed by the differential equation

$$f''' + \frac{1}{2}ff'' = 0, \quad f(0) = f'(0) = f'(\infty) - 1 = 0.$$

A comparison with the result of Brown [4] is demonstrated in figure 1, which is clear evidence of the accuracy of the numerical method.

Next, with the algorithm at hand, several test cases are considered so that the unknown initial conditions and the far field would not influence the outcomes within the accuracy of the method and machine precision. To be more specific, the domain of integration was fixed to 20 and divided into a 10000 uniform grid, and the integration was performed to give the initial values of $\psi''(0) = 0.51023$, $\bar{v}'(0) = -0.61592$, which are in excellent agreement with the values given in Malik [15].

Further properties of the basic velocity field can be captured from the graph shown in Figure 2(a). These profiles are in fact the same profiles as the Von-Karman's basic incompressible flow over a rotating disk and have been verified to be true in several studies, such as Lingwood [12, 13] and Malik [15], amongst others (see Figure 1 of Lingwood [11], Figure 4 of Lingwood [12] and Figure 2 of Balakumar and Malik [2]). In spite of the fact that these profiles are not the exact compressible flow profiles since they were obtained as a result of a series of self-consistent approximations, nevertheless we will use then for stability investigations of the generalized compressible Von-Karman's boundary layer flow.

Figure 1.

The Blasius profile $U = f'$ is shown against the normal coordinate y. A comparison of the solution obtained from the fourth order Runge-Kutta scheme employed for the present research is displayed with the solution of Brown [4] shown by the crosses.

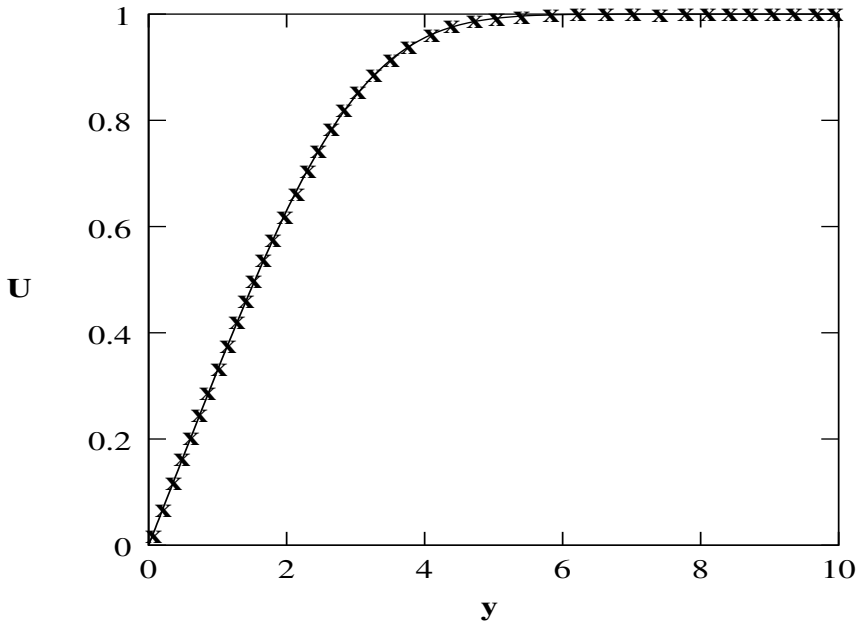

Equations (2.16–2.17) were then solved to compute the various temperature profiles corresponding to the several Mach numbers, Prandtl numbers and the wall temperatures as depicted in Figures (2–4). The insulated wall case is demonstrated first in Figures 2(b–d) for three different Prandtl numbers and with varying Mach numbers. The overall shapes of the profiles are seen to be similar and the influence of the Prandtl number is to change slightly the wall temperature.

The effect of the heat transfer and Prandtl number can be visualized next in Figures (3–4). It can be inferred from these pictures that the wall heating/cooling has a big impact on the formation of the temperature profiles. Although the far-field behavior of the profiles may be pursued using asymptotic means, it has not been implemented here. It is these graphs in Figures (2–3) that will determine the nature of the instabilities existing in the compressible generalized Von-Karman's flow. As mentioned above, this issue is currently under investigation.

4. Conclusions

The basic velocity field governing the compressible boundary layer flow over a rotating disk has been obtained using self-consistent assumptions. The resulting equations have then been solved numerically by a Runge-Kutta integrator accurate to the fourth order, and the behavior of the basic velocity and temperature field displayed graphically. The profiles determined will ultimately serve to explore the character of the compressible flow and this will constitute the basis of the oncoming research.

Figure 2.

(a) Basic velocity profiles of the generalized Von Karman's flow are shown for the boundary layer over the rotating disk. Temperature profiles for an insulated disk are shown in (b) for $\sigma = 0.5$, in (c) for $\sigma = 1$ and in (d) for $\sigma = 1.5$.

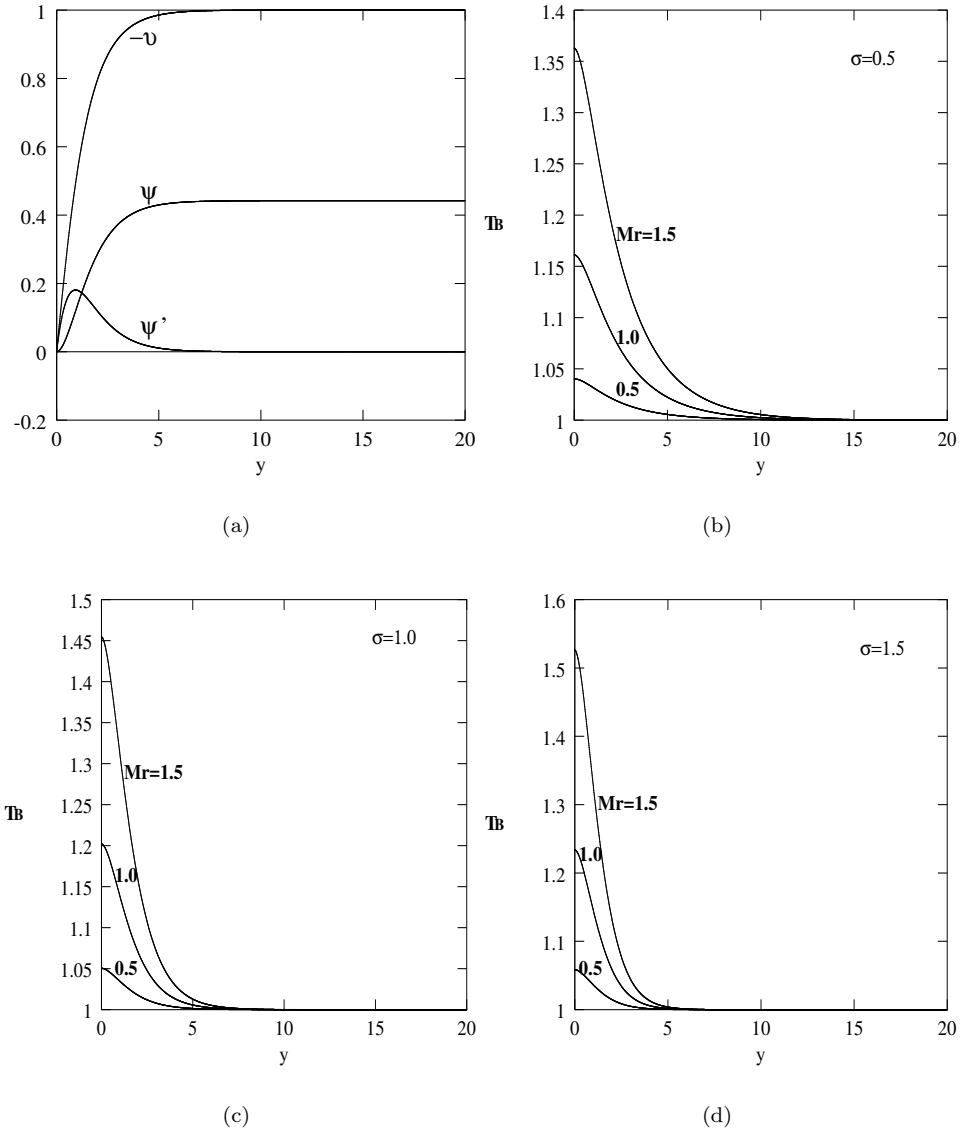

Figure 3.

Temperature profiles corresponding to the heat transfer case are shown at three different local Mach numbers, respectively in (a) for $\sigma = 0.5$, $T_w = 0.5$, in (b) for $\sigma = 0.5$, $T_w = 1.5$, in (c) for $\sigma = 1.0$, $T_w = 0.5$ and in (d) for $\sigma = 1.0$, $T_w = 1.5$. Dotted curves denote $M_r = 0.0$, straight curves $M_r = 0.5$ and broken curves $M_r = 1.5$.

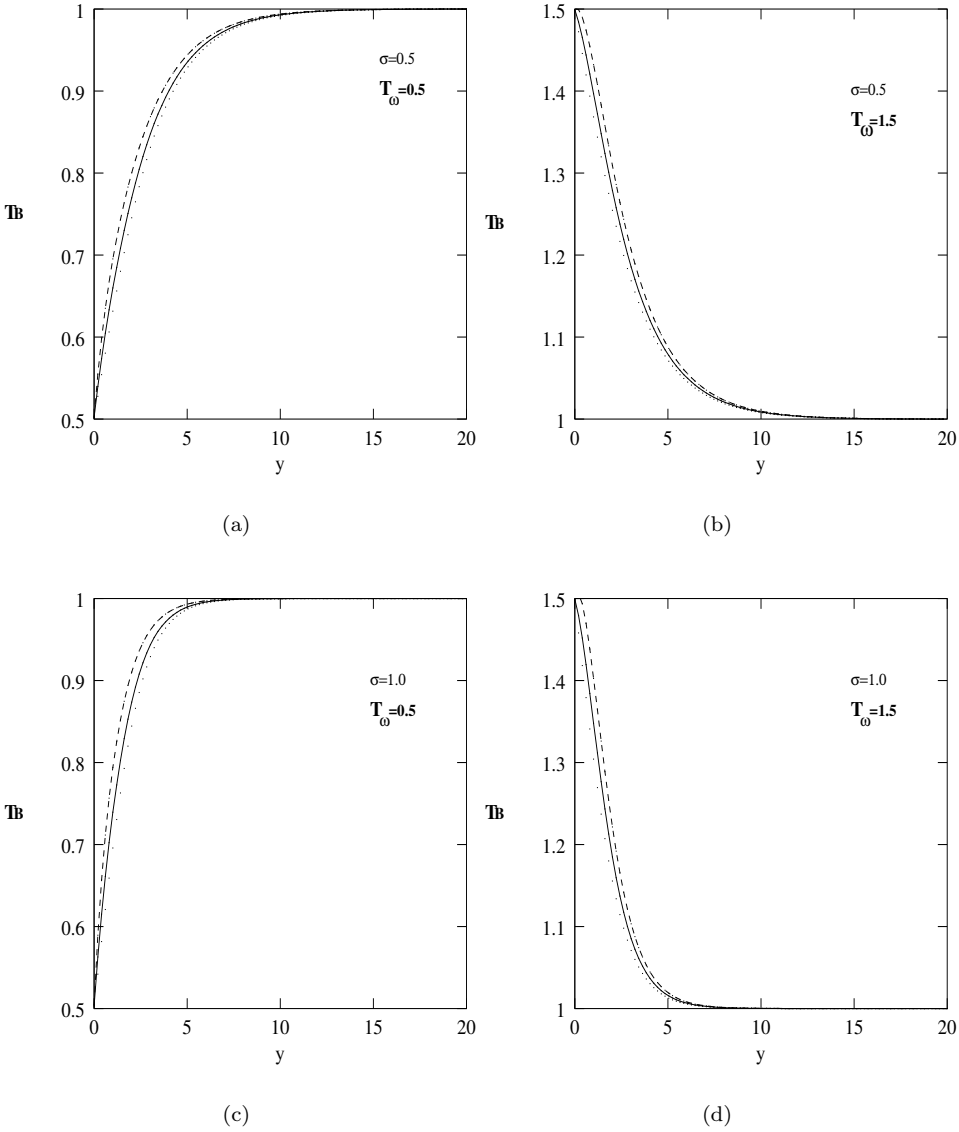

Figure 4

Temperature profiles corresponding to the heat transfer case are shown at three different local Mach numbers respectively, in (a) for $\sigma = 1.5$, $T_w = 0.5$ and in (b) for $\sigma = 1.5$, $T_w = 1.5$. Figures 3(c–d)) are redisplayed in combined form in (c). The effect of wall cooling is demonstrated in (d) for $\sigma = 1.0$, $M_r = 1.0$.

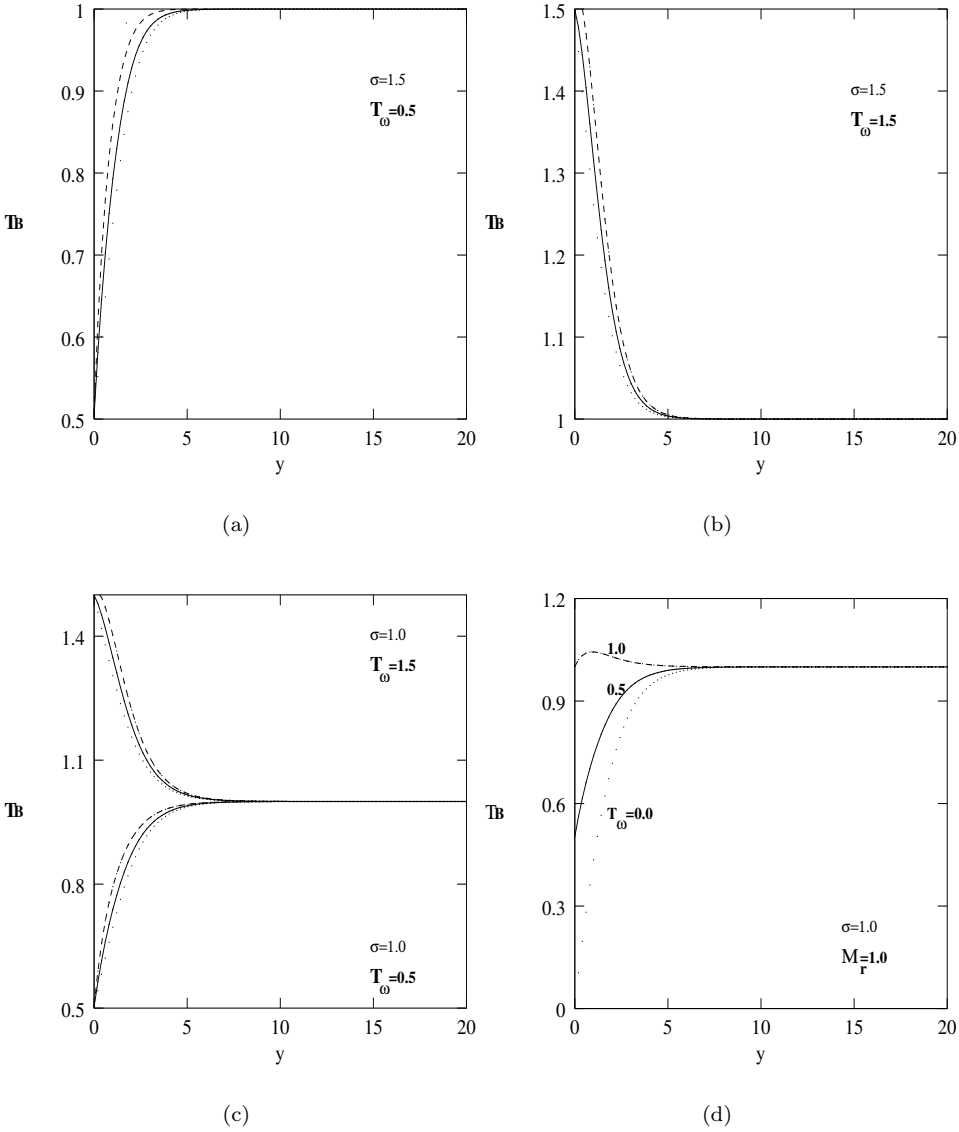

References

[1] Arnal, D. *Boundary layer transition: predictions based on linear theory*, (AGARD-VKI Special Cource on Progress in Transition Modelling, 1993).

[2] Balakumar, P. and Malik, M. R. *Travelling disturbances in rotating-disk flow*. Theoret. Comput. Fluid Dyn. **2**, 125–137, 1990.

[3] Bassom, A. P.and Gajjar J. S. B. *Non-Stationary cross-flow vortices in a three-dimensional boundary-layer*. Proc. Roy. Soc. London Ser. A **417**, 179–212, 1988.

[4] Brown, W. B. *Numerical calculation of the stability of cross flow profiles in laminar boundary layers on a rotating-disk and on a swept-wing and an exact calculation of the Blasius velocity profile*. (Northrop Aircraft Inc. Hawthorne, L. A. 59. 1959).

[5] Canuto, C., Hussaini, M. Y., Quarteroni, A. and Zang, T. A. *Spectral methods in fluid dynamics*, (Springer-Verlag, 1988).

[6] Cebeci, T. *Numerical and physical aspects of aerodynamic flows*. (Springer-Verlag, 1981-1983-1985).

[7] Gregory, N., Stuart, J. T. and Walker, W. S. *On the stability of three-dimensional boundary-layers with applications to the flow due to a rotating-disk*. Philos. Trans. R. Soc. London Ser. A **248**, 155–199, 1955.

[8] Hall, P. *An investigation of the stationary modes of instability of the boundary layer on a rotating-disk*. Proc. Roy. Soc. London Ser. A **406**, 93–106, 1986.

[9] Kármán, T. V. *Uber laminare und turbulente Reibung*. Zeitschnnift fur angewantee Mathematik und Mechanik. **1**, 233–252, 1921.

[10] Kohama, Y. *Study on boundary-layer transition of a rotating-disk*. Acta Mech. **50**, 193–199, 1984.

[11] Lingwood, R. J. *Absolute instability of the boundary layer on a rotating-disk*. J. Fluid Mech. **299**, 17–33, 1995.

[12] Lingwood, R. J. *An experimental study of absolute instability of the rotating-disk boundary-layer flow*. J. Fluid Mech. **314**, 373–405, 1996.

[13] Lingwood, R. J. *On the application of the Briggs' and steepest-descent method to a boundary layer flow*. Stud. Appl. Math. **98**, 213–254, 1997.

[14] Mack, L. M. *The wave pattern produced by a point source on a rotating-disk*. (AIAA Pap. No. 0490. 1985).

[15] Malik, M. R. *The neutral curve for stationary disturbances in rotating-disk flow*. J. Fluid Mech. **164**, 275–287, 1986.

[16] Malik, M. R. and Poll, D. I. A. *Effect of curvature on three-dimensional boundary-layer stability*. AIAA Journal **23**, 1362–1369, 1985.

[17] Malik, M. R., Wilkinson, S. P. and Orszag, S. A. *Instability and transition in rotating-disk flow*. AIAA Journal **19**, 1131–1138, 1981.

[18] Papageourgiou, D. T. *The stability of two dimensional wakes and shear layers at high Mach numbers*. Phys. Fluids **3**, 793–802, 1991.

[19] Rosenhead, L. *Laminar boundary layers*. (Oxford University Press, 1963).

[20] Stewartson, K. *The theory of laminar boundary layers in compressible fluids*, (Oxford University Press, 1964).

[21] Türkyılmazoğlu, M. *Linear Stability analysis of two and three-dimensional flows*, (PhD thesis, University of Manchester, 1998).

[22] Türkyılmazoğlu, M., Gajjar, J. S. B. and Ruban, A. I. *The absolute instability of thin wakes in an incompressible/compressible fluid*, Theoret. Comput. Fluid Dyn. **13**, 91–114, 1999.

[23] Wilkinson, S. P. and Malik, M. R. *Stability experiments in rotating-disk flow*. (AIAA Pap. No. 1760, 1983).

Hacettepe Journal of Mathematics and Statistics
Volume 33 (2004), 11 – 14

ON JORDAN GENERALIZED DERIVATIONS IN GAMMA RINGS

Yılmaz Çeven* and M. Ali Öztürk*

Received 23 : 09 : 2003 : Accepted 12 : 05 : 2004

Abstract

In this study, We define a generalized derivation and a Jordan generalized derivation on Γ-rings and show that a Jordan generalized derivation on some Γ-rings is a generalized derivation.

Keywords: Derivations, Generalized Derivations, Gamma ring.

2000 AMS Classification: 16 W 25, 16 N 60, 16 U 80, 16 A 78

1. Introduction

The notion of generalized derivation was introduced by Hvala [2]. Let R be an associative ring. An additive mapping $f : R \longrightarrow R$ is called a *generalized derivation* if there exists a derivation $d : R \longrightarrow R$ such that $f(xy) = f(x)y + xd(y)$ holds for all $x, y \in R$. We call an additive mapping $f : R \longrightarrow R$ a *Jordan generalized derivation* if there exists a derivation $d : R \longrightarrow R$ such that $f(x^2) = f(x)x + xd(x)$ holds for all $x \in R$.

Let M and Γ be additive Abelian groups. Then M is called a Γ- *ring* if for any $x, y, z \in M$ and $\alpha, \beta \in \Gamma$ the following conditions are satisfied.

(1) $x\alpha y \in M$,
(2) $(x + y)\alpha z = x\alpha z + y\alpha z$, $x(\alpha + \beta)z = x\alpha z + x\beta z$, $x\alpha(y + z) = x\alpha y + x\alpha z$, and
(3) $(x\alpha y)\beta z = x\alpha(y\beta z)$,

The notion of a Γ-ring was introduced by Nobusawa [5] and generalized by Barnes [1] as defined above. Many properties of Γ-rings were obtained by Barnes [1], Kyuno [3], Luh [4], Nobusawa [5] and others.

Let M be a $\Gamma-$ring and $D : M \longrightarrow M$ an additive map. Then D is called a derivation if

$$D(x\alpha y) = D(x)\alpha y + x\alpha D(y), \ (x, y \in M, \alpha \in \Gamma)$$

and D is called a Jordan derivation if

$$D(x\alpha x) = D(x)\alpha x + x\alpha D(x), \ (x \in M, \alpha \in \Gamma).$$

*Cumhuriyet University, Faculty of Arts and Science, Department of Mathematics, 58140-Sivas, Turkey.

Let M be a Γ-ring and $F : M \longrightarrow M$ an additive map. Then F is called a generalized derivation if there exists a derivation $D : M \longrightarrow M$ such that

$$F(x\alpha y) = F(x)\alpha y + x\alpha D(y)$$

for all $x, y \in M$ and $\alpha \in \Gamma$. Finally, F is called a Jordan generalized derivation if there exists a derivation $D : M \longrightarrow M$ such that

$$F(x\alpha x) = F(x)\alpha x + x\alpha D(x)$$

for all $x \in M$ and $\alpha \in \Gamma$.

The notions of derivation and Jordan derivation on a Γ-rings were defined by Sapanci and Nakajima in [6], where they showed that a Jordan derivation on a certain type of completely prime Γ-ring is a derivation. In this note we show that for our notions of generalized derivation and Jordan generalized derivation on a Γ-ring given above, a Jordan generalized derivation on certain Γ-rings is also a generalized derivation.

1.1. Example. Let $f : R \longrightarrow R$ be a generalized derivation on a ring R. Then there exists a derivation $d : R \longrightarrow R$ such that $f(xy) = f(x)y + xd(y)$ for all $x, y \in R$. We take $M = M_{1,2}(R)$ and $\Gamma = \left\{ \begin{pmatrix} n \cdot 1 \\ 0 \end{pmatrix} : \ n \text{ is an integer} \right\}$. Then M is a Γ-ring. If we define the map $D : M \longrightarrow M$ by $D\,(\,(x, y)\,) = (\,d(x), d(y)\,)$ then D is a derivation on M. Let $F : M \longrightarrow M$ be the additive map defined by $F\,(\,(x, y)\,) = (\,f(x), f(y)\,)$. Then F is a generalized derivation on M. Let N be the subset $\{(x, x) : x \in R\}$ of M. Then N is a Γ-ring, and the map $F : N \longrightarrow N$ defined in terms of the generalized Jordan derivation $f : R \longrightarrow R$ on R by $F\,(\,(x, x)\,) = (\,f(x), f(x)\,)$ is a generalized Jordan derivation on N.

2. The Main Results

Throughout the following, we assume that M is an arbitrary Γ-ring and F a generalized Jordan derivation on M. Clearly, every generalized derivation on M is a Jordan generalized derivation. The converse in general is not true. In the present paper, it is shown that every Jordan generalized derivation on certain Γ-rings is a generalized derivation.

2.1. Lemma. *Let $a, b, c \in M$ and $\alpha, \beta \in \Gamma$. Then*

(i) $F(a\alpha b + b\alpha a) = F(a)\alpha b + F(b)\alpha a + a\alpha D(b) + b\alpha D(a)$.

(ii) $F(a\alpha b\beta a + a\beta b\alpha a) = F(a)\alpha b\beta a + F(a)\beta b\alpha a + a\beta D(b)\alpha a + a\alpha D(b)\beta a + a\alpha b\beta D(a) + a\beta b\alpha D(a)$.

(iii) *In particular, if M is 2-torsion free then*

$$F(a\alpha b\alpha a) = F(a)\alpha b\alpha a + a\alpha D(b)\alpha a + a\alpha b\alpha D(a).$$

(iv) $F(a\alpha b\alpha c + c\alpha b\alpha a) = F(a)\alpha b\alpha c + F(c)\alpha b\alpha a + a\alpha D(b)\alpha c + c\alpha D(b)\alpha a + a\alpha b\alpha D(c) + c\alpha b\alpha D(a)$.

Proof. (i) is obtained by computing $F(\,(a + b)\alpha(a + b))$ and (ii) is also obtained by replacing b with $a\beta b + b\beta a$ in (i). Moreover, (iii) can be obtained by replacing β with α in (ii). If we replace a with $a + c$, we can get (iv). □

2.2. Lemma. *Let $\delta_\alpha(a, b) = F(a\alpha b) - F(a)\alpha b - a\alpha D(b)$ for $a, b \in M$ and $\alpha \in \Gamma$. Then*

(i) $\delta_\alpha(a, b) + \delta_\alpha(b, a) = 0$.

(ii) $\delta_\alpha(a, b + c) = \delta_\alpha(a, b) + \delta_\alpha(a, c)$

(iii) $\delta_\alpha(a + b, c) = \delta_\alpha(a, c) + \delta_\alpha(b, c)$.

(iv) $\delta_{\alpha+\beta}(a, b) = \delta_\alpha(a, b) + \delta_\beta(a, b)$ *for all $a, b, c \in M$ and $\alpha, \beta \in \Gamma$.*

Proof. These results follow easily by Lemma 1 (i) and the definition of $\delta_\alpha(a, b)$. □

Note that F is a generalized derivation iff $\delta_\alpha(a,b)=0$ for all $a,b\in M$ and $\alpha\in\Gamma$.

2.3. Lemma. *Let $a,b,c\in M$ and $\alpha,\beta\in\Gamma$. If M is 2-torsion free, then*

(i) $\delta_\alpha(a,b)\alpha[a,b]_\alpha=0$.
(ii) $\delta_\alpha(a,b)\beta x\beta[a,b]_\alpha=0$ *for any* $x\in M$.

Proof. (i) Replacing c by $a\alpha b$ in Lemma 1(iv), we obtain the proof.

(ii) We set $A=a\alpha b\beta x\beta b\alpha a+b\alpha a\beta x\beta a\alpha b$. Then, since $F(A)=F(a\alpha(b\beta x\beta b)\alpha a+b\alpha(a\beta x\beta a)\alpha b)$ and $F(A)=F(\,(a\alpha b)\beta x\beta(b\alpha a)+(b\alpha a)\beta x\beta(a\alpha b)\,)$, by Lemma 1(iii) and Lemma 1(iv), we have the proof. □

2.4. Theorem. *Let M be a 2-torsion free Γ-ring. If M has two elements a and b so that for any $\alpha\in\Gamma$ we have $c\gamma x\gamma[a,b]_\alpha=0$ or $[a,b]_\alpha\gamma x\gamma c=0$ implies $c=0$ for all $x\in M$, $\gamma\in\Gamma$, then every Jordan generalized derivation on M is a generalized derivation.*

Proof. Let u,v be fixed elements of M such that $c\gamma x\gamma[u,v]_\alpha=0$ or $[u,v]_\alpha\gamma x\gamma c=0$ implies $c=0$. Then by Lemma 3(ii), we get

$$\delta_\alpha(u,v)=0 \tag{2.1}$$

for all $\alpha\in\Gamma$. Our aim is to prove that $\delta_\alpha(a,b)=0$ for all $a,b\in M$ and $\alpha\in\Gamma$. In Lemma 3(ii), replacing a by $a+u$, we have $\delta_\alpha(a+u,b)\beta x\beta((a+u)\alpha b-b\alpha(a+u))=0$. Using Lemma 2(iii), we get $\delta_\alpha(a,b)\beta x\beta[a,b]_\alpha+\delta_\alpha(a,b)\beta x\beta[u,b]_\alpha+\delta_\alpha(u,b)\beta x\beta[a,b]_\alpha+\delta_\alpha(u,b)\beta x\beta[u,b]_\alpha=0$.

From Lemma 3(ii), since $\delta_\alpha(a,b)\beta x\beta[a,b]_\alpha=0$ and $\delta_\alpha(u,b)\beta x\beta[u,b]_\alpha=0$ then we have

$$\delta_\alpha(a,b)\beta x\beta[u,b]_\alpha+\delta_\alpha(u,b)\beta x\beta[a,b]_\alpha=0 \tag{2.2}$$

for all $x,a,b\in M$ and $\alpha,\beta\in\Gamma$. Now replacing b by $b+v$ in (2.2) and using Lemma 2(ii), we get $\delta_\alpha(a,b)\beta x\beta[u,b]_\alpha+\delta_\alpha(a,b)\beta x\beta[u,v]_\alpha+\delta_\alpha(a,v)\beta x\beta[u,b]_\alpha+\delta_\alpha(a,v)\beta x\beta[u,v]_\alpha+\delta_\alpha(u,b)\beta x\beta[a,b]_\alpha+\delta_\alpha(u,b)\beta x\beta[a,v]_\alpha+\delta_\alpha(u,v)\beta x\beta[a,b]_\alpha+\delta_\alpha(u,v)\beta x\beta[a,v]_\alpha=0$ or using equations (2.1) and 2.2 we have

$$\delta_\alpha(a,b)\beta x\beta[u,v]_\alpha+\delta_\alpha(a,v)\beta x\beta[u,b]_\alpha+\delta_\alpha(a,v)\beta x\beta[u,v]_\alpha+\delta_\alpha(u,b)\beta x\beta[a,v]_\alpha=0. \tag{2.3}$$

Replacing a by u in equation(2.3) and using equation (2.1) together with the fact that M is 2-torsion free, we have

$$\delta_\alpha(u,b)\beta x\beta[u,v]_\alpha=0 \tag{2.4}$$

for all $b,x\in M$ and $\alpha,\beta\in\Gamma$. Hence by hypothesis, we get

$$\delta_\alpha(u,b)=0 \tag{2.5}$$

for all $b\in M$, $\alpha\in\Gamma$. Again replacing b by v in equation (2.2), using equation (2.1) and the hypothesis, we obtain

$$\delta_\alpha(a,v)=0 \tag{2.6}$$

for all $a\in M$, $\alpha\in\Gamma$. Substituting equations (2.5) and (2.6) in equation (2.3) we have

$$\delta_\alpha(a,b)\beta x\beta[u,v]_\alpha=0,$$

and then from the hypothesis we obtain

$$\delta_\alpha(a,b)=0$$

for all $a,b\in M$, $\alpha\in\Gamma$, i.e. F is a generalized derivation on M. □

References

[1] Barnes, W. E. *On the* Γ*-rings of Nobusawa*, Pasific J. Math. **18**, 411–422, 1966.
[2] Hvala, B. *Generalized derivations in rings*, Comm. Algebra **26**, 1147–1166, 1998.
[3] Kyuno, S. *On prime gamma rings*, Pacific J. Math. **75**, 185–190, 1978.
[4] Luh, J. *On the theory of simple* Γ*-rings*, Michigan Math. J. **16**, 65–75, 1969.
[5] Nobusawa, N. *On a generalization of the ring theory*, Osaka J. Math. **1**, 81–89, 1964.
[6] Sapancı, M. and Nakajima, A. *Jordan derivations on completely prime gamma rings*, Math. Japonica, **46** No: 1, 47–51, 1997.

Hacettepe Journal of Mathematics and Statistics
Volume 33 (2004), 15 – 22

AN ALMOST 2–PARACONTACT STRUCTURE ON THE COTANGENT BUNDLE OF A CARTAN SPACE

M. Gîrţu*

Received 30 : 10 : 2003 : Accepted 17 : 01 : 2005

Abstract

A Cartan space is a pair (M, K), where M is a smooth manifold and K an Hamiltonean on the slit cotangent bundle $T_0^*M := TM \setminus \{(x, 0),\ x \in M\}$, that is positively homogeneous of degree 1 in momenta. We show that K induces an almost 2–paracontact Riemannian structure on T_0^*M whose restriction to the figuratrix bundle $\mathbb{K} = \{(x, p) \mid K(x, p) = 1\}$ is an almost paracontact structure. A condition for this almost paracontact structure to be normal is found, and its geometrical meaning is pointed out. Similar results for Finsler spaces can be found in [1] and [3].

Keywords:

2000 AMS Classification:

1. Introduction

Let (N, h) be an m–dimensional Riemannian manifold. If on N there exists a tensor field ϕ of type $(1, 1)$, r vector fields $\xi_1, \xi_2, \ldots, \xi_r$, $(r < m)$, and r, 1–forms $\eta^1, \eta^2, \ldots, \eta^r$ such that

(i) $\eta^a(\xi_b) = \delta^a_b$, $a, b \in (r) = \{1, 2, \ldots, r\}$,
(ii) $\phi^2 = I - \sum_a \eta^a \otimes \xi_a$,
(iii) $\eta^a(X) = h(X,\ \xi_a),\ a \in (r)$,
(iv) $h(\phi X, \phi Y) = h(X, Y) - \sum_a \eta^a(X)\eta^a(Y)$,

where X, Y are vector fields and I is the identity tensor field on N, then

$$\Sigma = (\phi,\ \xi_a,\ \eta^a)_{a\in(r)}$$

is said to be an *almost r–paracontact Riemannian structure on M*, and the pair (M, Σ) is called an *almost r–paracontact Riemannian manifold.*

*Faculty of Sciences, University of Bacău, Bacău, Romania. E-mail : manuelag@ub.ro

From (i) through (iv) it follows that (see [2]):

$$\phi(\xi_a) = 0,\ \eta^a \circ \phi = 0,\ a \in (r)$$
$$\phi(x, y) := h(\phi X,\ Y) = h(X,\ \phi Y).$$

A Cartan space is a pair $K^n = (M, K)$, where M is a smooth $n-$dimensional manifold and K is a positive function on the cotangent bundle $T_0^*M := T^*M \setminus \{(x, 0) \mid x \in M\}$ such that the function K^2 is a regular Hamiltonian which is homogeneous of degree 2 in momenta.

It is well known that T_0^*M is a Riemannian manifold with a Riemannian metric similar to the Sasaki metric, completely determined by K.

We show in Section 2 that, moreover, T_0^*M can be naturally endowed with an almost 2-paracontact Riemannian structure. Section 1 is devoted to some preliminaries, especially regarding the geometry of T^*M. In Section 3 we consider the figuratrix bundle $\mathbb{K} = \{u \in T^*M \mid K(u) = 1\}$ as a submanifold of T_0^*M of codimension one, and we show that it carries an almost paracontact Riemanian structure induced by the above mentioned almost 2-paracontact Riemannian structure on T_0^*M. A condition for this paracontact Riemannian structure to be normal is established and its geometric meaning is discussed.

2. Preliminaries

We recall from Chapter 6 of [4] some facts from the geometry of the cotangent bundle T^*M. We take $(x^i),\ i = 1, 2, \ldots, n$ as local coordinates on M. The induced local coordinates on T^*M will be denoted by $(x^i,\ p_i)$, where x^i is in fact $x^i \circ \tau^*$, for $\tau^* : T^*M \to M$ the natural projection, and p_i are the components of a covector from T_x^*M, $x(x^i)$, in the cobasis $(dx^i)_x$. The coordinates p_i will be called momenta.

The kernel of the differential $D\tau^*$ of τ^* is a subbundle of TT_0^*M, known as vertical and denoted by VT_0^*M. The vertical distribution $V : u \in T^*M \to V_uT_0^*M = \ker(D\tau^*)_u$ is locally spanned by $\dot\partial^i := \dfrac{\partial}{\partial p_i}$, hence it is integrable.

The vector field $C^* = p_i\ \dot\partial^i$ on T^*M is called the Liouville vector field.

Let $K^n = (M, K)$ be a Cartan space. Then the function $K : T^*M \to \mathbb{R}$ has the properties

(i) K is smooth on T_0^*M and only continuous on the set $\{(x, 0) \mid x \in M\}$,
(ii) $K > 0$ on T^*M,
(iii) $K(x,\ \lambda p) = \lambda K(x, p)$ for any $\lambda > 0$,
(iv) The matrix with entries $g^{ij}(x, p) = \frac{1}{2}\ \dot\partial^i \dot\partial^j\ K^2$ is positive definite.

If one sets $p^i = \frac{1}{2}\ \dot\partial^i\ K^2$then $g^{ij} = \dot\partial^j\ p^i$, and from the homogeneity condition (iii) there results

$$\begin{aligned} &p^i = g^{ij}p_j,\ K^2 = g^{ij}p_ip_j = p_ip^j, \\ &C^{ijk}p_k = 0,\ \text{where } C^{ijk} := \tfrac{1}{2}\ \dot\partial^i\ g^{jk}. \end{aligned} \tag{2.1}$$

As $\det(g^{ij}) \neq 0$, from the first equation in (1.1) it follows that $p_i = g_{ij}p^j$, where (g_{ij}) is the inverse of the matrix (g^{ij}).

In the following we restrict our considerations to the open submanifold T_0^*M of T^*M.

A nonlinear connection on T_0^*M is a distribution $u \to H_uT_0^*M$, called horizontal, which is supplementary to the vertical distribution. This is usually given by a local basis $\delta_i = \partial_i + N_{ij}(x, p)\ \dot\partial^j$ for some functions (N_{ij}) having a special behavior, by a change of coordinates on T^*M. It was proved by R. Miron [4, Chapter 4] that any Cartan space

has a canonical nonlinear connection, completely determined by K, whose coefficients $(N_{ij}(x,p))$ are positively homogeneous of degree 1 in momenta, and have the property $N_{ij} = N_{ji}$.

Thus we have a decomposition

$$T_u T_0^* M = V_u T_0^* M \oplus H_u T_0^* M, \tag{2.2}$$

and $(\delta_i, \dot{\partial}^i)$ is a basis adapted to it.

This suggests the following definition of an almost product structure Q on T^*M.

$$Q(\delta_i) = g_{ij}\, \dot{\partial}^j,\ Q(\dot{\partial}^i) = g^{ij}\delta_j. \tag{2.3}$$

It is easy to check that $Q^2 = I$.

Using the matrices (g_{ij}) and (g^{ij}) the following Riemannian metric on T_0^*M is defined

$$G = g_{ij}dx^i \otimes dx^j + g^{ij}\delta p_i \otimes \delta p_j, \tag{2.4}$$

where $\delta p_i = dp_i - N_{ij}(x,p)dx^j$ and $(dx^i, \delta p_i)$ is the dual basis of $(\delta_i, \dot{\partial}^i)$.

The Riemannian metric G is similar to the Sasaki metric on the tangent bundle. An easy calculation gives:

$$G(QX, QY) = G(X,Y), X, Y \in \mathcal{X}(T_0^*M). \tag{2.5}$$

Here $\mathcal{X}(T^*M)$ is the $\mathcal{F}(M)$–module of vector fields on T_0^*M.

3. An almost 2-paracontact Riemannian structure on T_0^*M when (M,K) is a Cartan space

We already know that (T_0^*M, G) is a Riemannian manifold. On T_0^*M there exist two globally defined vector fields:

$$\xi_1 = \frac{1}{K}p^i\delta_i \text{ and } \xi_2 = \frac{1}{K}p_i\ \dot{\partial}^i\ .$$

They are linearly independent. The second one is collinear with the Liouville vector field, while the first one is nothing but the Hamiltonian vector field of the function K.

Indeed, the Hamiltonian vector field of K is

$$\overrightarrow{K} = (\dot{\partial}^i\ K)\frac{\partial}{\partial x^i} - (\partial_i K)\frac{\partial}{\partial p_i} = (\dot{\partial}^i\ K)\delta_i - (\delta_i K)\ \dot{\partial}^i = \xi_1,$$

because for a Cartan space $\delta_i K = 0$ and $\dot{\partial}^i\ K = \frac{p^i}{K}$.

Now we consider the 2 1-forms

$$\eta^1 = \frac{1}{K}p_i dx^i \text{ and } \eta^2 = \frac{1}{K}p^i\delta p_i.$$

These are globally defined. It quickly follows that

$$\eta^a(\xi_b) = \delta^a_b,\ a,b \in \{1,2\}. \tag{3.1}$$

One easily checks that

$$Q(\xi_1) = \xi_2,\ Q(\xi_2) = \xi_1, \tag{3.2}$$

$$\eta^1 \circ Q = \eta^2,\ \eta^2 \circ Q = \eta^1. \tag{3.3}$$

Using $Q,\ \xi_a,\ \eta^a,\ a \in \{1,2\}$, we construct the tensor field

$$q = Q - \eta^2 \otimes \xi_1 - \eta^1 \otimes \xi_2.$$

Based on (3.1) - (3.3) it comes out that

$$q^2(X) = X - \eta^1(X)\xi_1 - \eta^2(X)\xi_2. \tag{3.4}$$

In the adapted frame $(\delta_i, \dot\partial^i)$ we have

$$G(\delta_i, \delta_j) = g_{ij}, G(\delta_i, \dot\partial^j) = 0,\ G(\dot\partial^i, \dot\partial^j) = g^{ij}.$$

These equations are used to verify that

$$\eta^a(X) = G(X, \xi_a),\ a \in \{1, 2\}, \tag{3.5}$$

holds for $X = \delta_i, \dot\partial^i$.

A direct calculation using (2.5), (3.5), as well as $G(\xi_a, \xi_b) = \delta_{ab}$, gives

$$G(qX, qY) = G(X, Y) - \eta^1(X)\eta^1(Y) - \eta^2(X)\eta^2(Y),\ X, Y \in \mathfrak{X}(T_0^*M). \tag{3.6}$$

The equations (3.1), (3.4) - (3.6) show that the following theorem holds good.

3.1. Theorem. *Let $K^n = (M, K)$ be a Cartan space. Then T_0^*M is an almost 2-paracontact Riemannian manifold with the almost 2-paracontact Riemannian structure $(q,\ \xi_a,\ \eta^a, G),\ a \in \{1, 2\}$.*

The next equations follow easily from (3.1) and (3.2)

$$q(\xi_a) = 0,\ \eta^a \circ q = 0. \tag{3.7}$$

By (3.4) and (3.7) we have

$$q^3 - q = 0. \tag{3.8}$$

Now we prove

3.2. Lemma. *The rank of q is $2n - 2$.*

Proof. By the first equation (3.7), the subspace span $\{\xi_1, \xi_2\}$ is contained in $\ker q$. Let now $X \in \ker q$. If $X = X^i\delta_i + Y_i\ \dot\partial^i$, the condition $q(X) = 0$ gives $X^i = \dfrac{X^j p_j}{K^2} p^i$, $Y_i = \dfrac{Y_i p^j}{K^2} p_i$, hence $X \in \operatorname{span}\{\xi_1, \xi_2\}$ □

Let $h(X, Y) = G(qX, Y),\ X, Y \in \mathfrak{X}(T_0^*M)$.

3.3. Theorem. *The mapping h is bilinear and symmetric and its null space is $\ker q$.*

Proof. The bilinearity is obvious. The symmetry holds even in a more general setting cf. Section 1. The null space of h is $\{X \mid h(X, Y) = 0,\ \forall Y\} = \{X \mid G(qX, Y) = 0,\ \forall Y\} = \{X \mid qX = 0\} = \ker q$. □

In the adapted basis $(\delta_i, \dot\partial^i)$ we have

$$\begin{aligned} &q(\delta_i) = A_{ij}\ \dot\partial^j,\ q(\dot\partial^i) = B^{ij}\delta_j, \\ &A_{ij} = g_{ij} - \frac{1}{K^2} p_i p_j,\ B^{ij} = g^{ij} - \frac{1}{K^2} p^i p^j. \end{aligned} \tag{3.9}$$

We notice that these matrices have rank $n - 1$ because of

$$A_{ij}p^j = 0,\ B^{ij}p_j = 0. \tag{3.10}$$

The mapping h has the form

$$h = A_{ij}dx^i \otimes dx^j - B^{ij}\delta p_i \otimes \delta p_j.$$

Thus it is a singular pseudo-Riemannian metric on T_0^*M.

4. An almost paracontact structure on the figuratrix bundle of a Cartan space K^n

The set $\mathbb{K} = \{(x,p) \in T_0^*M \mid K(x,p) = 1\}$ will be called the *figuratrix bundle* of the Cartan space K^n. It will be thought of as a hypersurface (submanifold of codimension 1) of T_0^*M, endowed with the almost 2-paracontact Riemannian structure from Theorem 3.1.

Let

$$\begin{cases} x^i = x^i(u^\alpha), \\ p_i = p_i(u^\alpha), \ \alpha = 1,2,\dots,2n-1, \end{cases} \tag{4.1}$$

with rank $\left(\dfrac{\partial x^i}{\partial u^\alpha}, \dfrac{\partial p_i}{\partial u^\alpha}\right) = 2n-1$, a parametrization of $\mathbb{K}$.

We consider the local vector fields $\dfrac{\partial}{\partial u^\alpha} = \dfrac{\partial x^i}{\partial u^\alpha}\partial_i + \dfrac{\partial p_i}{\partial u^\alpha}\ \dot\partial^i$, which provide a local basis in the tangent bundle to $\mathbb{K}$, and put them into the form

$$\frac{\partial}{\partial u^\alpha} = \frac{\partial x^i}{\partial u^\alpha}\delta_i + \left(\frac{\partial p_j}{\partial u^\alpha} - N_{ij}\frac{\partial x^i}{\partial u^\alpha}\right)\dot\partial^j\ .$$

It follows that $G\left(\dfrac{\partial}{\partial u^\alpha}, \xi_2\right) = \dfrac{1}{K}p^j\left(\dfrac{\partial p_j}{\partial u^\alpha} - N_{ij}\dfrac{\partial x^i}{\partial u^\alpha}\right)$. On the other hand, by deriving the identity $K^2(x^i(u^\alpha), p_i(u^\alpha)) = 1$ with respect to u^α we find

$$\begin{aligned} 0 &= (\partial_i K^2)\frac{\partial x^i}{\partial u^\alpha} + (\dot\partial^i\ K^2)\frac{\partial p_i}{\partial u^\alpha} \\ &= (\delta_i K^2)\frac{\partial x^i}{\partial u^\alpha} + (\dot\partial^i\ K^2)\left(\frac{\partial p_i}{\partial u^\alpha} - N_{ij}\frac{\partial x^j}{\partial u^\alpha}\right) \\ &= 2p^i\left(\frac{\partial p_i}{\partial u^\alpha} - N_{ij}\frac{\partial x^j}{\partial u^\alpha}\right) \end{aligned}$$

because, for a Cartan space, $\delta_i K = 0$. Thus on $\mathbb{K}$ we have $G = \left(\dfrac{\partial}{\partial u^\alpha}, \xi_2\right) = 0$ for every $\alpha = 1,2,\dots,2n-1$. In other words, the vector field ξ_2 restricted to $\mathbb{K}$ is normal to $\mathbb{K}$.

Recall that ξ_2 restricted to $\mathbb{K}$ is $\overline{\xi_2} = p_i(u^\alpha)\ \dot\partial^i$.

4.1. Lemma. *The hypersurface $\mathbb{K}$ is invariant with respect to q i.e. $q(T_u\mathbb{K}) \subset T_u\mathbb{K}$, $\forall u \in \mathbb{K}$.*

Proof. $G\left(q\left(\dfrac{\partial}{\partial u^\alpha}\right), \xi_2\right) = (\eta^2 \circ q)\left(\dfrac{\partial}{\partial u^\alpha}\right) = 0\ \forall\, \alpha = 1,2,\dots,2n-1.$ □

By item (i) in Theorem 3.1 from [2], and Lemma 4.1, there follows:

4.2. Theorem. *The almost 2-paracontact Riemannian structure $(q,\ \xi_a,\ \eta^a, G)$, $a \in \{1,2\}$, on T_0^*M induces by restriction an almost paracontact Riemannian structure on the figuratrix bundle $\mathbb{K}$.*

If we use overlines to denote the restrictions we have

- $\overline{\xi_1} = p^i\delta_i$, is tangent to $\mathbb{K}$
- $\overline{\eta_2} = 0$ because of $\eta^2(X) = G(X, \xi_2) = 0$ for every X tangent to $\mathbb{K}$,
- $\overline{G} = G|_{\mathbb{K}}$,
- $\overline{q} = \overline{Q} - \overline{\eta}^1 \otimes \overline{\eta}^2$ is an automorphism of $T_u\mathbb{K}$, $\forall u \in \mathbb{K}$.

We put $\xi = \overline{\xi}_1$, $\eta = \overline{\eta}_1$, so the almost paracontact Riemannian structure given by Theorem 4.2 is $(\overline{q}, \xi, \eta, \overline{G})$. We mention that

$$\overline{q}^2 = I - \eta \otimes \xi,\ \eta(X) = G(X, \xi), \tag{4.2}$$

$$\overline{G}(\overline{q}X, \overline{q}Y) = \overline{G}(X, Y) - \eta(X)\eta(Y),\ X, Y \in \mathfrak{X}(\mathbb{K}). \tag{4.3}$$

By Theorem 1.1 in [2], the almost paracontact Riemannian structure $(\overline{q}, \xi, \eta, \overline{G})$ is **normal** if and only if

$$N(X, Y) := N_{\overline{q}}(X, Y) - 2d\eta(X, Y)\xi = 0, \tag{4.4}$$

where $N_{\overline{q}}$ is the Nijenhuis tensor field of $\overline{q}$, i.e.

$$N_{\overline{q}}(X, Y) = [\overline{q}X, \overline{q}Y] + \overline{q}^2[X, Y] - \overline{q}[\overline{q}X, Y] - \overline{q}[X, \overline{q}Y],\ \forall X, Y \in \mathfrak{X}(\mathbb{K}). \tag{4.5}$$

Now we look for conditions under which $(\overline{q}, \xi, \eta, \overline{G})$ is normal.

If we put $\dot{\delta}_j = \overline{q}(\delta_j)$ we get n local vector fields that are tangent to $\mathbb{K}$, because $\mathbb{K}$ is an invariant hypersurface. These, together with δ_i, $i = 1, 2, \ldots, n$, are all tangent to $\mathbb{K}$ and they are not linearly independent. But if we consider δ_i, $i = 1, 2, \ldots, n$ and $\dot{\delta}_j$ with $j = 1, 2, \ldots, n-1$, we obtain a set $(\delta_i, \dot{\delta}_j)$ of local vector fields that form a local basis in the tangent bundle to $\mathbb{K}$. We shall compute N from (4.4) in this basis.

First, we note that

$$\begin{aligned} &\dot{\delta}_j = \overline{q}(\delta_j) = a_{jk}\ \dot{\partial}^k,\ a_{jk} = g_{jk} - p_j p_k \\ &\overline{q}(\dot{\partial}^k) = g^{ki}\delta_i. \end{aligned} \tag{4.6}$$

$$\begin{aligned} &\overline{q}^2(\delta_i) = b_i^k \delta_k,\ b_i^k = \delta_i^k - p_i p^k \\ &\overline{q}^2(\dot{\partial}^k) = b_i^k\ \dot{\partial}^i\ . \end{aligned} \tag{4.7}$$

Secondly, we recall some formulae related to K^n from [4],

$$\begin{aligned} &[\delta_i, \delta_j] = R_{kij}\ \dot{\partial}^k,\ R_{kij} = \delta_j N_{ki} - \delta_i N_{kj}, \\ &\left[\delta_i, \dot{\partial}^j\right] = -(\dot{\partial}^j N_{ik})\ \dot{\partial}^k\ . \end{aligned} \tag{4.8}$$

$$p_k\ \dot{\partial}^k\ N_{ij} = N_{ij} \text{ (the homogeneity of } N_{ij} \text{ in momenta)}. \tag{4.9}$$

Assume that K^n is endowed with the linear Cartan connection $(H^i_{jk}, C^j k_i = g_{is}C^{sjk})$. Denote by $_{|k}$ and $|^k$ the horizontal and vertical covariant derivatives, respectively. Then we have

$$\begin{aligned} &K^2_{|j} := \delta_j K^2 = 0, K^2|^j = 2p^j, p_{i|j} = 0,\ p_i|^j = \delta_i^j \\ &p^i_{|j} = 0, p^i|^j = g^{ij}. \end{aligned} \tag{4.10}$$

$$R_{kij}p^k = 0, P^i_{jk}p^j = 0,\ P^i_{jk} := H^i_{jk} - \dot{\partial}^i\ N_{jk}. \tag{4.11}$$

$$\delta_i g_{jk} = H^s_{ji}g_{sk} + H^s_{ki}g_{js}. \tag{4.12}$$

Now we compute:

$$2d\eta(\delta_i, \delta_j) = \delta_i p_j - \delta_j p_i = 0 \text{ since by (3.9), } \delta_i p_j = H^s_{ij}p_s,$$

$$2d\eta(\delta_i, \dot{\delta}_j) = -\dot{\delta}_j p_i = -a_{ij},$$

$$2d\eta(\dot{\partial}^i, \dot{\partial}^j) = 0.$$

And further,

$$
\begin{aligned}
&N(\delta_i,\delta_j)=A_{hij}g^{hk}\delta_k+(B_{kij}-R_{kij})\,\dot\partial^{\,j}\\
&N(\delta_i,\dot\delta_j)=(a_{ih}\,\dot\partial^{\,h}\,b^s_j-b^k_jR_{hik}g^{hs}-B_{hij}g^{hs}-B_{hij}g^{hs}+a_{ij}p^s)\delta_s-\\
&\qquad\qquad-\left[A_{kij}-p_jp^r(\delta_ra_{ik}-a_{ih}\,\dot\partial^{\,h}\,N_{rk})+a_{kr}\delta_ib^r_j\right]\dot\partial^{\,k},\\
&N(\dot\delta_i,\dot\delta_j)=(D^s_{ij}-D^s_{ji})\delta_s+(b^k_ib^h_jR_{rkh}-B_{rij}+a_{rk}E^k_{ij})\,\dot\partial^{\,r},
\end{aligned}
\tag{4.13}
$$

where

$$
\begin{aligned}
A_{kij}&=\delta_ia_{jk}-\delta_ja_{ik}+a_{ih}\,\dot\partial^{\,h}\,N_{jk}-a_{jh}\,\dot\partial^{\,h}\,N_{ik},\\
B_{kij}&=a_{ih}\,\dot\partial^{\,h}\,a_{jk}-a_{jh}\,\dot\partial^{\,h}\,a_{ik},\\
D^s_{ij}&=b^k_i\delta_kb^s_j+(b^k_j\delta_ka_{ih}+b^k_ia_{jh}\dot\partial^hN_{kr})g^{hs},\\
E^k_{ij}&=a_{ih}\,\dot\partial^{\,h}\,b^k_j-a_{jh}\,\dot\partial^{\,h}\,b^k_i.
\end{aligned}
\tag{4.14}
$$

The expressions from (4.14) can be simplified as follows.

First, using (1.1) one easily obtains that $B_{kij}=p_ig_{jk}-p_jg_{ik}$.

From $p^ka_{kr}=0$ it follows that $(\delta_ip^k)a_{kr}=-(\delta_ia_{kr})p^r$, and $p_{i|k}=0$ is equivalent to $\delta_ip_k=N_{ik}$. Based on these formulae we find that the vertical part of $N(\delta_i,\dot\delta_j)$ is $-b^k_jA_{rik}\,\dot\partial^{\,r}$ and its horizontal part takes the form $b^k_j(p_ig_{kh}-p_kg_{ih}-R_{hik})g^{hs}\delta_s$.

A tedious computation gives

$$D^s_{ij}-D^s_{ji}=A_{hij}g^{hs}+p^kP^r_{kh}(p_ig_{rj}-p_jg_{ir})=A_{hij}g^{hs}$$

by (4.11).

We have $E^k_{ij}=p_i\delta^k_j-p_j\delta^k_i$, and using this we get that the vertical part of $N(\dot\delta_i,\dot\delta_j)$ is $(R_{kij}+p_iR_{kjo}-p_jR_{rio})\partial^r$, where $R_{kjo}=R_{kjs}p^s$.

The tensor field A_{kij} takes the form $A_{kij}=\delta_ig_{jk}-\delta_jg_{ik}+g_{ih}\,\dot\partial^{\,h}\,N_{jk}-g_{jh}\,\dot\partial^{\,h}\,N_{ik}$ and by (iii) of Prop. 2.3 in Chapter 7 of [4], it vanishes for Cartan spaces.

Gathering together the above facts we obtain

4.3. Theorem. *In the frame $(\delta_i,\dot\delta_j)$, $j=1,2,\dots,n-1$, the tensor field N given by* (4.4) *has the form*

$$
\begin{aligned}
&N(\delta_i,\delta_j)=(p_ig_{jk}-p_jg_{ik}-R_{kij})\,\dot\partial^{\,j},\\
&N(\delta_i,\dot\delta_j)=-b^k_j(p_ig_{jk}-p_kg_{ih}-R_{hik})g^{hs}\delta_s,\\
&N(\dot\delta_i,\dot\delta_j)=(R_{kij}+p_iR_{kjo}-p_jR_{kio})\,\dot\partial^{\,k}\ .
\end{aligned}
$$

4.4. Corollary. *The almost paracontact Riemannian structure $(\overline{q},\,\xi,\,\eta,\,\overline{G})$ is normal if and only if*

$$R_{kij}=p_ig_{jk}-p_jg_{ik}. \tag{4.15}$$

Proof. One easily checks that if R_{kij} has the form given by (4.15), then $R_{kij}+p_iR_{kjo}-p_jR_{kio}=0$. Then the conclusion is obvious. □

We give a geometrical meaning to (4.15), showing that it implies that the Cartan space K^n is of constant scalar curvature -1.

A Cartan space K^n is of constant scalar curvature c if

$$H_{hijk}p^ip^jX^hX^k=c(g_{hj}g_{ik}-g_{hk}g_{ij})p^ip^jX^hX^k \tag{4.16}$$

for every $(x,p) \in T_0^*M$ and $X = (X^i) \in T_xM$. Here, H_{hijk} is the $(hh)h$–curvature of the linear Cartan connection of K^n.

We replace H_{hijk} in (4.16) with $g_{is}\ H^s_{hjk}$ and so it reduces to

(4.16') $\quad p_s H^s_{hjk} p^j X^h X^k = c(p_h p_k - g_{hk}) X^h X^k.$

on $\mathbb{K}$.

By Proposition 5.1 (ii) in Chapter 7 of [4], $p_s H^s_{hjk} = -R_{khj}$, hence we get $R_{kho} X^h X^k = c(g_{hk} - p_h p_k) X^h X^k$, or equivalently

(4.17) $\quad R_{kho} = c(g_{hk} - p_h p_k),$

because $(X^h),\ (X^k)$ are arbitrary vector fields on M.

Now it is easy to check that (4.17) follows from (4.15) when $c = -1$.

In general, (4.17) does not imply (4.15). But this happens when the (g^{ij}) do not depend on p. Indeed, in this case $N_{ij}(x,p) = \gamma^k_{ij} p_k$, where (γ^k_{ij}) are the Christoffel symbols constructed with $g_{ij}(x)$, and then $R_{kij} = R^h_{kij} p_h$, where R^h_{kij} is the curvature tensor derived from $g_{ij}(x)$.

The equation (4.17) now reads as follows:

(4.17') $\quad R^s_{khj}(x) p_s p^j = c(g_{kh} - p_k p_h).$

On the other hand we can write $g_{kh} - p_k p_h = (\delta^s_j g_{kh}(x) - \delta^s_h g_{kj}(x)) p_s p^j$, and making use of (4.17') we get

(4.18) $\quad R^s_{khj}(x) = c(\delta^s_j g_{kh} - \delta^s_h g_{kj}).$

Equation (4.15) becomes $R^h_{kij} = p_h(\delta^h_i g_{jk} - \delta^h_j g_{ik})$, or equivalently

(4.19) $\quad R^h_{kij} = \delta^h_i g_{jk} - \delta^h_j g_{ik},$

which is equivalent to (4.18) for $c = -1$.

Thus we have obtained:

4.5. Theorem. *Let (M,K) be the Cartan space with $K^2 = g^{ij}(x) p_i p_j$. Then the almost paracontact Riemannian structure $(\overline{q},\ \xi,\ \eta,\ \overline{G})$ on the figuratrix bundle $\mathbb{K}$ is normal if and only if the Riemannian manifold $(M, g_{ij}(x))$ is of constant curvature -1.*

References

[1] Anastasiei, M. *A framed f-structure on tangent manifold of a Finsler space*, Analele Univ. Bucuresti, Mat.-Inf., XLIX, 3–9, 2000.

[2] Bucki, A. *Hypersurfaces of almost r- paracontact Riemannian manifolds.* Tensor N. S. **48**, 245–251, 1989.

[3] Gîrţu, M. *An almost paracontact structure on the indicatrix bundle of a Finsler space*, BJGA **7**(2), 43–48, 2002.

[4] Miron, R., Hrimiuc, D., Shimada, H. and Sabău, V. S. *The Geometry of Hamilton and Lagrange Spaces* , (Kluwer Academic Publishers, FTPH 118, 2001).

Hacettepe Journal of Mathematics and Statistics
Volume 33 (2004), 23 – 30

A WAVELET-TYPE TRANSFORM GENERATED BY THE POISSON SEMIGROUP

Melih Eryiğit * and Ilham A. Aliev †

Received 11 : 05 : 2004 : Accepted 16 : 06 : 2004

Abstract

A wavelet-type transform generated with the aid of the Poisson Semigroup and a signed Borel measure is introduced. An analogue of the Calderón reproducing formula (in the framework of the L_2 and L_p-theory) is established.

Keywords: Wavelet transform, Poisson semigroup, Calderón's reproducing formula.

2000 AMS Classification: 65 R 10

1. Introduction

The Calderón reproducing formula is widely used in the theory of continuous wavelet transforms [3, 4], in fractional calculus and in integral geometry (see, e.g. [1, 2, 5, 6] and references therein). A version of the Calderón formula asserts that under certain conditions on $u(x)$, $(x \in \mathbb{R}^n)$

$$\lim_{\substack{\varepsilon \to 0 \\ \rho \to \infty}} \int_{\varepsilon}^{\rho} \frac{f * u_t}{t} dt = c_u f, \quad f \in L_2(\mathbb{R}^n), \tag{1.1}$$

where $u_t(x) = t^{-n} u(x/t), \quad t > 0$, "$*$" is a convolution operator and the limit is taken with respect to the L_2-norm. The convolution $(W_u f)(x,t) = (f * u_t)(x)$ is called the *continuous wavelet transform, generated by the "wavelet function" u.*

A generalization of (1.1) has the form [6] :

$$\int_0^{\infty} \frac{f * \mu_t}{t} dt \stackrel{def}{=} \lim_{\substack{\varepsilon \to 0 \\ \rho \to \infty}} \int_{\varepsilon}^{\rho} \frac{f * \mu_t}{t} dt = c_\mu f, \tag{1.2}$$

where μ is a suitable radial Borel measure, μ_t stands for the dilation of μ, and the limit is interpreted in the L_p-norm and in the pointwise (a.e.) sense.

*Institute of Science, Akdeniz University, 07058, Antalya, Turkey.
E-mail : eryigit@akdeniz.edu.tr
†Department of Mathematics, Akdeniz University, 07058, Antalya, Turkey.
E-mail: ialiev@akdeniz.edu.tr

In this paper we introduce a new wavelet-type transform by making use of the Poisson kernel and finite Borel measure μ. The main purpose of the paper is to prove the relevant Calderón-type reproducing formula. The L_2 and L_p, $(1 \le p \le \infty)$ cases are examined separately. The pointwise (a.e.) convergence of the corresponding "truncated integrals" $\int_{\varepsilon}^{\rho}(\cdots)$ is also studied.

2. Preliminiaries

Let

$$P(x,t) = \frac{\Gamma((n+1)/2)}{\pi^{(n+1)/2}} \cdot \frac{t}{(t^2+|x|^2)^{(n+1)/2}}, \qquad t>0\ ,\ x \in \mathbb{R}^n,$$

be the Poisson kernel which possess the following properties [7]:

$$\Big[P(.,t)\Big]^{\wedge}(\xi) \equiv \int_{\mathbb{R}^n} e^{-2\pi i x.\xi} P(x,t)\,dx = e^{-\pi t|\xi|}\,, \tag{2.1}$$

with $x.\xi = x_1\xi_1 + \cdots + x_n\xi_n$;

$$\int_{\mathbb{R}^n} P(x,t)\,dx = 1, \qquad \forall t>0\,; \tag{2.2}$$

$P(x,t)$ is homogeneous function of order $(-n)$, i.e

$$P(\lambda x, \lambda t) = \lambda^{-n} P(x,t), \qquad \forall \lambda > 0\,; \tag{2.3}$$

$$\int_{\mathbb{R}^n} P(y,t)P(x-y,\tau)dy = P(x,t+\tau). \tag{2.4}$$

Given a function $f \in L_p(\mathbb{R}^n)$ with the norm $\|f\|_p = (\int_{\mathbb{R}^n} |f(x)|^p dx)^{1/p}$ we denote by $P_t f(x),\ t>0$ the Poisson semigroup associated with f:

$$P_t f(x) = \int_{\mathbb{R}^n} f(x-z)P(z,t)dz,\ t>0; \quad P_0 f(x) = f(x). \tag{2.5}$$

It is well known that (see, e.g. [7, p. 8-16])

$$\|P_t f\|_p \le \|f\|_p, \quad (1 \le p \le \infty), \quad \forall t \ge 0\,; \tag{2.6}$$

$$P_t(P_\tau f)(x) = P_{t+\tau} f(x), \quad (t,\tau \ge 0)\,; \tag{2.7}$$

$$\lim_{t\to 0^+} P_t f(x) = f(x)\,, \tag{2.8}$$

with the limit being understood in the $L_p, (1 \le p < \infty)$– norm or pointwise for almost all $x \in \mathbb{R}^n$. If $f \in C^0$ (the space of continuous functions vanishing at infinity), then convergence is uniform. Furthermore,

$$\sup_{t>0} |P_t f(x)| \le M_f(x), \tag{2.9}$$

with the well known Hardy–Littlewood maximal function

$$M_f(x) = \sup_{r>0} \frac{1}{|B_r|} \int_{B_r} |f(x-z)|dz,\ B_r = \{x : |x| < r\}. \tag{2.10}$$

2.1. Definition. Let μ be a signed Borel measure on $\mathbb{R}^1$ such that

$$\text{supp}\mu \subset [0,\infty); \quad |\mu|(\mathbb{R}^1) < \infty, \quad \mu(\{0\}) = 0, \text{ and}$$

$$\mu(\mathbb{R}^1) \equiv \int_{\mathbb{R}^1} d\mu(t) = 0. \tag{2.11}$$

In addition let $P(y,t)$ be the Poisson kernel extended to $t \le 0$ by zero. We define a wavelet transform of $f : \mathbb{R}^n \to \mathbb{C}$ as

$$W_\mu f(x,\eta) = \int_{\mathbb{R}^{n+1}} P(y,t) f(x-\eta y)dy\, d\mu(t)$$

$$\overset{(2.11)}{=} \int_{\mathbb{R}^n \times (0,\infty)} P(y,t) f(x-\eta y)dy\, d\mu(t). \tag{2.12}$$

By setting ty instead of y and using (2.3) we have

$$W_\mu f(x,\eta) = \int_{\mathbb{R}^n \times (0,\infty)} P(y,1) f(x-\eta t y)dy\, d\mu(t). \tag{2.13}$$

2.2. Remark. For any fixed $\eta > 0$ the operator W_μ is $L_p \to L_p$ bounded. Indeed, by the Minkowski inequality,

$$\|W_\mu f(\,.\,,\eta)\|_p \le \|f\|_p \int_{\mathbb{R}^n \times (0,\infty)} P(y,t)dy\, d|\mu|(t) \overset{(2.2)}{=} \|f\|_p \|\mu\| < \infty$$

where

$$\|\mu\| = \int_{(0,\infty)} d|\mu|(t) < \infty.$$

2.3. Remark. For $f \in L_p(\mathbb{R}^n)$, due to the Fubini theorem, we get

$$W_\mu f(x,\eta) = \int_{\mathbb{R}^n} f(x-\eta y)\Big(\int_{(0,\infty)} P(y,t) d\mu(t)\Big) dy.$$

Setting $w(y) = \int_{(0,\infty)} P(y,t) d\mu(t)$, by the Fubini theorem we have

$$\int_{\mathbb{R}^n} w(y)dy \overset{(2.2)}{=} \int_{(0,\infty)} d\mu(t) \overset{(2.11)}{=} 0.$$

That is, the function $w(y)$ is a usual wavelet function. Further,

$$W_\mu f(x,\eta) = \int_{\mathbb{R}^n} f(x-\eta y) w(y) dy = \frac{1}{\eta^n} \int_{\mathbb{R}^n} f(y) w(\frac{x-y}{\eta}) dy.$$

Therefore, $W_\mu f(x,\eta)$ is a continuous wavelet transform generated by the wavelet function $w(y) = \int_{(0,\infty)} P(y,t) d\mu(t)$.

2.4. Remark. In the following we will use the convention $\int_a^b \varphi(t) d\mu(t) = \int_{[a,b)} \varphi(t) d\mu(t)$. In the case where $\lim_{t \to 0^+} \varphi(t) = \infty$ we assume that $\mu(0) = 0$ and $\int_0^b \varphi(t) d\mu(t) = \int_{(0,b)} \varphi(t) d\mu(t)$.

We will need the following lemmas.

2.5. Lemma. [5, p.189] *Let μ be a Borel measure satisfying the conditions* (2.11) *and* $\int\limits_0^\infty |\log t|\, d|\mu|(t) < \infty$. *Set* $k(s) = \frac{1}{s}\int\limits_0^s d\mu(t)$. *Then*

$$k(s) \in L_1(0,\infty) \text{ and } \int\limits_0^\infty k(s)ds = \int\limits_0^\infty \log\frac{1}{s} d\mu(s)$$

.

2.6. Lemma. [7, p.60] *Let $T_\varepsilon, \varepsilon > 0$ be a family of linear operators, mapping $L^p(\mathbb{R}^n)$, $1 \le p \le \infty$ into the space of measurable functions on $\mathbb{R}^n$. Define T^*f by setting*

$$(T^*f)(x) = \sup_{\varepsilon>0} |(T_\varepsilon f)(x)|,\ x \in \mathbb{R}^n.$$

Suppose that there exists a constant $c > 0$ and a real number $q \ge 1$ such that

$$\text{meas}\{ x : |(T^*f)(x)| > t\} \le (c\|f\|_{L^p} t^{-1})^q$$

for all $t > 0$ and $f \in L^p(\mathbb{R}^n)$. If there exists a dense subset $\mathcal{D}$ of $L^p(\mathbb{R}^n)$ such that $\lim\limits_{\varepsilon\to 0}(T_\varepsilon g)(x)$ exists and is finite almost everywhere (a.e.) whenever $g \in \mathcal{D}$, then for each $f \in L^p(\mathbb{R}^n)$, $\lim\limits_{\varepsilon\to 0}(T_\varepsilon f)(x)$ exists and is finite a.e.

3. A Calderon-type reproducing formula associated with the wavelet-type transform $W_\mu f$

We will examine the L_2 and L_p, $(1 \le p \le \infty)$ cases separately. In the L_2-case the conditions on μ are expressed in terms of the Laplace transform of μ, and in the general case – in terms of μ itself.

3.1. Theorem. *Let μ satisfy the conditions in (2.11). Suppose that* $\tilde{\mu}(t) = \int\limits_0^\infty e^{-st} d\mu(s)$ *is the Laplace transform of μ and the integral* $\tilde{c}_\mu = \int\limits_0^\infty \tilde{\mu}(t)dt/t$ *is finite. Then,*

$$\int\limits_0^\infty W_\mu f(x,\eta)\frac{d\eta}{\eta} \equiv \lim_{\substack{\varepsilon\to 0\\ \rho\to\infty}} \int\limits_\varepsilon^\rho W_\mu f(x,\eta)\frac{d\eta}{\eta} = \tilde{c}_\mu f(x), \quad \forall f \in L_2(\mathbb{R}^n),$$

where the limit is interpreted in the L_2-norm.

Proof. Let

$$f_{\varepsilon,\rho}(x) = \int\limits_\varepsilon^\rho W_\mu f(x,\eta)\frac{d\eta}{\eta}, \qquad 0 < \varepsilon < \rho < \infty; \quad f \in L_1 \cap L_2.$$

By employing the Fourier transform and the Fubini theorem, from (2.13) we have

$$f^{\wedge}_{\varepsilon,\rho}(y) = \int_{\varepsilon}^{\rho} \frac{d\eta}{\eta} \int_{\mathbb{R}^n \times (0,\infty)} P(z,1)\Big(\int_{\mathbb{R}^n} e^{-2\pi i x.y} f(x-\eta t z)dx\Big) dz d\mu(t)$$

(we replace x with $x+\eta tz$)

$$= f^{\wedge}(y) \int_{\varepsilon}^{\rho} \frac{d\eta}{\eta} \int_{\mathbb{R}^n \times (0,\infty)} P(z,1) e^{-2\pi i (z.y)\eta t} dz d\mu(t)$$

$$\overset{(2.1)}{=} f^{\wedge}(y) \int_{\varepsilon}^{\rho} \frac{d\eta}{\eta} \int_{0}^{\infty} e^{-\pi \eta t |y|} d\mu(t) \quad (\text{put } \eta = s/\pi|y|)$$

$$= f^{\wedge}(y) \int_{\varepsilon\pi|y|}^{\rho\pi|y|} \frac{ds}{s} \int_{0}^{\infty} e^{-st} d\mu(t) = f^{\wedge}(y) \int_{\varepsilon\pi|y|}^{\rho\pi|y|} \tilde{\mu}(s) \frac{ds}{s}.$$

Setting $k_{\varepsilon,\rho}(y) = \int_{\varepsilon\pi|y|}^{\rho\pi|y|} \tilde{\mu}(s)\frac{ds}{s}$, we have

$$f^{\wedge}_{\varepsilon,\rho}(y) = f^{\wedge}(y) k_{\varepsilon,\rho}(y). \tag{3.1}$$

Since $\tilde{c}_{\mu} = \int_{0}^{\infty} \tilde{\mu}(s)\frac{ds}{s}$ is finite and the function $\int_{0}^{t} \tilde{\mu}(s)\frac{ds}{s}$ continuous on $[0,\infty)$,

$$c \overset{def}{=} \sup_{t>0} \Big| \int_{0}^{t} \tilde{\mu}(s) \frac{ds}{s} \Big|$$

is finite. Hence

$$|k_{\varepsilon,\rho}(y)| = \Big| \int_{0}^{\rho\pi|y|} \tilde{\mu}(s)\frac{ds}{s} - \int_{0}^{\varepsilon\pi|y|} \tilde{\mu}(s)\frac{ds}{s} \Big| \leq 2c. \tag{3.2}$$

Now by the Plancherel and Lebesque Dominated Convergence theorems it follows that

$$\|f_{\varepsilon,\rho} - \tilde{c}_{\mu} f\|_2 = \|f^{\wedge}_{\varepsilon,\rho} - \tilde{c}_{\mu} f^{\wedge}\|_2 \overset{(3.1)}{=} \|f^{\wedge}(k_{\varepsilon,\rho} - \tilde{c}_{\mu})\|_2 \to 0 \text{ as } \varepsilon \to 0,\ \rho \to \infty.$$

Hence, for any $f \in L_1 \cap L_2$,

$$\lim_{\substack{\varepsilon \to 0 \\ \rho \to \infty}} \|f_{\varepsilon,\rho} - \tilde{c}_{\mu} f\|_2 = 0.$$

The statement for arbitrary $f \in L_2$ follows in a standard way by using uniform $L_2 \to L_2$ boundedness of the family of linear operators $A_{\varepsilon,\rho} f \equiv f_{\varepsilon,\rho}$:

$$\|A_{\varepsilon,\rho} f\|_2 = \|f_{\varepsilon,\rho}\|_2 = \|f^{\wedge}_{\varepsilon,\rho}\|_2 = \|f^{\wedge} k_{\varepsilon,\rho}\|_2 \overset{(3.2)}{\leq} 2c\|f^{\wedge}\|_2 = 2c\|f\|_2,$$

that is $\|A_{\varepsilon,\rho} f\|_2 \leq 2c\|f\|_2,\ \forall\, f \in L_1 \cap L_2$.

The General case follows by density. □

The following result gives a L_p-version of the Calderón-type reproducing formula for arbitrary $p \geq 1$.

3.2. Theorem. *Let $f \in L_p(\mathbb{R}^n)$, $1 \le p \le \infty$ ($L_\infty \equiv C^0$- the space of continuous functions vanishing at infinity). Let μ be a finite (signed) Borel measure on $\mathbb{R}^1$ such that*

$$\mu(\mathbb{R}^1) = 0,\ \mu(\{0\}) = 0,\ \ \operatorname{supp}\mu \subset [0,\infty) \quad \textit{and} \quad \int_0^\infty |\log t| d|\mu|(t) < \infty,$$

then

$$\int_0^\infty W_\mu f(x,\eta)\frac{d\eta}{\eta} \equiv \lim_{\varepsilon\to 0}\int_\varepsilon^\infty W_\mu f(x,\eta)\frac{d\eta}{\eta} = c_\mu f(x)\,, \tag{3.3}$$

where

$$c_\mu = \int_0^\infty \log\frac{1}{t} d\mu(t),$$

the limit being with respect to the L_p-norm ($1 \le p < \infty$), or taken pointwise for almost all $x \in \mathbb{R}^n$. In the case $p = \infty$ it is assumed that $L_\infty = C^0$ and the limit is understood in the sup-norm.

Proof. We need the following modification of the wavelet-type transform $W_\mu f$.

$$W_\mu f(x,\eta) = \int\limits_{\mathbb{R}^n\times(0,\infty)} P(y,t) f(x-\eta y)dy\, d\mu(t)$$

(we put $y = (1/\eta)z$, $dy = (1/\eta)^n dz$ and use (2.3))

$$= \int_0^\infty \Big(\int_{\mathbb{R}^n} P(z,\eta t) f(x-z)dz\Big) d\mu(t) \overset{(2.5)}{=} \int_0^\infty P_{t\eta} f(x)\, d\mu(t). \tag{3.4}$$

Let

$$V_\varepsilon f(x) = \int_\varepsilon^\infty W_\mu f(x,\eta)\frac{d\eta}{\eta}, \quad \varepsilon > 0. \tag{3.5}$$

Then, by using (3.4) and the Fubini theorem, we have

$$V_\varepsilon f(x) = \int_\varepsilon^\infty \Big(\int_0^\infty P_{t\eta} f(x)\, d\mu(t)\Big)\frac{d\eta}{\eta} = \int_0^\infty \Big(\int_\varepsilon^\infty P_{t\eta} f(x)\,\frac{d\eta}{\eta}\Big) d\mu(t)$$

$$= \int_0^\infty \Big(\int_{\varepsilon t}^\infty P_s f(x)\,\frac{ds}{s}\Big) d\mu(t) = \int_0^\infty \Big(\frac{1}{s}\int_0^{s/\varepsilon} d\mu(t)\Big) P_s f(x)\, ds. \tag{3.6}$$

Setting $k(s) = \frac{1}{s}\int\limits_0^s d\mu(t)$ and $k_\tau(s) = \frac{1}{\tau}k(s/\tau)$, we have $k_\tau(s) = \frac{1}{s}\int\limits_0^{s/\tau} d\mu(t)$ and therefore, $\frac{1}{s}\int\limits_0^{s/\varepsilon} d\mu(t) = k_\varepsilon(s)$. Making use of this in (3.6) we have

$$V_\varepsilon f(x) = \int_0^\infty k_\varepsilon(s) P_s f(x) ds. \tag{3.7}$$

By setting $\tilde{c}_\mu = \int\limits_0^\infty k(s)\,ds$ (which is finite and equal to $c_\mu \equiv \int\limits_0^\infty \log\frac{1}{\tau} d\mu(\tau)$ by Lemma 2.5), and using Minkowski inequality we have

$$\begin{aligned}\|V_\varepsilon f(x) - \tilde{c}_\mu f(x)\|_p &= \Big\| \int\limits_0^\infty k_\varepsilon(s) P_s f(x) ds - \int\limits_0^\infty k(s) f(x) ds \Big\|_p \\ &= \Big\| \int\limits_0^\infty k(s) P_{s\varepsilon} f(x) ds - \int\limits_0^\infty k(s) f(x) ds \Big\|_p \\ &\le \int\limits_0^\infty |k(s)| \|P_{s\varepsilon} f(x) - f(x)\|_p ds.\end{aligned}$$

From (2.6), (2.8) and Lebesgue's convergence theorem it follows that the last expression tends to zero as $\varepsilon \to 0$. For similar reasons the convergence is uniform for $f \in C^0$.

It remains to show the pointwise (a.e) convergence in (3.3). For $f \in L_p,\ (1 \le p < \infty)$, we have

$$\begin{aligned}|V_\varepsilon f(x)| &\le \int\limits_0^\infty |k_\varepsilon(s)||P_s f(x)| ds \\ &\le \sup_{s>0} |P_s f(x)| \int\limits_0^\infty |k_\varepsilon(s)| ds = c \cdot \sup_{s>0} |P_s f(x)|, \qquad (3.8)\end{aligned}$$

where $c = \int\limits_0^\infty |k_\varepsilon(s)| ds = \int\limits_0^\infty |k(s)| ds < \infty$ by Lemma 2.5. From (3.8) and (2.9) it follows that for any $\lambda > 0$

$$\text{meas}\{\, x \in \mathbb{R}^n : \sup_{\varepsilon>0} |V_\varepsilon f(x)| > \lambda\} \le c_1 . \text{meas}\{x \in \mathbb{R}^n : M_f(x)| > \lambda\} \le \Big(c_2 \frac{\|f\|_p}{\lambda}\Big)^p.$$

Thus the maximal operator $\sup\limits_{\varepsilon>0} |V_\varepsilon f(x)|$ is of weak (p,p)-type. Now by employing Lemma 2.6 and keeping in mind that $V_\varepsilon f(x) \to \tilde{c}_\mu f(x)$ pointwise as $\varepsilon \to 0$ for any $f \in C^0$ (this class of functions is dense in $L_p,\ (1 \le p < \infty)$), we obtain for any $f \in L_p$ that $V_\varepsilon f(x) \to \tilde{c}_\mu f(x)$ a.e. as $\varepsilon \to 0$. To complete the proof of the theorem it remains only to recall that

$$\tilde{c}_\mu = c_\mu \equiv \int\limits_0^\infty \log\frac{1}{s} d\mu(s) \quad \text{(see Lemma 2.5)}.$$

□

References

[1] Aliev, I. A. and Rubin, B. *Parabolic wavelet transforms and Lebesgue spaces of parabolic potentials*, Rocky Mountain Journal of Math. **32** No 2, 391–408, 2002.

[2] Aliev, I. A. and Eryigit, M. *Inversion of Bessel Potentials with the aid of weighted wavelet transforms*, Math. Nachrichten. **242**, 27–37, 2002.

[3] Frazier, M., Jawerth B. and Weiss G. *Littlewood-Paley theory and the study of function spaces*, CBMS Reg. Conf. Ser. in Math. No. 79 (Amer. Math. Soc., Providence, R.I., 1991).

[4] Meyer, Y. *Wavelet and operators*, (Univ. Press, Cambridge, 1992).

[5] Rubin, B. *Fractional Integrals and Potentials*, (Addison Wesley Longman, Essex U. K., 1996).

[6] Rubin, B. *The Calderón reproducing formula, windowed X–Ray transforms and Radon transforms in L^p–spaces*, The Journal of Fourier Anal. and Appl. **4** No 2, 175–197, 1998.
[7] Stein, E. M. and Weiss G. *Introduction to Fourier analysis on Euclidean spaces*, (Princeton Univ. Press, Princeton N. J., 1971).

Hacettepe Journal of Mathematics and Statistics
Volume 33 (2004), 31 – 50

GRINDING FROM THE MATHEMATICAL POINT OF VIEW

Georgi V. Smirnov*

Received 02 : 07 : 2004 : Accepted 17 : 12 : 2004

Abstract

A rigorous mathematical description of grinding processes used in powder technologies is developed. A grinding equation, an operator equation, connecting the final particle size distribution function to the particle size distribution function before the grinding process is studied. The mathematical model introduced here can be used to predict the results of grinding, to construct grinding systems with desired properties, and to improve the particle size measurement.

Keywords: Grinding equation, Operator equation, Particle size distribution function.

2000 AMS Classification: 45 N 05, 47 B 38, 47 G 10.

1. Introduction

Powder technologies have many industrial applications in powder coating [5] and pharmaceutics [6], for example. The powder production is based on the use of special grinding systems [3]. The aim of this work is to develop a rigorous mathematical description of grinding processes.

Any grinding system contains grinders and classifiers. The grinder is responsible for the particle size reduction and the classifier separates small particles and takes them out from the grinder. These two principal elements of grinding systems can be described in terms of operators defined in spaces of particle size distribution functions. This allows to derive a grinding equation, an operator equation, connecting the grinding system 'output', the final particle size distribution, to the 'input', the particle size distribution before the grinding process. This mathematical model can be used to predict the results of grinding, to construct grinding systems with desired properties, and to improve the particle size measurement.

The paper is organized as follows. In the second section an informal outline of the approach is presented. The third section is devoted to geometric partition models and

*Centro de Matemática da Universidade do Porto, Departamento de Matemática Aplicada, Faculdade de Ciências, Universidade do Porto, Rua do Campo Alegre 687, 4169-007 Porto, Portugal. E-mail : gsmirnov@fc.up.pt

moment analysis. The partition operator and the classifier are studied in the fourth section. The fifth section deals with the grinding equation. Finally, the last section contains concluding remarks.

2. Informal Outline of the Approach

Consider a set of particles. Let $\nu(V)dV$ be the number of particles with the volumes in the interval $[V, V + dV]$. The density function f for the random value V(the particle volume) is given by

$$f(V) = \frac{\nu(V)}{\int_0^\infty \nu(V)dV}. \tag{1}$$

2.1. Partition operator. Suppose that a particle with the volume V is divided into n parts with the volumes $\xi_k V$, $k = \overline{1,n}$, where

$$\bar{\xi} = (\xi_1, \ldots, \xi_n) \in \Xi = \{(\xi_1, \ldots, \xi_n) \mid \xi_k \geq 0,\ \xi_1 + \ldots + \xi_n = 1\}.$$

Let the probability of getting particles with the volumes belonging to the intervals $[\xi_k V, (\xi_k + d\xi_k)V]$ be $\phi(\bar{\xi})d\bar{\xi}$, where $\phi : \Xi \to \mathbb{R}$ is a symmetric density function. Denote by $\mathcal{P}(f)$ the density function for the particle volume after the partition. Obviously

$$\mathcal{P}(f)(V)dV = \frac{\mathcal{P}(\nu)(V)dV}{\int_0^\infty \mathcal{P}(\nu)(V)dV}, \tag{2}$$

where $\mathcal{P}(\nu)(V)dV$ stands for the number of particles with the volumes in the interval $[V, V + dV]$ after the partition. Observe that the number $\mathcal{P}(\nu)(V)dV$ can be written as a superficial integral

$$\mathcal{P}(\nu)(V)dV = \int_\Xi \sum_{k=1}^n \nu\left(\frac{V}{\xi_k}\right) d\left(\frac{V}{\xi_k}\right) \phi(\bar{\xi})dS_{\bar{\xi}}.$$

Dividing this equality by

$$\int_0^\infty \mathcal{P}(\nu)(V)dV = n\int_0^\infty \nu(V)dV$$

and invoking (1) and (2), we get

$$\mathcal{P}(f)(V) = \frac{1}{n}\int_\Xi \sum_{k=1}^n f\left(\frac{V}{\xi_k}\right) d\left(\frac{V}{\xi_k}\right) \phi(\bar{\xi})dS_{\bar{\xi}}.$$

Since the function ϕ is symmetric, we obtain

$$\mathcal{P}(f)(V) = \int_0^1 f\left(\frac{V}{\eta}\right) \psi(\eta)\, d\eta, \tag{3}$$

where

$$\psi(\eta) = \frac{1}{\eta}\int_{\Xi_\eta} \phi(\eta, \xi_2, \ldots, \xi_n)dS_{\tilde{\xi}},$$

and

$$\Xi_\eta = \{\tilde{\xi} = (\xi_2, \ldots, \xi_n) \mid \xi_k \geq 0,\ \eta + \xi_2 + \ldots + \xi_n = 1\}.$$

Obviously

$$\int_0^1 \eta\psi(\eta)\, d\eta = \int_\Xi \phi(\bar{\xi})dS_{\bar{\xi}} = 1. \tag{4}$$

Thus equation (3) gives a general form of the partition operator. The function ψ satisfying (4) can be found experimentally or derived theoretically from partition models.

2.2. Two types of grinding. Classifier. The grinding process can be modelled as a successive application of the partition operator given by (3):

$$f_{\text{out}} = \mathcal{P}^N(f_{\text{in}}),$$

where f_{out} and f_{in} stand for the the final particle size density function and the initial particle size density function, respectively. During this process the particles do not leave the grinder. If, for example, $\psi(\eta) = 2\delta(\eta - 1/2)$, then all particles are divided into two equal parts independently on their shapes. Consider the input density function

$$f_{\text{in}}(V) = \begin{cases} (aV^{a-1}/b^a)e^{-(x/b)^a}, & x \geq 0, \\ 0, & x < 0, \end{cases}$$

known as the Rosin-Rammler density function [1]. Then we have

$$f_{\text{out}}(V) = 2^N f_{\text{in}}\left(2^N V\right),$$

that is, the output is again a Rosin-Rammler density function with a new parameter b. Obviously, this density function can be used to describe particle sizes only in this special case $\psi(\eta) = 2\delta(\eta - 1/2)$.

Another type of grinding includes a separation process. A special device, known as classifier, separates small particles and takes them out from the grinder. To model this separation introduce a classifier operator $\mathcal{C}_\alpha$, $\alpha > 0$, defined by

$$\mathcal{C}_\alpha(f)(V) = c_\alpha(V)f(V),$$

where

$$c_\alpha(V) = \begin{cases} 0, & V < \alpha, \\ 1, & V \geq \alpha. \end{cases}$$

The physical meaning of the parameter α is very simple. If $V < \alpha$, then the particle leaves the grinder. The grinding process with classification can be represented in the following form

$$f_{\text{out}} = \sum_{k=0}^{\infty} (\mathcal{I} - \mathcal{C}_\alpha)(\mathcal{P} \circ \mathcal{C}_\alpha)^k(f_{\text{in}}),$$

where $\mathcal{I}$ is the identity operator.

2.3. Grinding equation. Equivalently the output can be written as

$$f_{\text{out}} = (\mathcal{I} - \mathcal{C}_\alpha)(g), \tag{5}$$

where

$$g = \sum_{k=0}^{\infty} (\mathcal{P} \circ \mathcal{C}_\alpha)^k(f_{\text{in}}). \tag{6}$$

Applying (formally) the operator $(\mathcal{I} - \mathcal{P} \circ \mathcal{C}_\alpha)$ to (6), we obtain the grinding equation

$$g = \mathcal{P} \circ \mathcal{C}_\alpha(g) + f_{\text{in}}. \tag{7}$$

Using (3) the grinding equation (7) can be written in the integral form

$$g(V) = \int_0^1 c_\alpha\left(\frac{V}{\eta}\right) g\left(\frac{V}{\eta}\right) \psi(\eta)\, d\eta + f_{\text{in}}(V) = \int_0^{V/\alpha} g\left(\frac{V}{\eta}\right) \psi(\eta)\, d\eta + f_{\text{in}}(V). \tag{8}$$

From (5) we have

$$f_{\text{out}}(V) = g(V), \quad V < \alpha.$$

Therefore (8) implies

$$f_{\text{out}}(V) = \int_0^{V/\alpha} g\left(\frac{V}{\eta}\right)\psi(\eta)\,d\eta + f_{\text{in}}(V), \quad V < \alpha. \tag{9}$$

It is easy to see that the integral in (9) depends only on the values $g(V)$, with $V \in [\alpha, \infty[$. Hence to find the output from (9) it suffices to solve integral equation (8) in the interval $[\alpha, \infty[$, that is, to solve the equation

$$g(V) = \int_0^1 g\left(\frac{V}{\eta}\right)\psi(\eta)\,d\eta + f_{\text{in}}(V), \quad V \geq \alpha. \tag{10}$$

2.4. Connection with the integro-differential batch grinding equation. It turns out that the grinding equation can be easily obtained from existing comminution models. The fundamental equation of fragmentation, known as the batch grinding equation, has the form

$$\frac{\partial f(V,t)}{\partial t} = -s(V)f(V,t) + \int_V^\infty b(V,W)s(W)f(W,t)dW, \tag{11}$$

where $f(V,t)$ is the size density function at the moment t, $b(V,W)$ is the breakage function, giving the fraction of particles with volumes in the range $[V, V+dV]$ obtained by breakage of a particle of volume W, and $s(V)$ is the breakage rate of particles of volume V (see [8], for example). This is a simple balance law similar to that of population dynamics. Equation (11) is in a good agreement with the experimental data [7].

Integrating equation (11) and setting

$$g(V) = s(V)\int_0^\infty f(V,t)dt,$$

we get

$$\lim_{t\to\infty} f(V,t) + g(V) = \int_V^\infty b(V,W)g(W)dW + f(V,0).$$

All known breakage functions have the form

$$b(V,W) = \psi\left(\frac{V}{W}\right)\frac{V}{W^2}.$$

(This structure of b was confirmed by numerous experiments [7].) After the change of variables $\eta = V/W$ in the integral we obtain

$$\lim_{t\to\infty} f(V,t) + g(V) = \int_0^1 g\left(\frac{V}{\eta}\right)\psi(\eta)\,d\eta + f(V,0). \tag{12}$$

Assume that $s(V) = 0$, whenever $V < \alpha$. Then we have

$$\lim_{t\to\infty} f(V,t) = \int_0^{V/\alpha} g\left(\frac{V}{\eta}\right)\psi(\eta)\,d\eta + f(V,0), \quad V < \alpha. \tag{13}$$

Since $\lim_{t\to\infty} f(V,t) = 0$ whenever $V \geq \alpha$, equation (12) implies

$$g(V) = \int_0^1 g\left(\frac{V}{\eta}\right)\psi(\eta)\,d\eta + f(V,0), \quad V \geq \alpha. \tag{14}$$

Equalities (13) and (14) coincide with (9) and (10), respectively. This is, probably, the easiest way to derive the grinding equation, although the structure of the partition operator must be postulated.

The batch grinding integro-differential equation describes distribution at any stage of the grinding process and contains the breakage rate function $s(V)$. Theoretical or experimental determination of this function causes serious difficulties. Equations (13) and (14) do not contain $s(V)$ and are more suitable to predict the final distribution, for

any given feed distribution. Since system (13) and (14) is a consequence of (11), it does not contradict the experimental data.

2.5. Geometric partition models. The fragmentation of a particle in the grinder obviously depends on the particle shape. For the sake of simplicity assume that there exists only a finite number M of shapes and any particle of the shape $m = \overline{1, M}$ is divided into at most two particles of shapes $m' = \overline{1, M}$ and $m'' = \overline{1, M}$. Such a partition model can be obtained using some approximation rules. For example, if we have only spherical particles (M=1), then any particle is divided into two particles (obviously non-spherical) with volumes V_1 and V_2. To form a one-shape partition model we have to approximate the new particles by spheres with volumes V_1 and V_2. The partition model can be completely artificial or based on a physical hypothesis. The shape set should be chosen to be rather simple, a finite number of ellipsoids or polyhedrons, for example. Consider one possible partition model. The dust is formed by ellipsoids of shapes $m = \overline{1, M}$. If the particle is sufficiently small, the geometry of the grinder is not important. Any fragmentation can be seen as a result of collision of a particle with an infinite rigid plane Π_0. An ellipsoid-shaped particle E is divided into two particles by a plane Π containing the normal vector to the plane Π_0 at the point of collision $\Pi_0 \cap E$, and such that the area of the ellipse $E \cap \Pi$ is minimal. This hypothesis is quite natural: in this case the energy needed to divide the particle is the minimal one. Each of the new particles is approximated by ellipsoids E' and E'' of shapes $m' = \overline{1, M}$ and $m'' = \overline{1, M}$, respectively. If V is the volume of the ellipsoid E, then the ellipsoids E' and E'' have volumes V' and V'' satisfying $V = V' + V''$. To model the grinding process it suffices to consider only a finite number of possible orientations $l = \overline{1, L}$, of the particles with respect to the plane Π_0. For example, the normal vector to the plane Π_0 at the point of collision $\Pi_0 \cap E$ is parallel to one of the ellipsoid axes.

A geometric partition model can be described by a finite number of rules

$$\mathcal{R}(m, l) = (m'(m, l), m''(m, l), \gamma), \ m = \overline{1, M}, \ l = \overline{1, L},$$

which establish a correspondence between a pair (m, l) (shape and orientation) and a pair of new shapes m' and m'', and the ratio of the volumes $\gamma = V'/V''$, $0 \le V' \le V''$. Obviously

$$V' = \frac{\gamma}{1+\gamma} V \text{ and } V'' = \frac{1}{1+\gamma} V. \tag{15}$$

If a particle of the shape m with the orientation l is not divided, we use the rule $\mathcal{R}(m, l) = (0, m, 0)$. Three simple illustrative examples of geometric partition models are considered in the next section. If the number of shapes M and of orientations L are big enough, one can get a partition model close to reality.

Let $\nu_m(V)dV$ be the number of particles of the shape m with the volumes in the interval $[V, V + dV]$. Consider the functions f_m, $m = \overline{1, M}$, given by

$$f_m(V) = \frac{\nu_m(V)}{\sum_{n=1}^{M} \int_0^\infty \nu_n(V)dV}.$$

Put

$$\mathcal{P}(f_m)(V) = \frac{\mathcal{P}(\nu_m)(V)}{\sum_{n=1}^{M} \int_0^\infty \mathcal{P}(\nu_m)(V)dV},$$

where $\mathcal{P}(\nu_m)(V)dV$ stands for the number of particles with the shape m and the volumes in the interval $[V, V+dV]$, after the partition. Assume that all orientations of the particles with respect to the plane Π_0 are equally likely. This is a natural assumption in the case of non-isotropic materials. (If materials with a crystalline structure are considered, then

it is necessary to introduce corresponding probabilities of the orientations.) Using (15) we have

$$\mathcal{P}(\nu_k)(V)dV = \frac{1}{L}\sum_{l=1}^{L}\sum_{(m,\theta)\in N(k,l)}\nu_m(\theta V)d(\theta V), \tag{16}$$

where

$$N(k,l) = \{(m,\theta) \mid \mathcal{R}(m,l) = (k,n,1/(\theta-1)) \text{ or } \mathcal{R}(m,l) = (n,k,\theta-1)\}.$$

Set

$$\tau(m,l) = \begin{cases} 1, & m'(m,l) = 0, \\ 2, & m'(m,l) \neq 0. \end{cases}$$

Assume that their exists a number τ satisfying

$$\tau = \frac{1}{L}\sum_{l=1}^{L}\tau(m,l), \quad m = \overline{1,M}. \tag{17}$$

For example, if all particles are divided into two parts, then this condition is satisfied and $\tau = 2$. Since

$$\sum_{n=1}^{M}\int_0^\infty \mathcal{P}(\nu_n)(V)dV = \tau\sum_{n=1}^{M}\int_0^\infty \nu_n(V)dV,$$

dividing (16) by

$$\sum_{n=1}^{M}\int_0^\infty \mathcal{P}(\nu_n)(W)dWdV,$$

we get

$$\mathcal{P}(f_k)(V) = \frac{1}{\tau L}\sum_{l=1}^{L}\sum_{(m,\theta)\in N(k,l)}\theta f_m(\theta V). \tag{18}$$

The density function f can be represented in the form

$$f(V) = \sum_{m=1}^{M} f_m(V).$$

The partition operator now takes the form

$$\mathcal{P}(f) = \sum_{m=1}^{M}\mathcal{P}(f_m), \tag{19}$$

where $\mathcal{P}(f_m)$, $m = \overline{1,M}$, are given by (18).

2.6. Moments. The partition operator given by (19) cannot be reduced to form (3). The study of moments helps to understand the relation between (19) and (3) and to develop a rigorous mathematical theory of grinding. Set

$$\mu_s^{(m)} = \int_0^\infty V^s f_m(V)dV, \text{ and}$$
$$\mathcal{P}(\mu_s^{(m)}) = \int_0^\infty V^s\mathcal{P}(f_m(V))dV, \ m = \overline{1,M}, \ s = 0,1,\ldots.$$

From (18) we have

$$\mathcal{P}(\mu_s^{(k)}) = \frac{1}{\tau L}\sum_{l=1}^{L}\sum_{(m,\theta)\in N(k,l)}\theta^{-s}\mu_s^{(m)}, \quad k=\overline{1,M}, \quad s=0,1,\dots. \tag{20}$$

Introducing column-vectors $\bar{\mu}_s$ and $\mathcal{P}(\bar{\mu}_s)$ with the components $\mu_s^{(m)}$ and $\mathcal{P}(\mu_s^{(m)})$, $m=\overline{1,M}$, respectively, equalities (20) can be written as

$$\mathcal{P}(\bar{\mu}_s) = P_s\bar{\mu}_s, \quad s=0,1,\dots, \tag{21}$$

where P_s is a $M\times M$ matrix with the elements

$$(P_s)_{km} = \frac{1}{\tau L}\sum_{l=1}^{L}\sum_{\{\theta|(m,\theta)\in N(k,l)\}}\theta^{-s}.$$

Note that (17) implies

$$\sum_{k=1}^{M}(P_0)_{km} = \frac{1}{\tau L}\sum_{l=1}^{L}\tau(m,l) = 1, \quad m=\overline{1,M},$$

that is the matrix P_0 is stochastic.

Consider the moments of the density functions f and $\mathcal{P}(f)$:

$$\mu_s = \int_0^\infty V^s f(V)dV = \sum_{m=1}^{M}\mu_s^{(m)}, \quad s=0,1,\dots,$$

and

$$\mathcal{P}(\mu_s) = \int_0^\infty V^s\mathcal{P}(f)(V)dV, \quad s=0,1,\dots.$$

If $\mathcal{P}(f)$ is given by (3), then we have

$$\mathcal{P}(\mu_s) = \nu_{s+1}\mu_s, \quad s=0,1,\dots, \tag{22}$$

where

$$\nu_s = \int_0^\infty \eta^s\psi(\eta)\,d\eta, \ \ s=0,1,\dots.$$

On the other hand, if $\mathcal{P}(f)$ is given by (19), then we obtain

$$\mathcal{P}(\mu_s) = \sum_{m=1}^{M}\mathcal{P}(\mu_s^{(m)}), \ \ s=0,1,\dots, \tag{23}$$

where $\mathcal{P}(\mu_s^{(m)})$, $m=\overline{1,M}$, are defined by (20) or, equivalently, by (21). Moment transformation (22) is a special case of (23). Indeed, if $P_s\bar{\mu}_s = \nu_{s+1}\bar{\mu}_s$, $s=0,1,\dots$, then (22) and (23) coincide.

2.7. Main objectives. The first issue we address in this paper is the construction of geometric partition models and the study of the moment sequences generated by the dominant eigenvalues λ_s of the corresponding matrices P_s, $s=0,1,\dots$.

We show that under some natural conditions the sequences $\lambda_s^{-N}P_s^N\bar{\mu}_s$ tend to eigenvectors $\hat{\bar{\mu}}_s$ of the matrices P_s as N goes to infinity. This implies that

$$\sum_{m=1}^{M}\mathcal{P}^N(\mu_s^{(m)}) \approx \lambda_s^N\mu_s,$$

whenever N is big enough, that is, after many partitions the transformation of the moments is described (approximately) by (22) and $\nu_{s+1}=\lambda_s$. This observation allows us to

obtain the partition operator representation (3) from geometrical partition models, but formula (3) should be understood in some generalized sense.

A rigorous theory of the grinding equation is the second main objective of this work. We show that the equation has a unique solution in an appropriate space.

3. Geometric Partition Models

We shall consider geometric partition models satisfying the following conditions:

(C1): The matrices P_s, $s = 0, 1, \ldots$, have the form

$$P_s = pI + \eta^s(D + \hat{P}_s),$$

where $p \in [0, 1[$, $\eta \in]0, 1]$, I is the identity matrix, D is a diagonal matrix with the elements $d_m \geq 0$ such that $\max_{m=\overline{1,M}} d_m = d_{\hat{m}} > d_m$, $m \neq \hat{m}$, $\hat{P}_s = \hat{P}(\eta_1^s, \ldots, \eta_K^s)$, $\eta_k \in]0, 1[$, $k = \overline{1, K}$, and $\hat{P}(z_1, \ldots, z_K)$ is a matrix with the elements

$$(\hat{P})_{ij} = \sum_{k=1}^{K} a_{ijk} z_k, \quad a_{ijk} \geq 0, \quad i, j = \overline{1, M}, \quad k = \overline{1, K}.$$

(C2): There exists n such that the matrices $(D + \hat{P}(z_1, \ldots, z_K))^n$ are positive, whenever $z_k > 0$, $k = \overline{1, K}$.

3.1. Examples. Here we present three simple examples of geometric partition models. All these models satisfy conditions (C1) and (C2).

Example 1 Consider a two-dimensional dust composed of ellipses

$$E = \left\{ (x, y) \in \mathbb{R}^2 \;\middle|\; \frac{x^2}{a^2} + \frac{b^2}{b^2} \leq 1 \right\}$$

of two types: $a = b$ and $a = 2b$. Assume that there are three possible orientations of the ellipses with respect to the plane (in this case the line) Π_0: the normal vector to Π_0 is parallel to the axis $0x$, to a line between the axes $0x$ and $0y$, and to the axis $0y$. The corresponding geometric partition model is described by the following rules:

$$\mathcal{R}(1, l) = (2, 2, 1), \; l = \overline{1, 3},$$

$$\mathcal{R}(2, l) = \begin{cases} (1, 1, 1), & l = 1, \\ (2, 2, \gamma), & l = 2, \\ (2, 2, 1), & l = 3, \end{cases}$$

where $\gamma \in]0, 1[$. Transformation (18) of the functions f_1 and f_2 is given by

$$\mathcal{P}(f_1)(V) = \frac{1}{6}(4 f_2(2V)),$$

$$\mathcal{P}(f_2)(V) = \frac{1}{6}(12 f_1(2V) + 4 f_2(2V) + (1 + 1/\gamma) f_2((1 + 1/\gamma)V) + \\ + (1 + \gamma) f_2((1 + \gamma)V)).$$

Formula (21) takes the form

$$\mathcal{P} \begin{pmatrix} \mu_s^{(1)} \\ \mu_s^{(2)} \end{pmatrix} = \frac{1}{6} \begin{pmatrix} 0 & 1/2^{s-1} \\ 3/2^{s-1} & 1/2^{s-1} + (\gamma/(1 + \gamma))^s + 1/(1 + \gamma)^s \end{pmatrix} \begin{pmatrix} \mu_s^{(1)} \\ \mu_s^{(2)} \end{pmatrix}$$

Condition (C1) is satisfied with $p = 0$, $\eta = 1/(1+\gamma)$, and

$$D = \begin{pmatrix} 0 & 0 \\ 0 & 1/6 \end{pmatrix}$$

Obviously condition (C2) is satisfied with $n = 2$.

Example 2 Consider a three-dimensional dust composed of ellipsoids

$$E = \left\{ (x,y,z) \in \mathbb{R}^3 \;\middle|\; \frac{x^2}{a^2} + \frac{b^2}{b^2} + \frac{z^2}{c^2} \le 1 \right\}$$

of three types: $a = b = c$, $a = b = 2c$, and $a = 2b = 2c$. Assume that there are seven possible orientations of the ellipsoids with respect to the plane Π_0: the normal vector to the plane is parallel to the lines generated by the vectors $(0,0,1)$, $(0,1,0)$, $(1,0,0)$, (ξ,ζ,η), $(-\xi,\zeta,\eta)$, $(\xi,-\zeta,\eta)$, and $(-\xi,-\zeta,\eta)$. The corresponding geometric partition model is described by the following rules:

$$\mathcal{R}(1,l) = (2,2,1),\ l = \overline{1,7},$$
$$\mathcal{R}(2,l) = (3,3,1),\ l = \overline{1,7},$$
$$\mathcal{R}(3,l) = \begin{cases} (1,1,1), & l = 1,2 \\ (3,3,1), & l = 3, \\ (2,3,\gamma), & l = \overline{4,7}, \end{cases}$$

where $\gamma \in]0,1[$. Transformation (18) of the functions f_1, f_2, and f_3 is given by

$$\mathcal{P}(f_1)(V) = \frac{1}{14}(8 f_3(2V)),$$
$$\mathcal{P}(f_2)(V) = \frac{1}{14}(28 f_1(2V) + 4(1+1/\gamma) f_3((1+1/\gamma)V)),$$
$$\mathcal{P}(f_3)(V) = \frac{1}{14}(28 f_2(2V) + 4 f_3(2V) + 4(1+\gamma) f_3((1+\gamma)V)).$$

Formula (21) takes the form

$$\mathcal{P}\begin{pmatrix} \mu_s^{(1)} \\ \mu_s^{(2)} \\ \mu_s^{(3)} \end{pmatrix} = \frac{1}{14}\begin{pmatrix} 0 & 0 & 1/2^{s-2} \\ 7/2^{s-1} & 0 & 4\left(\gamma/(1+\gamma)\right)^s \\ 0 & 7/2^{s-1} & 1/2^{s-1} + 4/(1+\gamma)^s \end{pmatrix}\begin{pmatrix} \mu_s^{(1)} \\ \mu_s^{(2)} \\ \mu_s^{(3)} \end{pmatrix}$$

In this case condition (C1) is satisfied with $p = 0$, $\eta = 1/(1+\gamma)$, and

$$D = \begin{pmatrix} 0 & 0 & 0 \\ 0 & 0 & 0 \\ 0 & 0 & 2/7 \end{pmatrix}$$

It is easy to verify that condition (C2) is satisfied and $n = 4$.

Example 3 Consider a two-dimensional dust composed of triangles with the angles

$$(\pi/3, \pi/3, \pi/3),\ (\pi/2, \pi/3, \pi/6),\ \text{and } (\pi/6, \pi/6, 2\pi/3).$$

The first and the second vertices of the triangles belong to the axis $0x$. The third vertex is in the upper half-plane. Assume that there are twelve possible orientations of the triangles with respect to the plane (line) Π_0: the angle between the axes $0x$ and the

normal vector to Π_0 is equal to $(l-1)\pi/6$, $l=\overline{1,12}$. The corresponding geometric partition model is described by the following rules:

$$\mathcal{R}(1,l)=\begin{cases}(0,1,0), & l\neq 4,8,12\\ (2,2,1), & l=4,8,12,\end{cases}$$

$$\mathcal{R}(2,l)=\begin{cases}(0,2,0), & l\neq 8,9,12\\ (2,2,1/3), & l=8,\\ (1,3,1), & l=9,\\ (2,3,1/2), & l=12,\end{cases}$$

$$\mathcal{R}(3,l)=\begin{cases}(0,3,0), & l\neq 3,4,5\\ (3,2,1/2), & l=3,5,\\ (2,2,1), & l=4.\end{cases}$$

The equality $m'(m,l)=0$ in these rules implies that the particle with the shape m and the orientation l is not divided. In this model the parameter τ is equal to $5/4$. Transformation (18) of the functions f_1, f_2, and f_3 is given by

$$\mathcal{P}(f_1)(V)=\frac{1}{15}(9f_1(V)+2f_2(2V)),$$

$$\mathcal{P}(f_2)(V)=\frac{1}{15}(12f_1(2V)+9f_2(V)+4f_2(4V)+(4/3)f_2((4/3)V)+3f_2(3V)+ \\ +4f_3(2V)+3f_3((3/2)V)),$$

$$\mathcal{P}(f_3)(V)=\frac{1}{15}(2f_2(2V)+(3/2)f_2((3/2)V)+9f_3(V)+6f_3(3V)).$$

Formula (21) takes the form

$$\mathcal{P}\begin{pmatrix}\mu_s^{(1)}\\ \mu_s^{(2)}\\ \mu_s^{(3)}\end{pmatrix}=\frac{1}{15}\begin{pmatrix}9 & 1/2^s & 0\\ 6/2^s & 9+1/4^s+(3/4)^s+1/3^s & 2/2^s+2\,(2/3)^s\\ 0 & 1/2^s+(2/3)^s & 9+2/3^s\end{pmatrix}\begin{pmatrix}\mu_s^{(1)}\\ \mu_s^{(2)}\\ \mu_s^{(3)}\end{pmatrix}$$

Condition (C1) is satisfied with $p=3/5$, $\eta=3/4$, and

$$D=\begin{pmatrix}0 & 0 & 0\\ 0 & 1/15 & 0\\ 0 & 0 & 0\end{pmatrix}$$

Obviously condition (C2) is satisfied with $n=2$.

3.2. Auxiliary results. Recall the following corollary of the Frobenius theorem [2].

3.1. Theorem. *Let A be a non-negative $M\times M$ matrix. Assume that there exists n such that the matrix A^n is positive. Then there exists a simple eigenvalue $\lambda>0$ of A (called the dominant eigenvalue of A) corresponding to an eigenvector with positive coordinates and such that $\lambda>|\lambda'|$ for any eigenvalue $\lambda'\neq\lambda$ of A.*

Let $\bar\mu=(\mu^{(1)},\dots,\mu^{(M)})\in C^M$ and $\bar\nu=(\nu^{(1)},\dots,\nu^{(M)})\in C^M$ be complex vectors. The inner product is denoted by $\langle\bar\mu,\bar\nu\rangle$. The norm is defined as $|\bar\mu|=\sum_{m=1}^M|\mu^{(m)}|$. If A is a matrix, then the transposed matrix is denoted by A^T.

Set $\bar z=(z_1,\dots,z_K)\in C^K$. From condition (C2) and Theorem 3.1 we see that the matrices $(D+\hat P(\bar z))$ and $(D+\hat P^T(\bar z))$ have a dominant eigenvalue $\mu(\bar z)$, whenever $z_k>0$, $k=\overline{1,K}$. Denote by $\hat{\bar\mu}(\bar z)$ and $\check{\bar\mu}(\bar z)$ the corresponding eigenvectors satisfying

$|\hat{\bar{\mu}}(\bar{z})| = |\check{\bar{\mu}}(\bar{z})| = 1$. If $\bar{z} = 0$, then we have $\hat{\bar{\mu}}(0) = \check{\bar{\mu}}(0) = \breve{\bar{\mu}}$, where the vector $\breve{\bar{\mu}}$ has the components $\breve{\mu}^m = 0$, $m \neq \hat{m}$, and $\breve{\mu}^{\hat{m}} = 1$ (see condition (C1)).

Suppose that $z_k > 0$, $k = \overline{1,K}$. Then the subspace $E(\bar{z}) = \{\bar{e} \mid \langle \check{\bar{\mu}}(\bar{z}),\ \bar{e}\rangle = 0\}$ satisfies $(D + \hat{P}(\bar{z}))E(\bar{z}) \subset E(\bar{z})$, and its dimension is equal to $M-1$. Consider a vector $\bar{v} = (v^{(1)}, \dots, v^{(M)}) \in C^M$. Then the linear system

$$\begin{cases} \alpha\hat{\bar{\mu}}(\bar{z}) + \bar{e} = \bar{v}, \\ \langle \check{\bar{\mu}}(\bar{z}), \bar{e}\rangle = 0 \end{cases} \tag{24}$$

has a unique solution $(\alpha(\bar{z},\bar{v}), \bar{e}(\bar{z},\bar{v}))$. The scalar $\alpha(\bar{z},\bar{v})$ can be written as

$$\alpha(\bar{z},\bar{v}) = \sum_{m=1}^{M} \alpha^{(m)}(\bar{z}) v^{(m)}. \tag{25}$$

3.2. Proposition. *The functions $\mu(\bar{z})$, $\hat{\bar{\mu}}(\bar{z})$, and $\alpha^{(m)}(\bar{z})$, $m = \overline{1,M}$, are analytic in a neighborhood of zero.*

Proof. 1. Consider the characteristic equation

$$\Delta(\mu,\bar{z}) = \det(D + \hat{P}(\bar{z}) - \mu I) = 0.$$

Obviously

$$\frac{\partial\Delta(\mu,0)}{\partial\mu}\bigg|_{\mu=d_{\hat{m}}} = -\prod_{m\neq\hat{m}} (d_m - d_{\hat{m}}) \neq 0.$$

By the Implicit Function theorem [4] the function $\mu(\bar{z})$ is analytic in a neighborhood of zero.

2. Denote by I_*, D_*, and $\hat{P}_*$ the $(M-1)\times M$ matrices obtained after the elimination of the $\hat{m}$-th row from the matrices I, D, and $\hat{P}$, respectively. Consider the equation

$$\Phi(\bar{\mu},\bar{z}) = \begin{pmatrix} (D_* + \hat{P}_*(\bar{z}) - \mu(\bar{z})I_*)\bar{\mu} \\ \sum_{m=1}^{M} \mu^{(m)} - 1 \end{pmatrix} = \begin{pmatrix} 0 \\ 0 \end{pmatrix}$$

Since

$$\det\frac{\partial\Phi(\bar{\mu},0)}{\partial\bar{\mu}}\bigg|_{\bar{\mu}=\check{\bar{\mu}}} = \pm\prod_{m\neq\hat{m}} (d_m - d_{\hat{m}}) \neq 0,$$

by the Implicit Function theorem the function $\hat{\bar{\mu}}(\bar{z})$ is analytic in a neighborhood of zero. Analogously one can prove that the function $\check{\bar{\mu}}(\bar{z})$ is analytic in a neighborhood of zero.

3. Consider the equation

$$\Phi(\alpha,\bar{e},\bar{z},\bar{v}) = \begin{pmatrix} \alpha\hat{\bar{\mu}}(\bar{z}) + \bar{e} - \bar{v}, \\ \langle \check{\bar{\mu}}(\bar{z}), \bar{e}\rangle \end{pmatrix} = \begin{pmatrix} 0 \\ 0 \end{pmatrix}.$$

Let $(\alpha_0, \bar{e}_0)$ be a solution to system (24) with $\bar{z} = 0$. Since

$$\det\frac{\partial\Phi(\alpha,\bar{e},\bar{z},\bar{v})}{\partial(\alpha,\bar{e})}\bigg|_{(\alpha,\bar{e},\bar{z},\bar{v})=(\alpha_0,\bar{e}_0,0,\bar{v})} = (-1)^{M+1} \neq 0,$$

and the functions $\hat{\bar{\mu}}(\bar{z})$ and $\check{\bar{\mu}}(\bar{z})$ are analytic in a neighborhood of zero, by the Implicit Function theorem the functions $\alpha^{(m)}(\bar{z})$ are analytic in a neighborhood of zero. □

3.3. The Condition (S). In the sequel we shall consider numerical sequences $\{q_s\}_{s\geq 0}$ satisfying the following condition:

(S): There exist an integer $\hat{s} \geq 0$ and numbers $1 > \xi_1 > \xi_2 > \ldots > 0$ such that

$$q_s = \sum_{j\geq 0} q^{(j)} \xi_j^s, \ s \geq \hat{s},$$

and the series converges absolutely.

Obviously the sum and the product of two sequences satisfying condition (S) satisfy condition (S).

3.3. Proposition. *Assume that conditions (C1) and (C2) are satisfied. Then sequences of the dominant eigenvalues λ_s of the matrices P_s and of the components of the corresponding eigenvectors $\hat{\bar{\mu}}_s$, $|\hat{\bar{\mu}}_s| = 1$, $s = 0, 1, \ldots$, satisfy condition (S). Moreover, if the components of vectors $\bar{v}_s$, $s = 0, 1, \ldots$, form sequences satisfying condition (S), then the sequence α_s of solutions to systems (24) with $\bar{v} = \bar{v}_s$, $s = 0, 1, \ldots$, satisfies condition (S).*

Proof. Since by Proposition 3.2 the functions $\mu(\bar{z})$, $\hat{\mu}^{(m)}(\bar{z})$, and $\alpha^{(m)}(\bar{z})$, $m = \overline{1, M}$, are analytic in a neighborhood of zero and

$$\lambda_s = p + \eta^s \mu(\eta_1^s, \ldots, \eta_K^s), \ \hat{\bar{\mu}}_s = \hat{\bar{\mu}}(\eta_1^s, \ldots, \eta_K^s),$$

and

$$\alpha_s = \sum_{m=1}^{M} \alpha^{(m)}(\eta_1^s, \ldots, \eta_K^s) v_s^{(m)}$$

(see (25)), we obtain the result. □

Note that in the case of Examples 1-3, using the formulae for the roots of the corresponding characteristic polynomials of the matrices P_s, we can found explicitly the representation

$$\lambda_s = p + \eta^s \sum_{m_1,\ldots,m_K} a_{m_1,\ldots,m_K} (\eta_1^{m_1} \ldots \eta_K^{m_K})^s, \ s \geq \hat{s}.$$

4. The Main Operators

In this section we give a correct definition of the partition operator and the classifier. To this end we have to introduce appropriate spaces, which are a generalization of the space of functions of bounded variation. Since the sizes of the particles forming a dust are limited, it suffices to consider particles with the volumes $V \in [0, 1]$.

4.1. The Spaces. The sequence $\{\lambda_s\}_{s=0}^{\infty}$ of the dominant eigenvalues of the matrices P_s may not be a moment sequence of a function of bounded variation. But it can be associated with an element of a larger space, which we construct as a dual space to a subspace of the space of continuous functions. Denote by $C(0, 1)$ the space of continuous functions on the interval $[0, 1]$ and by $BV(0, 1)$ the space of functions of bounded variation on the interval $[0, 1]$. Consider the space

$$X(n) = \{h(x) = a_0 + a_1 x + \ldots + a_{n-1} x^{n-1} + x^n \tilde{h}(x) \mid \tilde{h} \in C(0, 1)\}$$

with the norm

$$|h|_n = |a_0| + \ldots + |a_{n-1}| + |\tilde{h}|_{C(0,1)}.$$

It is easy to see that $X(n) \cong \mathbb{R}^n \times C(0, 1)$ is a Banach space. Its conjugate space is

$$X^*(n) \cong \mathbb{R}^n \times BV(0, 1) = \{\Psi^* = (\mu_0, \ldots, \mu_{n-1}, \tilde{\Psi}^*) \mid \mu_k \in \mathbb{R}, \ \tilde{\Psi}^* \in BV(0, 1)\},$$

and the elements $\Psi^* \in X^*(n)$ and $h \in X(n)$ satisfy the identity

$$\langle \Psi^*, h\rangle = a_0\mu_0 + \ldots + a_{n-1}\mu_{n-1} + \int_0^1 \tilde{h}(x)d\tilde{\Psi}^*(x).$$

For example, we have

$$\langle \Psi^*, x^k\rangle = \mu_k,\ k = \overline{0, n-1},\ \text{and}\ \langle \Psi^*, x^k\rangle = \int_0^1 x^{k-n}\, d\tilde{\Psi}^*(x),\ k \geq n.$$

The norm of a functional $\Psi^* \in X^*(n)$ is given by

$$|\Psi^*| = \max\left\{|\mu_0|, \ldots, |\mu_{n-1}|, \bigvee_0^1(\tilde{\Psi}^*)\right\},$$

where $\bigvee_0^1(\tilde{\Psi}^*)$ is the total variation of the function $\tilde{\Psi}^*$. Obviously $X(n+1) \subset X(n)$ and $X^*(n+1) \supset X^*(n)$.

4.1. Proposition. *Assume that the sequence $\{q_s\}_{s\geq 0}$ satisfies condition (S). Let $k \geq 0$ be an integer. Then there exists $\Psi^* \in X^*(\hat{s}+k)$ such that $q_s = \langle \Psi^*, x^{s+k}\rangle$, $s = 0, 1, \ldots$.*

Proof. The function $\tilde{\Psi}^*$ given by

$$\tilde{\Psi}^*(x) = \begin{cases} \sum_{\{j\geq 1 | \xi_j < x\}} q^{(j)}\xi_j^{\hat{s}+k}, & x \in]0,1[, \\ \sum_{j\geq 0} q^{(j)}, & x = 1, \end{cases} \tag{26}$$

belongs to the space $BV(0,1)$ (the series converges absolutely). Setting

$$\Psi^* = (q_{-k}, \ldots, q_{-1}, q_0, \ldots, q_{\hat{s}-1}, \tilde{\Psi}^*),$$

where q_{-s}, $s = \overline{1,k}$, are arbitrary numbers, we get the result. □

4.2. The Partition Operator. Suppose that functions $\Psi^*, F^* \in BV(0,1)$ are continuously differentiable, $(\Psi^*)' = \psi^*$ and $(F^*)' = f^*$. Then for any $h \in C(0,1)$ from (3) we have

$$\langle \mathcal{P}(f^*), h\rangle = \int_0^1\int_0^1 f^*\left(\frac{V}{\eta}\right)\psi^*(\eta)\, d\eta h(V)\, dV.$$

Since $\operatorname{supp} f^* \subset [0,1]$, this can be rewritten as

$$\int_0^1\int_V^1 f^*\left(\frac{V}{\eta}\right)\psi^*(\eta)\, d\eta h(V) dV = \int_0^1\int_0^\eta f^*\left(\frac{V}{\eta}\right)h(V) dV\psi^*(\eta)\, d\eta.$$

After the change of variables $V = \eta W$ we obtain

$$\langle \mathcal{P}(f^*), h\rangle = \int_0^1\int_0^1 f^*(W)\eta h(\eta W) dW\psi^*(\eta)\, d\eta = \langle \Psi^*, \phi_{F^*,h}\rangle,$$

where $\phi_{F^*,h}(\eta) = \eta\langle F^*, h_\eta\rangle$ and $h_\eta(w) = h(\eta W)$. This observation allows to give a correct definition of the partition operator $\mathcal{P}_{\Psi^*} : X^*(n) \to X^*(n)$, associated to a functional $\Psi^* \in X^*(n+1)$.

4.2. Lemma. *Consider $F^* \in X^*(n)$ and $h \in X(n)$. Then $\phi_{F^*,h} \in X(n+1)$.*

Proof. Let $F^* = (\mu_0, \ldots, \mu_{n-1}, \tilde{F}^*)$ and $h(x) = a_0 + a_1x + \ldots + a_{n-1}x^{n-1} + x^n\tilde{h}(x)$. Then we have

$$\phi_{F^*,h}(\eta) = \eta\langle F^*, h_\eta\rangle = \eta a_0\mu_0 + \ldots + \eta^n a_{n-1}\mu_{n-1} + \eta^{n+1}\int_0^1 \tilde{h}(\eta x)\, d\tilde{F}^*(x). \tag{27}$$

It suffice to prove that the function $\int_0^1 \tilde{h}(\eta x)\, d\tilde{F}^*(x)$ is continuous. Since the function $\tilde{h} : [0,1] \to \mathbb{R}$ is continuous, for any $\epsilon > 0$ there exists $\delta > 0$ such that $|\tilde{h}(x) - \tilde{h}(y)| < \epsilon$, whenever $|x - y| < \delta$. Hence if $|\eta - \xi| < \delta$, we get

$$\left| \int_0^1 (\tilde{h}(\eta x) - \tilde{h}(\xi x))\, d\tilde{F}^*(x) \right| \le \sup_{x\in[0,1]} |\tilde{h}(\eta x) - \tilde{h}(\xi x)| \bigvee_0^1 (\tilde{F}^*) < \epsilon \bigvee_0^1 (\tilde{F}^*).$$

□

Let $\Psi^* \in X^*(n+1)$, $F^* \in X^*(n)$, and $h \in X(n)$. Set

$$\langle \mathcal{P}_{\Psi^*}(F^*), h\rangle = \langle \Psi^*, \phi_{F^*,h}\rangle,$$

where $\phi_{F^*,h}(\eta) = \eta\langle F^*, h_\eta\rangle$ and $h_\eta(w) = h(\eta W)$. From Lemma 4.2 we see that this equality defines a functional $\mathcal{P}_{\Psi^*}(F^*) \in X^*(n)$.

4.3. Proposition. *The operator $\mathcal{P}_{\Psi^*} : X^*(n) \to X^*(n)$ is linear and continuous. Its norm does not exceed $|\Psi^*|_{X^*(n+1)}$.*

Proof. The linearity of this operator is obvious. Let $\Psi^* = (\lambda, \lambda_0, \ldots, \lambda_{n-1}, \tilde{\Psi}^*)$, $F^* = (\mu_0, \ldots, \mu_{n-1}, \tilde{F}^*)$, and $h(x) = a_0 + a_1 x + \ldots + a_{n-1}x^{n-1} + x^n \tilde{h}(x)$. Then using (27) we have

$$\begin{aligned} |\langle \mathcal{P}_{\Psi^*}(F^*), h\rangle| &= |\langle \Psi^*, \phi_{F^*,h}\rangle| \\ &= \left| a_0\lambda_0\mu_0 + \ldots + a_{n-1}\lambda_{n-1}\mu_{n-1} + \int_0^1\int_0^1 \tilde{h}(\eta x)\, d\tilde{F}^*(x)\, d\tilde{\Psi}^*(\eta) \right| \\ &\le |\Psi^*|_{X^*(n+1)} |F^*|_{X^*(n)} |h|_{X(n)}. \end{aligned}$$

This implies $|\mathcal{P}_{\Psi^*}| \le |\Psi^*|_{X^*(n+1)}$. □

Let $\Psi^* = (\lambda, \lambda_0, \ldots, \lambda_{n-1}, \tilde{\Psi}^*)$ and $F^* = (\mu_0, \ldots, \mu_{n-1}, \tilde{F}^*)$. Since

$$\phi_{F^*,x^s}(\eta) = \eta\langle F^*, (\eta y)^s\rangle = \eta^{s+1}\langle F^*, y^s\rangle = \eta^{s+1}\mu_s, \quad s = 0, 1, \ldots,$$

we have

$$\langle \mathcal{P}_{\Psi^*}(F^*), x^s\rangle = \langle \Psi^*, \phi_{F^*,x^s}\rangle = \langle \Psi^*, \eta^{s+1}\rangle\mu_s = \lambda_s\mu_s = \nu_{s+1}\mu_s, \quad s = 0, 1, \ldots,$$

where $\mu_s = \langle F^*, x^s\rangle$ and $\nu_s = \langle \Psi^*, x^s\rangle$, $s = 0, 1, \ldots$, that is, the operator $\mathcal{P}_{\Psi^*}$ satisfies (22).

4.3. Asymptotic behavior of the grinding process. Consider functions $f_m : [0,1] \to \mathbb{R}$, $m = \overline{1, M}$, describing the initial volume distributions of the particles with the shape m (see Section 2). Set $\bar{f}(V) = (f_1(V), \ldots, f_M(V))$. Then we have $f(V) = |\bar{f}(V)|$ and

$$\bar{\mu}_s = \int_0^1 V^s \bar{f}(V) dV.$$

Obviously

$$|\bar{\mu}_s| = \int_0^1 V^s |\bar{f}(V)| dV \le \int_0^1 f(V) dV = 1. \tag{28}$$

Below we obtain an asymptotic representation for the vectors $P_s^N \bar{\mu}_s$ when N goes to infinity. We obtain an especially interesting result if the components of the moment vectors $\bar{\mu}_s$, $s = 0, 1, \ldots$, satisfy condition (S). This take place if, for example, initially we have only particles of one shape, say shape 1, with the same volume V_0. In this case $\bar{f}(V) = (\delta(V - V_0), 0, \ldots, 0)$ and $\bar{\mu}_s = (V_0^s, 0, \ldots, 0)$.

4.4. Theorem. *Assume that conditions (C1) and (C2) are satisfied. Let p in condition (C1) be zero. Then there exists a bounded sequence $\alpha_s \geq 0$ such that*

$$P_s^N \bar{\mu}_s = (\tilde{\mu}_s \eta^s)^N (\alpha_s \hat{\bar{\mu}}_s + r_s^{(N)}), \tag{29}$$

where $|r_s^{(N)}| \leq ce^{-\tau N}$, $\tau > 0$, and $\tilde{\mu}_s = \mu(\eta_1^s, \ldots, \eta_K^s)$. Moreover, if the components of the moment vectors $\bar{\mu}_s$, $s = 0, 1, \ldots$, satisfy condition (S), then there exist $n \geq 0$, $F^* \in X^*(n)$, and $\Psi^* \in X^*(n+1)$ such that $\langle F^*, x^s \rangle = \alpha_s$ and $\langle \Psi^*, x^{s+1} \rangle = \tilde{\mu}_s \eta^s = \lambda_s$, $s = 0, 1, \ldots$.

Remark This theorem implies that $\mathcal{P}^N(f) \approx \mathcal{P}^N_{\Psi^*}(F^*)$ when N is large enough. This justifies formula (3) for the partition operator, but this formula should be understood in the general form introduced above. A knowledge of the dominant eigenvalues of the matrices P_s allows us to compute the functional Ψ^*, and therefore to find the partition operator $\mathcal{P}_{\Psi^*}$.

Proof of Theorem 4.4. Setting $\bar{v} = \bar{\mu}_s$ in (24) we see that there exist α_s and $\bar{e}_s$ such that

$$\bar{\mu}_s = \alpha_s \hat{\bar{\mu}}_s + \bar{e}_s, \tag{30}$$

$$\langle \check{\bar{\mu}}_s, \bar{e}_s \rangle = 0. \tag{31}$$

To show that the sequence α_s is bounded, suppose that there exists a subsequence s_i such that $\lim_{i\to\infty} \alpha_{s_i} = \infty$. Then multiplying (30) by $\check{\bar{\mu}}_s$, dividing by α_s, and using (31), we obtain $\langle \bar{\mu}_s, \check{\bar{\mu}}_s \rangle / \alpha_s = \langle \hat{\bar{\mu}}_s, \check{\bar{\mu}}_s \rangle$. Since $\lim_{s\to\infty} \hat{\bar{\mu}}_s = \lim_{s\to\infty} \check{\bar{\mu}}_s = \check{\bar{\mu}}$, using (28), setting $s = s_i$, and passing to the limit as i goes to infinity, we get $0 = \langle \check{\bar{\mu}}, \check{\bar{\mu}} \rangle$, a contradiction. Thus the sequence α_s is bounded. Combining (28) and (30), we see that the sequence $\bar{e}_s$ is also bounded.

Applying P_s^N to (30), we obtain (29) with

$$r_s^{(N)} = \tilde{\mu}_s^{-N} (D + \hat{P}_s)^N \bar{e}_s.$$

Since the eigenvalue $\tilde{\mu}_s$ is dominant, the modules of the eigenvalues of the linear operator $\tilde{\mu}_s^{-1}(D + \hat{P}_s)\Big|_{E_s}$, where $E_s = E(\eta_1^s, \ldots, \eta_K^S)$, are less than 1. Hence there exist norms $\|\cdot\|_s$ in $\mathbb{R}^M$ such that $\|r_s^{(N)}\|_s \leq \gamma_s^N \|\bar{e}\|_s$, $\gamma_s \in [0, 1[$, $s, N = 0, 1, \ldots$. Since there are constants c_s satisfying $|\cdot| \leq c_s \|\cdot\|_s$, $s = 0, 1, \ldots$, we see that $|r_s^{(N)}|$, $s = 0, 1, \ldots$, tend to zero as N goes to infinity. Dividing (29) by $(\tilde{\mu}_s \eta^s)^N$ and passing to the limit as N goes to infinity, we obtain

$$\lim_{N\to\infty} \tilde{\mu}_s^{-N} (D + \hat{P}_s) \bar{\mu}_s = \alpha_s \hat{\bar{\mu}}.$$

Since the components of the vectors $\bar{\mu}_s$ are non-negative, this implies that all the numbers α_s, $s = 0, 1, \ldots$, are non-negative.

Set $E = \{\bar{e} \mid \langle \check{\bar{\mu}}, \bar{e} \rangle = 0\}$. Obviously if $\bar{e} \in E$, then we have

$$|d_{\hat{m}}^{-1} D\bar{e}| \leq \gamma |\bar{e}|, \tag{32}$$

where $\gamma = \max_{m \neq \hat{m}} d_m / d_{\hat{m}} < 1$.

We show that there exists s_0 such that for all $\bar{e} \in E_s$, $s \geq s_0$ the inequality

$$|\tilde{\mu}_s^{-1}(D + \hat{P}_s)\bar{e}| \leq \frac{1+\gamma}{2} |\bar{e}|$$

holds. Suppose that there exist a subsequence s_i, $i = 1, 2, \ldots$, and a sequence $\bar{e}_{s_i} \in E_{s_i}$, $|\bar{e}_{s_i}| = 1$, such that

$$|\tilde{\mu}_{s_i}^{-1}(D + \hat{P}_{s_i})\bar{e}_{s_i}| > \frac{1+\gamma}{2}. \tag{33}$$

Without loss of generality the sequence $\bar{e}_{s_i}$ converges to a vector $\bar{e} \in E$, $|\bar{e}| = 1$. Passing to the limit in (33) as i goes to infinity, we obtain

$$|d_{\hat{m}}^{-1} D\bar{e}| \geq \frac{1+\gamma}{2}.$$

This contradicts (32). Thus we have $|r_s^{(N)}| \leq ce^{-\tau N}$, where

$$\tau = \ln \max \left\{ \frac{1+\gamma}{2}, \gamma_0, \ldots, \gamma_{s_0} \right\}$$

and

$$c = \max \left\{ \sup_{s>s_0} |\bar{e}_s|, c_0 \|\bar{e}_0\|, \ldots, c_{s_0} \|\bar{e}_{s_0}\| \right\}.$$

Assume that the components of the moment vectors $\bar{\mu}_s$, $s = 0, 1, \ldots$, satisfy condition (S). Then by Proposition 3.3 the sequences $\{\alpha_s\}_{s\geq 0}$ and $\{\lambda_s\}_{s\geq 0}$ satisfy condition S. Hence Proposition 4.1 implies the existence of $n \geq 0$, $F^* \in X^*(n)$, and $\Psi^* \in X^*(n+1)$ such that $\langle F^*, x^s \rangle = \alpha_s$ and $\langle \Psi^*, x^{s+1} \rangle = \tilde{\mu}_s \eta^s = \lambda_s$, $s = 0, 1, \ldots$. □

4.4. The Classifier. Suppose that a function $F^* \in BV(0,1)$ is continuously differentiable and $(F^*)' = f^*$. Let $\alpha \in]0,1[$. Then for any $h \in C(0,1)$ we have

$$\langle \mathcal{C}_\alpha(F^*), h \rangle = \int_\alpha^1 f^*(V) h(V)\, dV = \langle F^*, h\chi_{[\alpha,1]} \rangle,$$

where

$$\chi_{[\alpha,1]}(x) = \begin{cases} 1, & x \in [\alpha, 1], \\ 0, & x \notin [\alpha, 1]. \end{cases}$$

We use this identity to introduce a definition of the classifier operator $\mathcal{C}_\alpha : X^*(n) \to X^*(n)$.

Denote by $B(0,1)$ the space of bounded functions on the interval $[0,1]$ with the sup-norm. Consider the space

$$Y(n) = \{h(x) = a_0 + a_1 x + \cdots + a_{n-1} x^{n-1} + x^n \tilde{h}(x) \mid \tilde{h} \in B(0,1)\}$$

with the norm

$$|h|_{Y(n)} = |a_0| + \cdots + |a_{n-1}| + |\tilde{h}|_{B(0,1)}.$$

Clearly $X(n) \subset Y(n)$. For example $Y(n)$ contains all functions of the form $h(x)\chi_{[\alpha,1]}(x)$. Let $F^* \in X^*(n)$. By the Hahn-Banach theorem, F^* can be considered as an element of the dual space $Y^*(n)$ and $|F^*|_{Y^*(n)} = |F^*|_{X^*(n)}$. Consider $\alpha \in]0,1[$, $F^* \in X^*(n)$, and $h \in X(n)$. Introduce a linear operator $\mathcal{H}_\alpha : X(n) \to Y(n)$ defined by

$$\mathcal{H}_\alpha(h)(x) = x^n \tilde{h}(x) \chi_{[\alpha,1]}(x).$$

Define the classifier by

$$\langle \mathcal{C}_\alpha(F^*), h \rangle = \langle F^*, \mathcal{H}_\alpha(h) \rangle.$$

Obviously we have

$$\langle F^*, \mathcal{H}_\alpha(h) \rangle = \int_\alpha^1 \tilde{h}(x) d\tilde{F}^*(x).$$

4.5. Proposition. *The operator $\mathcal{C}_\alpha : X^*(n) \to X^*(n)$ is linear and continuous. Its norm is less than or equal to one.*

Proof. The linearity of this operator is obvious. Let $F^* = (\mu_0, \dots, \mu_{n-1}, \tilde{F}^*)$ and $h(x) = a_0 + a_1 x + \dots + a_{n-1}x^{n-1} + x^n \tilde{h}(x)$. Then we have

$$\begin{aligned}\big|\langle \mathcal{C}_\alpha(F*), h\rangle\big| &= \left| \int_\alpha^1 \tilde{h}(x)\, d\tilde{F}^*(x) \right| \\ &\le \sup_{x\in[\alpha,1]} |\tilde{h}(x)| \bigvee_\alpha^1 (\tilde{F}^*) \\ &\le |h|_{X(n)} |F^*|_{X^*(n)}.\end{aligned}$$

This implies $|\mathcal{C}_\alpha| \le 1$. □

5. The Grinding Equation

Let $\Psi^* \in X(n+1)$. We can write (5) and (7) as equalities in the space $X^*(n)$:

$$F^*_{\text{out}} = (\mathcal{I} - \mathcal{C}_\alpha)(G^*)$$

and

$$G^* = \mathcal{P}_{\Psi^*} \circ \mathcal{C}_\alpha(G^*) + F^*_{\text{in}}. \tag{34}$$

Applying $\mathcal{C}_\alpha$ to (34) and setting $H^* = \mathcal{C}_\alpha(G^*)$, we obtain

$$H^* = \mathcal{C}_\alpha \circ \mathcal{P}_{\Psi^*}(H^*) + \mathcal{C}_\alpha(F^*_{\text{in}}). \tag{35}$$

Applying $\mathcal{I} - \mathcal{C}_\alpha$ to (34) we have

$$F^*_{\text{out}} = \mathcal{P}_{\Psi^*}(H^*) - \mathcal{C}_\alpha \circ \mathcal{P}_{\Psi^*}(H^*) + (\mathcal{I} - \mathcal{C}_\alpha)(F^*_{\text{in}}),$$

that is, to find the output F^*_{out}, it suffices to solve equation (35).

5.1. Theorem. *Let $\Psi^* = (\lambda, \lambda_0, \dots, \lambda_{n-1}, \tilde{\Psi}^*) \in X^*(n+1)$. Assume that*

$$\lim_{\sigma\uparrow 1} \int_\sigma^1 |d\tilde{\Psi}^*| = 0. \tag{36}$$

Then there exists $m \ge 0$ such that equation (35) has one and only one solution $H^* \in X^*(n+m)$.

Proof. We show that the norm of the operator $\mathcal{C}_\alpha \circ \mathcal{P}_{\Psi^*} : X^*(n+m) \to X^*(n+m)$ is less than one, whenever m is big enough. The functional Ψ^* can be considered as an element of the space $X^*(n+m+1)$:

$$\Psi^* = \left(\lambda, \lambda_0, \dots, \lambda_{n+m-1}, \int_0^x y^m d\tilde{\Psi}^*(y)\right),$$

where $\lambda_s = \langle \Psi^*, x^{s+1}\rangle$, $s = \overline{n, n+m-1}$. Let $F^* = (\mu_0, \dots, \mu_{n+m-1}, \tilde{F}^*) \in X^*(n+m)$ and $h(x) = a_0 + \dots + a_{n+m-1}x^{n+m-1} + x^{n+m}\tilde{h}(x) \in X(n+m)$. The functional $\mathcal{P}_{\Psi^*}(F^*) \in X^*(n+m)$ is given by

$$\mathcal{P}_{\Psi^*}(F^*) = (\lambda_0\mu_0, \dots, \lambda_{n+m-1}\mu_{n+m-1}, \tilde{\Phi}^*).$$

Therefore we have

$$\langle \mathcal{P}_{\Psi^*}(F^*), h\rangle = \sum_{j=0}^{n+m-1} \lambda_j \mu_j a_j + \int_0^1 \tilde{h}(y) d\tilde{\Phi}^*(y). \tag{37}$$

The functional $\mathcal{C}_\alpha \circ \mathcal{P}_{\Psi^*}(F^*) \in X^*(n+m)$ has the form

$$\mathcal{C}_\alpha \circ \mathcal{P}_{\Psi^*}(F^*) = (0, \dots, 0, \tilde{\Phi}^*(x)\chi_{[\alpha,1]}(x)),$$

and the equality

$$\langle \mathcal{C}_\alpha \circ \mathcal{P}_{\Psi^*}(F^*), h\rangle = \int_\alpha^1 x^m \tilde{h}(x)\, d\tilde{\Phi}^*(x) \tag{38}$$

holds. Since

$$\begin{aligned}\langle \mathcal{P}_{\Psi^*}(F^*), h\rangle &= \sum_{j=0}^{n+m-1} \lambda_j \mu_j a_j + \int_0^1 \int_0^1 \eta^m \tilde{h}(\eta x)\, d\tilde{F}^*(x) d\tilde{\Psi}^*(\eta) \\ &= \sum_{j=0}^{n+m-1} \lambda_j \mu_j a_j + \int_0^1 \eta^m \int_0^\eta \tilde{h}(y)\, d\tilde{F}^*\left(\frac{y}{\eta}\right)\, d\tilde{\Psi}^*(\eta),\end{aligned}$$

from (37) and (38) we obtain

$$\begin{aligned}\int_\alpha^1 x^m \tilde{h}(x)\, d\tilde{\Phi}^*(x) &= \int_\alpha^1 \eta^m \int_\alpha^\eta \tilde{h}(y)\, d\tilde{F}^*\left(\frac{y}{\eta}\right)\, d\tilde{\Psi}^*(\eta) \\ &= \int_\alpha^1 \eta^m \int_{\alpha/\eta}^1 \tilde{h}(\eta x)\, d\tilde{F}^*(x)\, d\tilde{\Psi}^*(\eta).\end{aligned}$$

Thus we have

$$\begin{aligned}\langle \mathcal{C}_\alpha \circ \mathcal{P}_{\Psi^*}(F^*), h\rangle &= \int_\alpha^1 \eta^m \int_{\alpha/\eta}^1 \tilde{h}(\eta x)\, d\tilde{F}^*(x)\, d\tilde{\Psi}^*(\eta) \\ &\le |\tilde{h}|_{C(0,1)} \bigvee_0^1 (\tilde{F}^*) \int_\alpha^1 \eta^m |\, d\tilde{\Psi}^*(\eta)| \\ &\le |h|_{X(n+m)} |F^*|_{X^*(n+m)} \int_\alpha^1 \eta^m |\, d\tilde{\Psi}^*(\eta)|. \qquad (39)\end{aligned}$$

We have that $\lim_{m\to\infty} \int_\alpha^1 \eta^m |\, d\tilde{\Psi}^*(\eta)| = 0$. Indeed, if $\sigma \in]\alpha, 1[$, then we have

$$\begin{aligned}\int_\alpha^1 \eta^m |\, d\tilde{\Psi}^*(\eta)| &\le \sigma^m \int_\alpha^\sigma |\, d\tilde{\Psi}^*(\eta)| + \int_\sigma^1 |d\tilde{\Psi}^*(\eta)| \\ &\le \sigma^m \bigvee_\alpha^1 (\tilde{\Psi}^*) + \int_\sigma^1 |d\tilde{\Psi}^*(\eta)|. \qquad (40)\end{aligned}$$

Consider a number $\epsilon > 0$. From (36) we see that there exists $\sigma \in]\alpha, 1[$ such that the second integral in (40) is less than $\epsilon/2$. Hence sum (40) is less than ϵ, whenever m is big enough. From (39) we see that the norm of the operator $\mathcal{C}_\alpha \circ \mathcal{P}_{\Psi^*} : X^*(n+m) \to X^*(n+m)$ is less than one, if m is big enough. Therefore there exists $m \ge 0$ such that equation (35) has one and only one solution $H^* \in X^*(n+m)$. □

Consider a geometric partition model satisfying conditions (C1) and (C2). Assume that p in condition (C1) is equal to zero. Then from Proposition 4.1 we see that there exist a functional $\Psi^* \in X^*(n+1)$ such that $\lambda_s = \langle \Psi^*, x^{s+1}\rangle$, where λ_s, $s = 0, 1, \ldots$, is the sequence of the dominant eigenvalues λ_s of the matrices P_s. The condition $p = 0$ implies that $q^{(0)} = 0$ in (26). Therefore condition (36) is satisfied, and we get the following result.

5.2. Theorem. *Assume that conditions (C1) and (C2) are satisfied. Let p in condition (C1) be zero. Then there exist a functional $\Psi^* \in X^*(n+1)$ such that $\lambda_s = \langle \Psi^*, x^{s+1}\rangle$, where λ_s, $s = 0, 1, \ldots$, is the sequence of the dominant eigenvalues of the matrices P_s, and a number m such that equation (35) has one and only one solution $H^* \in X^*(n+m)$.*

The condition $p = 0$ essential in Theorems 4.4 and 5.2 is not restrictive. Indeed, if $p > 0$, then we have $\Psi^* = \Psi_0^* + p\Psi_1^*$, where $\Psi_0^* = (\lambda, \lambda_0, \dots, \lambda_{n-1}, \tilde{\Psi}_0^*)$ and $\Psi_1^* = (1, \dots, 1, \tilde{\Psi}_1^*)$. The function $\tilde{\Psi}_0^*$ satisfies condition (36) and

$$\tilde{\Psi}_1^* = \begin{cases} 0, & x \in [0, 1[, \\ 1, & x = 1. \end{cases}$$

Equation (35) takes the form

$$H^* = \mathcal{C}_\alpha \circ \mathcal{P}_{\Psi_0^*}(H^*) + p\mathcal{C}_\alpha \circ \mathcal{P}_{\Psi_1^*}(H^*) + \mathcal{C}_\alpha(F_{\text{in}}^*).$$

From this, after simple calculations we have

$$(1-p)H^* = \mathcal{C}_\alpha \circ \mathcal{P}_{\Psi_0^*}(H^*) + \mathcal{C}_\alpha(F_{\text{in}}^*).$$

Dividing by $(1-p)$, we obtain an equation with a partition operator satisfying the conditions of Theorems 4.4 and 5.2:

$$H^* = \mathcal{C}_\alpha \circ \mathcal{P}_{(1-p)^{-1}\Psi_0^*}(H^*) + (1-p)^{-1}\mathcal{C}_\alpha(F_{\text{in}}^*).$$

6. Conclusion

We have shown that the grinding process can be described in term of partition operators $\mathcal{P}_{\Psi^*}$ and classifier operators $\mathcal{C}_\alpha$ defined in the spaces $X^*(n)$. The dynamics of the grinding process is approximately described as $\mathcal{P}^N(f) \approx \mathcal{P}_{\Psi^*}^N(F^*)$ whenever N is big enough. Here $F^* \in X^*(n)$ is a generalized distribution function. This implies that the input and the output of a grinding system are related (approximately) by the grinding equation. The equation has a unique solution in an appropriate space $X^*(n)$. The study of geometric partition models, especially the study of the dominant eigenvalues of the matrices P_s, allows one to compute the functional Ψ^*, and therefore to determine the partition operator $\mathcal{P}_{\Psi^*}$.

Let us mention possible applications of the theory developed above. A grinding system can be composed of various grinders and classifiers. The grinding equation is an adequate mathematical model, which allows us to predict the results of grinding and construct grinding systems with desired properties.

An experimental verification of mathematical models describing grinding processes is rather difficult because different instruments used in particle size measurement give different results [1]. Usually sizers interpret all particles as spheres independently of the particle shapes. For example, if a sizer uses laser light scattering, then the results of the scattered radiation measurements are interpreted as the far-field diffraction pattern of an assembly of spheres. The moment analysis can help to recover the 'true' particle size distributions from the results of the measurements.

Consider a particle of volume V and the shape m having an orientation $\omega \in \Omega$, where Ω is a set of possible orientations of particles in the sizer. Assume that the sizer interprets the particle as a ball of volume $T(m, \omega)V$. Then the density function measured by the device is given by

$$f^{\text{b}}(V) = \sum_{m=1}^{M} \int_\Omega f_m\left(\frac{V}{T(m,\omega)}\right) h_m(\omega)\, d\omega,$$

where h_m are the density functions of the random value ω, the orientation of a particle of the shape m. It is easy to calculate

$$\begin{aligned}\mu_s^{\mathrm{b}} &= \int_0^\infty V^s f^{\mathrm{b}}(V) dV \\ &= \sum_{m=1}^{M} \int_\Omega \int_0^\infty V^s f_m \left(\frac{V}{T(m,\omega)} \right) dV h_m(\omega)\, d\omega \\ &= \sum_{m=1}^{M} \theta_{s+1}^{(m)} \mu_s^{(m)},\end{aligned}$$

where

$$\theta_s^{(m)} = \int_\Omega T^s(m,\omega) h_m(\omega)\, d\omega.$$

As we know from Theorem 4.4, the vector $\bar{\mu}_s$ (see (21)) approximately has the form $\bar{\mu}_s \approx \mu_s \hat{\bar{\mu}}_s$, where $\hat{\bar{\mu}}_s$ is an eigenvector of the matrix P_s with the coordinates $\hat{\mu}_s^{(m)}$, $m = \overline{1, M}$, satisfying $\sum_m \hat{\mu}_s^{(m)} = 1$. Therefore

$$\mu_s^{\mathrm{b}} = \mu_s \sum_{m=1}^{M} \theta_{s+1}^{(m)} \hat{\mu}_s^{(m)}.$$

From this we can find the moments μ_s and estimate the density function f.

Acknowledgements. The author is grateful to Nelson Oliveira and José Carlos Lopes from CIN (Portugal) for helpful discussions of the problem and bibliographical support.

References

[1] Allen, T. *Particle size measurement*, 4th edition, (Chapman and Hall, London, 1990).
[2] Gantmacher, F. R. *The Theory of Matrices*, (Chelsea, New York, 1974).
[3] Giersemehl, M. and Plihal, G. *Fine grinding system with impact classifier mill and cyclone classifier*, Powder Handling and Processing **11** (3), 1999.
[4] Hörmander, L. *An Introduction to Complex Analysis in Several Variables*, (D. van Norstrand Company, Inc., Princeton, 1966).
[5] Lambourne, R. and Strivens, T. A. Eds. *Paint and Surface Coating: Theory and Practice*, 2nd edition, (Woodhead Publishing Limited, Cambridge, 1999).
[6] Oguchi, T. and Yamamoto, K. *Recent technology of grinding and pharmaceutical technology*, J. Jpn. Soc. Pharm. Machinery Eng. **4**, 32–38, 1995.
[7] Peterson, T. W., Scotto, M. V. and Sarofim, A. F. *Comparison of comminution data with analytical solutions of the fragmentation equation*, Powder Technology **45**, 87–93, 1985.
[8] Reid, K. J. *A solution to the batch grinding equation*, Chemical Engineering Science **20**, 953–963, 1965.

Hacettepe Journal of Mathematics and Statistics
Volume 33 (2004), 51 – 56

CONTINUOUS DEPENDENCE ON THE PARAMETERS OF PHASE FIELD EQUATIONS

Şevket Gür *

Received 13 : 07 : 2004 : Accepted 27 : 10 : 2004

Abstract

Phase field equations are analyzed. It is shown that the solution of the problem considered depends continuously on changes in the parameters.

Keywords: System of equations of phase field, A priori estimates, Nonlinear equations, Continuous dependence.

2000 AMS Classification: 35 K 60, 35 B 30, 35 B 45

1. Introduction

We consider the problem

$$\tau\phi_t - \xi^2\Delta\phi + f(x,\phi) = 2u + h_1(x,t),\ (x,t) \in Q_T \tag{1}$$

$$u_t + \frac{l}{2}\phi_t = K\Delta u + h_2(x,t),\ (x,t) \in Q_T \tag{2}$$

$$\phi\,|_\Gamma = \phi_\partial(x,t),\ u\,|_\Gamma = u_\partial(x,t),\ (x,t) \in \partial\Omega \times (0,T] \tag{3}$$

$$\phi(x,0) = \phi_0(x),\ u(x,0) = u_0(x),\ x \in \Omega, \tag{4}$$

where $Q_T = \Omega \times (0,T]$, $T > 0$, $\Omega \subset \mathbb{R}^n$, $(n \geq 1)$ is a bounded domain with a sufficiently smooth boundary, $\partial\Omega$; ξ, τ, l and K are positive constants characterizing the length scale, the relaxation time, the latent heat and the thermal diffusivity, respectively. Also, $\phi_0(x)$, $u_0(x)$, $\phi_\partial(x,t)$, $u_\partial(x,t)$, $h_1(x,t)$, $h_2(x,t)$ and $f(x,s)$ are given functions.

In [1], G. Caginalp considered the following system of equations as a model describing the phase transitions with a separation surface of finite thickness:

$$\tau\phi_t = \xi^2\Delta\phi + \frac{1}{2}(\phi - \phi^3) + 2u,\ x \in \Omega,\ t \in \mathbb{R}^+ \tag{5}$$

$$u_t + \frac{l}{2}\phi_t = K\Delta u,\ x \in \Omega,\ t \in \mathbb{R}^+. \tag{6}$$

*Sakarya University, Department of Mathematics, Sakarya, Turkey.

Under the assumption $\frac{\xi^2}{\tau} < K$, a global existence theorem was proved for the classical solution of the initial boundary value problem for the system (5)-(6) with non-homogeneous Dirichlet boundary conditions of the form

$$\phi(t,x)\,|_{\partial\Omega} = \phi_\partial(x),\ u(t,x)\,|_{\partial\Omega} = u_\partial(x),\ t \in \mathbb{R}^+. \tag{7}$$

Several scientists have investigated problems based on Caginalp's model, and made a few modifications. In [2], Caginalp and Hastings investigated the existence of stationary solutions of problem (5)-(7) in $\Omega \subset \mathbb{R}^1$. In [3], C. M. Eliott and Song Mu Zheng proved the global unique solvability of initial boundary value problems for the system (5)-(6) in the class $H^2(\Omega) \times H^2(\Omega),\ \Omega \subset \mathbb{R}^n, n \le 3$, without the assumption $\frac{\xi^2}{\tau} < K$, for boundary conditions of the form (7), as well as for conditions of the form

$$\frac{\partial\phi}{\partial n}\,|_{\partial\Omega} = 0,\ \frac{\partial u}{\partial n}\,|_{\partial\Omega} = 0,\ t \in \mathbb{R}^+,$$
$$\phi\,|_{\partial\Omega} = \phi_\partial(x), \quad \frac{\partial u}{\partial n}\,|_{\partial\Omega} = 0,\ t \in \mathbb{R}^+.$$

They also studied the behaviour of the solutions of the system (5),(6) when $t \to \infty$. In [4], Kalantarov proved that the initial boundary value problem for system (5)-(6), under homogeneous boundary conditions of the form (7), is globally uniquely solvable in $C(\mathbb{R}^+, X),\ X = \overset{0}{H}{}^1(\Omega) \times \overset{0}{H}{}^1(\Omega)$, and established the existence of a global attractor. In [5], Brochet, Hilhorst and Chen investigated problem (1)-(4), considering $v = u + \frac{l}{2}\phi$, $f(s) = \sum_{j=0}^{2p-1} b_j s^j$, $b_{2p-1} > 0$, $p \ge 2$, $h_i(x,t) = 0,\ (i = 1,2)$ and homogeneous Neumann boundary conditions, proving this problem to be well posed if $(\phi_0, u_0) \in (L_2(\Omega))^2$.

2. Continuous Dependence of Solutions

We investigate the continuous dependence on the parameters $\xi,\ \tau,\ l$ and K of solutions of problem (1)–(4) in the class $V(Q_T) \times V(Q_T)$, where

$$V(Q_T) = W_2^1(Q_T) \cap \{v(x,t) : \Delta v \in L_2(Q_T)\}. \tag{8}$$

The existence of a solution to this problem can be seen from the general results of [7] and [8], but to the best of our knowledge an investigation of continuous dependence does not occur in the literature. Investigations of this type are of interest in physical problems, and can lead to useful applications.

We assume that $f(x,\phi)$ is the Caratheodory function which satisfies the local Lipschitz condition:

$$|f(x,s_1) - f(x,s_2)| \le c(1 + |s_1|^{p-1} + |s_2|^{p-1})\,|s_1 - s_2|,\ \forall\, s_1,\ s_2 \in \mathbb{R}^1, \tag{9}$$

where $p \in [1,\infty)$ if $n = 1,2$, and $p \in \left[1, \frac{n}{n-2}\right]$ if $n \ge 3$. We have used standard techniques for the calculations (cf. [6], which considers this type of question for a different problem). Let $\{\phi_1, u_1\}$ and $\{\phi_2, u_2\}$ be the solutions from $V(Q_T) \times V(Q_T)$ of the following initial-boundary value problems for different coefficients ξ_1, τ_1, l_1, K_1 and ξ_2, τ_2, l_2, K_2

respectively.

$$
\begin{aligned}
&\tau_1(\phi_1)_t - \xi_1^2\Delta\phi_1 + f(x,\phi_1) = 2u_1 + h_1(x,t),\ (x,t)\in Q_T\\
&(u_1)_t + \frac{l_1}{2}(\phi_1)_t = K_1\Delta u_1 + h_2(x,t),\ (x,t)\in Q_T\\
&\phi_1\,|_\Gamma = \phi_\partial(x,t), u_1\,|_\Gamma = u_\partial(x,t),\ (x,t)\in\partial\Omega\times(0,T]\\
&\phi_1(x,0) = \phi_0(x),\ u_1(x,0) = u_0(x),\ x\in\Omega\\
&\tau_2(\phi_2)_t - \xi_2^2\Delta\phi_2 + f(x,\phi_2) = 2u_2 + h_1(x,t),\ (x,t)\in Q_T\\
&(u_2)_t + \frac{l_2}{2}(\phi_2)_t = K_2\Delta u_2 + h_2(x,t),\ (x,t)\in Q_T\\
&\phi_2\,|_\Gamma = \phi_\partial(x,t),\ u_2\,|_\Gamma = u_\partial(x,t),\ (x,t)\in\partial\Omega\times(0,T]\\
&\phi_2(x,0) = \phi_0(x),\ u_2(x,0) = u_0(x),\ x\in\Omega.
\end{aligned}
$$

We define the difference variables ϕ, u, ξ, τ, l and K by

$$
\begin{aligned}
\phi &= \phi_1 - \phi_2, \qquad & \tau &= \tau_1 - \tau_2,\\
u &= u_1 - u_2, & l &= l_1 - l_2,\\
\xi^2 &= \xi_1^2 - \xi_2^2, & K &= K_1 - K_2
\end{aligned}
$$

Then $\{\phi, u\}$ satisfies the initial-boundary value problem:

$$\tau_1\phi_t + \tau(\phi_2)_t - \xi_1^2\Delta\phi - \xi^2\Delta\phi_2 + f(x,\phi_1) - f(x,\phi_2) = 2u, \tag{10}$$

$$u_t + \frac{l_1}{2}\phi_t + \frac{l}{2}(\phi_2)_t = K_1\Delta u + K\Delta u_2 \tag{11}$$

$$\phi\,|_\Gamma = u\,|_\Gamma = 0 \tag{12}$$

$$\phi(x,0) = u(x,0) = 0 \tag{13}$$

If we take the inner product in $L_2(\Omega)$ of (10) by $\phi_t + \phi$ and of (11) by $\frac{2\tau_1}{l_1^2}u_t + \frac{4}{l_1}u$ and then add the equations obtained, we obtain

$$
\begin{aligned}
&\tau_1\|\phi_t\|^2 + \xi_1^2\|\nabla\phi\|^2 + \frac{4K_1}{l_1}\|\nabla u\|^2 + \frac{2\tau_1}{l_1^2}\|u_t\|^2 +\\
&+ \frac{d}{dt}\left[\frac{\xi_1^2}{2}\|\nabla\phi\|^2 + \frac{2}{l_1}\|u\|^2 + \frac{\tau_1}{2}\|\phi\|^2 + \frac{\tau_1 K_1}{l_1^2}\|\nabla u\|^2\right] \le\\
\le\ &\left|\int_\Omega (f(x,\phi_1) - f(x,\phi_2))\,\phi_t dx\right| + \left|\int_\Omega (f(x,\phi_1) - f(x,\phi_2))\,\phi dx\right| +\\
&+ 2|(u,\phi)| + \frac{4|K|}{l_1}|(\Delta u_2, u)| + \frac{2\tau_1|K|}{l_1^2}|(\Delta u_2, u_t)| + \frac{\tau_1}{l_1}|(\phi_t, u_t)| +\\
&+ |\tau|\,|((\phi_2)_t, \phi_t)| + |\tau|\,|((\phi_2)_t, \phi)| + |\xi^2|\,|(\Delta\phi_2, \phi_t)| + |\xi^2|\,|(\Delta\phi_2, \phi)| +\\
&\frac{2|l|}{l_1}|((\phi_2)_t, u)| + \frac{\tau_1|l|}{l_1^2}|((\phi_2)_t, u_t)|,
\end{aligned}
\tag{14}
$$

where $\|.\|$ denotes the norm on $L_2(\Omega)$. Using (9) and Hölder's inequality, the first term on the right hand side of (14) can be estimated in the following manner:

$$\left| \int_\Omega (f(x,\phi_1) - f(x,\phi_2))\,\phi_t dx \right| \le \int_\Omega |(f(x,\phi_1) - f(x,\phi_2))|\,|\phi_t|\,dx \le$$
$$\le \int_\Omega c(1 + |\phi_1|^{p-1} + |\phi_2|^{p-1})\,|\phi|\,|\phi_t|\,dx \le$$
$$\le c\,\|\phi\|\,\|\phi_t\| + c\int_\Omega |\phi_1|^{p-1}\,|\phi|\,|\phi_t|\,dx + c\int_\Omega |\phi_2|^{p-1}\,|\phi|\,|\phi_t|\,dx \le$$
$$\le c\,\|\phi\|\,\|\phi_t\| + c\,\|\phi\|_{L_{\frac{2n}{n-2}}}\,\|\phi_t\|\left(\|\phi_1\|^{p-1}_{L_{(p-1)n}} + \|\phi_2\|^{p-1}_{L_{(p-1)n}}\right).$$

By the Sobolev imbedding theorem the following inequality holds:

$$\|\phi\|_{L_{\frac{2n}{n-2}}(\Omega)} \le c_2\,\|\nabla\phi\|\,.$$

Therefore,

$$\left| \int_\Omega (f(x,\phi_1) - f(x,\phi_2))\,\phi_t dx \right| \le c\,\|\phi\|\,\|\phi_t\| +$$
$$+ cc_2\,\|\phi_t\|\,\|\nabla\phi\|\left(\|\phi_1\|^{p-1}_{L_{(p-1)n}} + \|\phi_2\|^{p-1}_{L_{(p-1)n}}\right).$$

Since $\{\phi_i, u_i\} \in V(Q_T) \times V(Q_T)$ are fixed,

$$\|\phi_1\|^{p-1}_{L_{(p-1)n}} + \|\phi_2\|^{p-1}_{L_{(p-1)n}} \le c_1(t).$$

Hence

$$\left| \int_\Omega (f(x,\phi_1) - f(x,\phi_2))\,\phi_t dx \right| \le c\,\|\phi\|\,\|\phi_t\| + cc_1(t)c_2\,\|\phi_t\|\,\|\nabla\phi\|\,, \tag{15}$$

and similarly,

$$\left| \int_\Omega (f(x,\phi_1) - f(x,\phi_2))\,\phi dx \right| \le c\,\|\phi\|^2 + cc_1(t)c_2\,\|\phi\|\,\|\nabla\phi\|\,. \tag{16}$$

Taking into account (15) and (16), we obtain from (14)

$$\begin{aligned} & \tau_1\,\|\phi_t\|^2 + \xi_1^2\,\|\nabla\phi\|^2 + \frac{4K_1}{l_1}\,\|\nabla u\|^2 + \frac{2\tau_1}{l_1^2}\,\|u_t\|^2 + \\ & + \frac{d}{dt}\left[\frac{\xi_1^2}{2}\,\|\nabla\phi\|^2 + \frac{2}{l_1}\,\|u\|^2 + \frac{\tau_1}{2}\,\|\phi\|^2 + \frac{\tau_1 K_1}{l_1^2}\,\|\nabla u\|^2\right] \le \\ \le\ & 2\,|(u,\phi)| + \frac{4\,|K|}{l_1}\,|(\Delta u_2, u)| + \frac{2\tau_1\,|K|}{l_1^2}\,|(\Delta u_2, u_t)| + \frac{\tau_1}{l_1}\,|(\phi_t, u_t)| + \\ & + |\tau|\,|((\phi_2)_t, \phi_t)| + |\tau|\,|((\phi_2)_t, \phi)| + \left|\xi^2\right|\,|(\Delta\phi_2, \phi_t)| + \left|\xi^2\right|\,|(\Delta\phi_2, \phi)| + \\ & + \frac{2\,|l|}{l_1}\,|((\phi_2)_t, u)| + \frac{\tau_1\,|l|}{l_1^2}\,|((\phi_2)_t, u_t)| + c\,\|\phi\|\,\|\phi_t\| + \\ & + cc_1(t)c_2\,\|\phi_t\|\,\|\nabla\phi\| + c\,\|\phi\|^2 + cc_1(t)c_2\,\|\phi\|\,\|\nabla\phi\|\,. \end{aligned} \tag{17}$$

Making use of Cauchy's inequality with ε, the right hand side of (17) can be estimated. If we select the number $\varepsilon > 0$ sufficiently small then we obtain

$$\begin{aligned}
&\frac{\tau_1}{4}\|\phi_t\|^2 + \frac{4K_1}{l_1}\|\nabla u\|^2 + \frac{\tau_1}{2l_1^2}\|u_t\|^2 + \\
&\frac{d}{dt}\left[\frac{\xi_1^2}{2}\|\nabla\phi\|^2 + \frac{2}{l_1}\|u\|^2 + \frac{\tau_1}{2}\|\phi\|^2 + \frac{\tau_1 K_1}{l_1^2}\|\nabla u\|^2\right] \leq \\
\leq\ & a_1(t)\|\nabla\phi\|^2 + (\frac{3+l_1}{l_1})\|u\|^2 + a_2(t)\|\phi\|^2 + \\
&+\left[\left(\frac{\tau_1+2l_1}{2l_1^2}\right)l^2 + \left(\frac{8+\tau_1}{2\tau_1}\right)\tau^2\right]\|(\phi_2)_t\|^2 + \\
&+\left(\frac{2(\tau_1+l_1)}{l_1^2}\right)K^2\|\Delta u_2\|^2 + \left(\frac{8+\tau_1}{2\tau_1}\right)\xi^4\|\Delta\phi_2\|^2,
\end{aligned} \tag{18}$$

where,

$$a_1(t) = \frac{4c^2c_1^2(t)c_2^2}{\tau_1} \text{ and } a_2(t) = \frac{4c^2}{\tau_1} + \frac{c^2c_1^2(t)c_2^2}{4\xi_1^2} + c + 2.$$

If we set

$$c_2(t) = \max\left\{\frac{2a_1(t)}{\xi_1^2}, \frac{3+l_1}{2}, \frac{2a_2(t)}{\tau_1}, 1\right\},$$

and

$$Y(t) = \frac{\xi_1^2}{2}\|\nabla\phi\|^2 + \frac{2}{l_1}\|u\|^2 + \frac{\tau_1}{2}\|\phi\|^2 + \frac{\tau_1K_1}{l_1^2}\|\nabla u\|^2,$$

then from (18) we obtain

$$\begin{cases} \dfrac{dY(t)}{dt} \leq c_2(t)Y(t) + \left(c_3l^2 + c_4\tau^2\right)\|(\phi_2)_t\|^2 + c_4\xi^4\|\Delta\phi_2\|^2 + c_5K^2\|\Delta u_2\|^2, \\ Y(0) = 0, \end{cases}$$

where, $c_3 = \frac{\tau_1+2l_1}{2l_1^2}$, $c_4 = \frac{8+\tau_1}{2\tau_1}$ and $c_5 = \frac{2(\tau_1+l_1)}{l_1^2}$. According to Gronwall's lemma, we have

$$\begin{aligned}
Y(t) \leq \exp\left\{\int_0^T c_2(s)ds\right\}\Big\{&(c_3l^2 + c_4\tau^2)\|(\phi_2)_t\|^2_{L_2(Q_T)} + \\
&+c_4\xi^4\|\Delta\phi_2\|^2_{L_2(Q_T)} + c_5K^2\|\Delta u_2\|^2_{L_2(Q_T)}\Big\}.
\end{aligned} \tag{19}$$

Since $\{\phi_i, u_i\} \in V(Q_T) \times V(Q_T)$, we have

$$\begin{aligned}
&\|(\phi_2)_t\|^2_{L_2(Q_T)} \leq C, \\
&\|\Delta\phi_2\|^2_{L_2(Q_T)} \leq C, \text{ and} \\
&\|\Delta u_2\|^2_{L_2(Q_T)} \leq C.
\end{aligned}$$

If we set

$$\max\{c_3C, c_4C, c_4C, c_5C\} = C_6$$

and

$$C_6\exp\left\{\int_0^T c_2(s)ds\right\} = C_7$$

then from (19) we have

$$Y(t) \leq C_7 \left[K^2 + \xi^4 + \tau^2 + l^2\right]$$

Hence we have proved the following theorem.

2.1. Theorem. *Assume that (9) is satisfied. Then the solution of problem (1)-(4) from* $V(Q_T) \times V(Q_T)$ *depends continuously on the parameters* ξ, τ, l *and* K. *Moreover,*

$$\|\phi_1 - \phi_2\|^2_{C\left(0,T;W_2^1(\Omega)\right)} \leq C_7 \left[(K_1 - K_2)^2 + (\xi_1 - \xi_2)^4 + (\tau_1 - \tau_2)^2 + (l_1 - l_2)^2\right],$$

and

$$\|u_1 - u_2\|^2_{C\left(0,T;W_2^1(\Omega)\right)} \leq C_7 \left[(K_1 - K_2)^2 + (\xi_1 - \xi_2)^4 + (\tau_1 - \tau_2)^2 + (l_1 - l_2)^2\right].$$

References

[1] Caginalp, G. *An analysis of a phase field model of a free boundary*, Arch. Rat. Mech. Anal. **92**, 205–245, 1986.

[2] Caginalp, G. and Hastings, S. *Properties of some ordinary differential equations related to free boundary problems*, Proc. Roy. Soc. Edinburgh **104** A, 217–234, 1986.

[3] Elliot, C. M. and Zheng, S. M. *Global existence and stability of solutions to the phase field equations*, in: *Free boundary value problems*, Internat. Ser. Number. Math. **95**, Birkhause, Basel, 46–58, 1990.

[4] Kalantarov, V. K. *On the minimal global attractor of a system of phase field equations*, Zap. Nauchn. Semin. LOMI **188**, 70–86, 1991.

[5] Brochet, D., Hilhorst, D. and Chen, X. *Finite dimensional exponential attractor for the phase field model*, Appl. Analysis **49**, 197–212, 1993.

[6] Payne, L. E. and Straughan, B. *Convergence and continuous dependence for the Birkman-Forchmeier equations*, Studies in applied mathematics **102**, 419–439, 1999.

[7] Soltanov, K. N. *On nonlinear equations of the form* $F(x, u, Du, \Delta u) = 0$, Russian Acad. Sic. Sb. Math. **80** no:2, 367–3923, 1995.

[8] Soltanov, K. N. *Some imbedding theorems and nonlinear differential equations*, Trans. Acad. Sci. Azerb. Ser. Phys.-Tech. Math. Sci. **19**, 125–146, 1999.

Hacettepe Journal of Mathematics and Statistics
Volume 33 (2004), 57 – 67

NONPARAMETRIC CONTROL CHARTS BASED ON MAHALANOBIS DEPTH

Canan Hamurkaroğlu*, Mehmet Mert* and Yasemin Saykan*

Received 22 : 01 : 2003 : Accepted 23 : 02 : 2004

Abstract

This study concerns the use of r and Q control charts based on data depth to control process involving multivariate quality measurements. In this paper, firstly the concept of data depth is introduced in order to construct quality control chart structures, the characteristics of data depth are given and statistics based on this concept are obtained. Following this, the structures and interpretations of mainly nonparametric r and Q control charts are explained for the Mahalanobis depth measure used in statistical quality control by means of an example.

Keywords: Control Charts, r Chart, Q Chart, Multivariate statistical process control, Depth function.

1. Introduction

In statistical process control, control charts are very important tools for monitoring and/or controlling whether a manufacturing process is statistically in control or not. Shewart's $(X, \overline{X})$ and CUSUM charts are widely used for this purpose. In addition to their efficiency, these charts are preferred because they are simple to construct and interpret. However, as these charts are based on an assumption of normality of the quality variable and are used when there is only one quality variable, they are not always appropriate. In many cases, two or more variables may need to be monitored, and following these two (or more) quality variables separately may be misleading. The Type I error α occurring when the variables are monitored separately differs from the Type I error α occurring when the variables are monitored simultaneously. Therefore, multivariate control charts are required when there is more than one quality variable. Monitoring the process of related variables is usually called a *multivariate quality control* problem.

Studies of multivariate quality control were first carried out by Hotelling in 1947; later, Hicks, Jackson, Crosier, Hawkins, Lowry, Montgomery, Pignatiello, Runger, Tracy, Young, Mason, Wadsworth, Alt and others also carried out studies on this subject. The work of these authors is given in [5], together with detailed references. The multivariate control charts considered by these authors are also based on the normality assumption

*Hacettepe University, Faculty of Science, Department of Statistics, Beytepe, Ankara, Turkey,

for the quality variable. Widely used multivariate control charts are χ^2 and Hotelling's T^2 charts.

Liu defined the new, mainly nonparametric, control charts (r, Q and S) by using a depth data concept in order to monitor the process of multivariate quality measurements [4]. These charts, like $(X, \overline{X})$ and CUSUM charts, are important as they bring out the shift in location and the increase in scale, in addition to having a two dimensional graphic representation which makes them easy to interpret. Unlike χ^2 and Hotelling's T^2, the normality assumption on the quality variable is not required, which is another advantage of these charts. So, these charts serve as an important measure in quality assurance [5].

In this study, r and Q control charts based on the Mahalanobis depth for elliptical distributions are given. Firstly, depth function, its properties and statistics obtained from depth function to construct control charts based on Mahalanobis depth are explained.

2. Data Depth

Statistical depth functions are widely used in nonparametric derivations for multivariate data. A depth function suitable for a distribution F in R^p, denoted by $D(F;x)$, brings out the non-central ranking of X in R^p with respect to F. A higher value of $D(F;x)$ for X in R^p means that X based on the distribution F is deeper (more central), and vice versa. That is, a smaller value of $D(F;x)$ for X in R^p shows that the sample point is further away from the center with respect to F. Depth functions have some important characteristics, which are given as follows:

Affine Invariance: Let $\mathcal{F}$ denote the family of distributions in R^p. If X is a random vector having distribution function F in R^p, then $D(F_{Ax+b}; Ax+b) = D(F;x)$.

Here, A is a non-singular $p \times p$ dimensional matrix and b is p-dimensional vector.

Maximality at the Center: When a F$\in \mathcal{F}$ is symmetric around any point θ_0 (that is, if the distribution function of the random variable X is F, then $(X-\theta_0)$ and $(\theta_0 - X)$ have the same distribution), then

$D(F;\theta_0) = \max_{x \in R^p} D(F;x)$.

Monotonicity Relative to the Deepest Point: When $F \in \mathcal{F}$ is symmetric around a point θ_0, in other words θ_0 is the deepest point of the distribution F, then $D(F;x)$ has the monotonicity characteristic if $D(F;x) \leq D(F;\theta_0 + \alpha(x-\theta_0))$.

Here $\alpha \in [0,1]$.

Vanishing at Infinity: For all $F \in \mathcal{F}$, if $\|x\| \to \infty$ then $D(F;x) \to 0$ [6].

Many data depth concepts have been given having all of the above properties. Tukey's depth, Majority depth, Mahalanobis depth and simplicial depth are the most popular of these.

In this study, as the control charts based on Mahalanobis depth are to be used, only Mahalanobis depth is given in detail here.

Liu defined Mahalanobis depth as follows [4]:

Let X denote a random vector having distribution function F in R^p. Then the Mahalanobis measure of depth for any point x (a $p \times 1$-dimensional vector) in R^p with respect to the distribution F is defined as follows:

$$MD(F;x) = \frac{1}{[1 + (x-\mu_F)\Sigma^{-1}(x-\mu_F)]} \tag{1}$$

In (1), μ_F and Σ_F are the mean vector and covariance matrix of the distribution function F, respectively. Hence, $MD(F;x)$ is a measure showing how 'deep' or 'central' x is with

respect to the distribution F. When F is unknown and a sample taken from distribution F is given, then the definition of Mahalanobis depth is:

$$MD(F_m; x) = \frac{1}{\left[1 + (x - \overline{X})' S^{-1} (x - \overline{X})\right]} \tag{2}$$

In (2), $\overline{X}$ is a $(p \times 1)$ sample mean vector and S a $(p \times p)$ sample covariance matrix. The depth function $MD(F; \cdot)$ is a depth function satisfying all of the above properties [3, 4].

3. Some Statistics Based on Data Depth used in Constructing Control Charts

Let F and G be the distribution functions of two independent p-dimensional populations and $X = \{X_1, \ldots, X_m\}$ be a sample taken from a population having distribution F. In quality control, F can be thought of as a 'good population,' in another words considered as measurements of products produced by an in-control process.

Let $Y = \{Y_1, \ldots, Y_n\}$ be a random sample taken from a population having distribution G (that is, new measurements taken from the process). In order to test whether the process is in control, or if there is any deterioration in the quality of the product by using the observations Y_i's, the distributions F and G need to be compared. If the Y_i's do not approach to the distribution F, this means that the quality of product has deteriorated. The hypotheses to test this can be given as follows:

$$H_o : F = G \text{ vs.}$$

$$H_A : \text{ There is a location shift and / or a scale increase from } F \text{ to } G \tag{3}$$

To test this hypothesis, the statistic $R(F; Y)$ which characterises the distance between F and G with respect to data depth when $X \sim F$ and $Y \sim G$ for a Y_i in R^p with respect to the given data depth $D(\cdot\,; \cdot)$ is defined as follows [2, 4]:

$$R(F; Y_i) = P_F \{X : D(F; X) \leq D(F; Y_i) / X \sim F\} \tag{4}$$

When $D(F; \cdot)$ has affine- invariance, then $R(F; Y)$ also has affine-invariance:

$$R(F; Y) = R(AY + b; F_{AY+b}).$$

Under the hypothesis $F = G$, if the distribution of $D(F; Y)$ is continuous, then the distribution of $R(F; Y)$ in (4) is uniformly distributed in $[0, 1]$:

$$R(F; Y) \sim U(0, 1). \tag{5}$$

The mean of the ratios $R(F; Y)$ for all y generated from population G, denoted by $Q(F, G)$, is found as follows:

$$\begin{aligned} Q(F, G) &= P\{D(F; X) \leq D(F; Y) / X \sim F, Y \sim G\} \\ &\quad (= E_G[R(F; Y)]) \end{aligned} \tag{6}$$

The parameter $Q(F, G)$ given in (6) is called the 'quality index' and takes values between 0 and 1 [2]. The quality index $Q(F, G)$ shows whether or not there is a difference in location and/or dispersion by comparing G and F.

When $D(F; \cdot)$ has affine-invariance, then $Q(F, G)$ also has affine-invariance:

$$Q(F, G) = Q(F_{AX+b}; G_{AY+b}). \tag{7}$$

In (7), A is a $(p \times p)$ non-singular matrix and b is a $(p \times 1)$ vector.

Let us denote by $\text{ell}(h; \theta, \Sigma)$ an elliptical distribution with parameters θ and Σ, where $h(\,.\,)$ is a function from R to R and Σ is positive definite. When there is only a location shift but no change in dispersion, the function $Q(F; G)$ decreases as θ_1 moves away from θ_0 along any line when $F \sim \text{ell}(h; \theta_0, \Sigma_0)$ and $G \sim \text{ell}(h; \theta_1, \Sigma_0)$.

When the locations are the same but there is a difference in dispersion, for $F \sim \text{ell}(h;\theta_0,\Sigma_0)D(F;\,\cdot\,)$ and $G \sim \text{ell}(h;\theta_0,\Sigma_1)$, $R(F;Y) \overset{ss}{\leq} R(F;X)$ and $Q(F;G) \leq \frac{1}{2}$ (here "ss" denotes stochastically smaller). When there are both location shift and scale change, then for $F \sim \text{ell}(h;\theta_0,\Sigma_0)$ and $G \sim \text{ell}(h;\theta_1,\Sigma_1)$, while the parameter θ_1 moves away from θ_0 along any line, the function $Q(F;G)$ decreases uniformly [2].

The statistics obtained from (4) and (6) will be used while constructing the structure of the control charts, and their limit distributions are given as follows:

a. Assuming the distribution F is known (meaning that F is either regarded as the collection of one (or several) acceptable lot(s) or an elliptical distribution with μ and Σ obtained from the measurements of a large acceptable batch).

When $Y = \{Y_1,\ldots,Y_n\}$ is a random sample taken from the distribution, $Q(F;G)$ is the mean of the random variables $R(F;Y)$:

$$Q(F,G_n) = \frac{1}{n}\sum_{i=1}^{n} R(F;Y_i). \tag{8}$$

If D(F;X) has a continuous distribution, under hypothesis H_0 the distribution of $Q(F,G_n)$ is the same as the distribution of $\sum_{i=1}^{n}\frac{U_i}{n}$, when $U_1,\ U_2,\ldots,U_n$ are independent and uniformly distributed random variables in $(0,1)$.

As a result of the Central Limit Theorem,

$$For\ n\to\infty\ ,\ \left[Q(F,G_n)-\frac{1}{2}\right] \to^{k} N(0,\frac{1}{12n}). \tag{9}$$

In (9), "k" means convergence in law.

b. If $X = \{X_1,\ldots,X_m\}$ is a random sample taken from the unknown distribution F and $Y = \{Y_1,\ldots,Y_n\}$ a random sample taken from the distribution G, then the estimation of $Q(F;G)$ is:

$$Q(F_m,G_n) = \frac{1}{n}\sum_{i=1}^{n} R(F_m;Y_i). \tag{10}$$

In (10), $R(F_m;Y_i)$ is the ratio of the X_j's satisfying $D(F_m;X_j) \leq D(F_m;Y_i)$ when the distribution F is unknown:

$$R(F_m;Y_i) = \#\left\{D(F_m;X_j) \leq D(F_m;Y_i),\ j=1,\ldots,m\right\}/m. \tag{11}$$

Here the values of $D(F_m;\,\cdot\,)$ are empirical depth values calculated with respect to F_m, and if the distribution F is continuous, $D(F_m;\,\cdot\,)$ converges to $D(F;\,\cdot\,)$ uniformly as $m\to\infty$. Therefore:

$$R(F_m;Y_i) \to^{k} U\,[0,1] \text{ as } m\to\infty, \text{ for all } X. \tag{12}$$

The uniform convergence of $D(F_m;\,\cdot\,)$ obtained by using Mahalanobis depth is valid when F is an elliptical distribution and the second absolute moment of the distribution F exists $\left(E_F\left\|X\right\|^2<\infty\right)$.

As a result of this, when F is an elliptical distribution and $\left(E_F\left\|X\right\|^2<\infty\right)$, then $MD(F_m;x)$ converges to $MD(F;x)$ uniformly as $m\to\infty$ [2, 4].

In the same way, when $D(F;Y)$ has continuous distribution, then it has also been shown that $Q(F_m,G_n)$ in (10) converges to $Q(F;G)$ as $\min(m,n)\to\infty$.

Under the condition that (11) holds, the limit distribution of $Q(F_m,G_n)$ is:

$$\left[Q(F_m,G_n)-\frac{1}{2}\right] \to^{k} N\left(0,\left[\frac{1}{m}+\frac{1}{n}\right]\Big/12\right),\ \text{as}\ \min(m,n)\to\infty. \tag{13}$$

In (13), if $Q(\,.\,,\,.\,)$ is used for the Mahalanobis depth then this equation is valid when F is continuous and the forth absolute moment exists $\left(E_F \left\|X\right\|^4 < \infty\right)$ [2, 4].

4. r and Q Control Charts based on the Mahalanobis Depth

A r control chart is alike to a univariate X chart. An X control chart reveals whether there is a deviation from a pre-determined process mean, or a trend or a non-random pattern of an observation set. However, although this chart is very simple and efficient when used to observe a univariate process, it cannot be easily generalized to a multivariate process. In studies of the bivariate normal distribution, the control limits are given as elliptical limits named as the control ellipse [1]. However, it cannot be said that they are efficient for a multivariate data set as they require a normality assumption, Type I Error α changes and the ranking of sample points with respect to time losses. An r control chart with $LCL = \alpha$ corresponds to an α-level test of the following hypothesis:

$H_0 : F = G$, vs.

H_A : there is a location shift and/or a scale increase from F to G.

In order to construct a r control chart, the values of $R(F; Y_i)$ are obtained using (4) and (11) when the distribution F is known, or the values of $R(F_m; Y_i)$, $i = 1, \ldots, n$ are calculated for $X_1, \ldots, X_m$ only, when the distribution F is unknown. When the distribution F is elliptical we denote by $R_{MD}(F, Y_i)$ the value of $R(F, Y_i)$ obtained by using the Mahalanobis depth given in (1) and (2). When the distribution F is known, $\mathrm{R}_{MD}(F, Y_i)$ is given by:

$$R_{MD}(F; Y_i) = P_F \left\{X : MD(F; X) \leq MD(F; Y)/X \sim F\right\}, \tag{14}$$

and when the distribution F is unknown, $\mathrm{R}_{MD}(F_m; Y_i)$ is given by:

$$R_{MD}(F_m; Y_i) = \#\left\{MD(F_m; X_j) \leq MD(F_m; Y_i),\ j = 1, \ldots, m\right\}/m. \tag{15}$$

It is known from [4] that $R_{MD}(F; Y_i)$ has all the properties of $R(F, Y_i)$.

A r control chart is constructed by plotting the $R(F, Y_i)$'s or the $R(F_m, Y_i)$'s for sample points $i = 1, \ldots, n$.

The center line (CL) and the lower control limit (LCL) of the chart are:

$$CL = 0.5,$$
$$LCL = \alpha. \tag{16}$$

Equation (16) can be obtained from (4) and (12). As seen from these equations, the expected values of $R(F, Y_i)$ and $R(F_m, Y_i)$ are 0.5. Therefore, in a r control chart it is suitable to take CL as 0.5. Also, the values of the $R(F, Y_i)$ or the $R(F_m, Y_i)$ being higher than 0.5 indicates a decrease in scale or an omittable shift in location. This is thought of as a gain not a loss in the quality concept of statistical process control. The process is not said to be out-of-control. Therefore, in a r control chart there exists only a lower control limit LCL. However, although a UCL does not exist, CL plays the role of a reference point enabling the observation of a possible trend or non-random pattern. In a r control chart, when the values of $R(F, Y_i)$ or $R(F_m, Y_i)$ are in the region of α, this means that process is statistically out-of-control. That is, there is signal of possible quality deterioration or an out-of-control process. $R(F_m, Y_i)$ given in (11) shows how far away from the center Y is with respect to the data set X_j. If the values of the $R(F_m, Y_i)$ are small the ratio of the X_j's further from the center than Y is also small. So, Y is not fitted centrally to a good data set. Therefore, under the assumption of $Y \sim G$, a small value of the values $R(F_m, Y_i)$ shows a possible deviation of G from F. As $R(F_m, Y_i)$ is

defined with respect to data depth, a possible deviation means a shift in location and/or an increase in scale [4].

The aim of a Q control chart is similar to that of a univariate $\overline{X}$ control chart. The hypotheses for a Q control chart are:

$H_0 : F = G, Q(F, G) = \frac{1}{2}$

$HA : Q(F, G) < \frac{1}{2}$

The acceptance of the hypothesis $H_A : Q(F, G) < \frac{1}{2}$ means that on average more than 50% of the population F are deeper (more central) than any of the observations Y generated from the distribution G. This shows a possible shift in location and/or an increase in scale from F to G. If $Q(F, G) > \frac{1}{2}$, then G has a very small dispersion.

As a multivariate Q chart is similar to a univariate $\overline{X}$ control chart, in order to construct Q control chart the mean of $R(F, Y_i)$ or of $R(F_m, Y_i)$ for k subgroups, each of which have equal size, needs to be calculated. Assuming that the size of each subset is t, the Q control chart for $k \times t = n$, is constructed using (8) and (10) by plotting $\left\{Q(F, G_t^1), Q(F, G_t^2), \ldots\right\}$ when F is known and $\left\{Q(F_m, G_t^1), Q(F_m, G_t^2) \ldots\right\}$ when F is unknown. Here G_t^k denotes the k^{th} $(k = 1, 2, \ldots)$ subgroup of the Y_i's with size t.

The values of the CL and the LCL of a Q chart depend on the choice of the size of the subgroup. When t is large, the CL and LCL of the Q control chart for the $\left\{Q(F, G_t^k)\right\}$'s are obtained from (9):

$$CL = 0.5 \text{ and } LCL = \left\{ .5 - z_\alpha \sqrt{\frac{1}{12t}} \right\}, \tag{17}$$

and for the $\left\{Q(F_m, G_t^k)\right\}$'s they are obtained from (13):

$$CL = 0.5 \text{ and } LCL = \left\{ .5 - z_\alpha \sqrt{\frac{1}{12t}} \left[\left(\frac{1}{k} + \frac{1}{t} \right) \right] \right\}. \tag{18}$$

This approach is valid until t=5. In applications, t can be taken as 3 or 4. In this case, the parameters for the Q chart are given as follows [4]:

$$CL = 0.5 \text{ and } LCL = \frac{(t!\alpha)^{\frac{1}{t}}}{t}. \tag{19}$$

The means of the ratios of Y's more out-of-centre than X with respect to the Mahalanobis depth given by (14) and (15) are respectively [4]:

$$Q_{MD}(F, G_t^k) = \frac{1}{t} \sum_{i=1}^{t} R_{MD}(F; Y_i), \ k = 1, 2, \ldots \tag{20}$$

and

$$Q_{MD}(F_m, G_t^k) = \frac{1}{t} \sum_{i=1}^{t} R_{MD}(F_m; Y_i), \ k = 1, 2, \ldots \tag{21}$$

Hence, r control charts are constructed with respect to Mahalanobis depth by using (14) and (15) and Q control chart by using (20) and (21). It is obvious that there is no change in the central line and the control limits for these control charts obtained using Mahalanobis depht.

5. An Application

In this study, r and Q control charts based on Mahalanobis depth are obtained and interpreted for a bivariate data set by taking into account the application in the study of Liu [4]. Firstly, a random sample of size 540 is generated from the distribution $F \sim N\left[\binom{0}{0}, \left(\begin{smallmatrix}1 & 0\\ 0 & 1\end{smallmatrix}\right)\right]$ using the MINITAB software. And then, a sample of size 40 is generated from the distribution $G \sim N\left[\binom{2}{2}, \left(\begin{smallmatrix}4 & 0\\ 0 & 4\end{smallmatrix}\right)\right]$. Although the normality assumption is not required for the construction of these charts, a normal distribution is chosen to make the evaluation of the outcome easier.

The last 40 of the 540 sample points generated from distribution F are considered as if they were generated from distribution G. So, in the charts constructed 40 sample points generated from distribution F are expected to be in-control and 40 sample points generated from distribution G are expected to reveal a shift in location and/or a change in dispersion.

For every X_i, $(i = 1, 2, \ldots, 500)$ and Y_i, $(i = 1, 2, \ldots, 80)$, the Mahalanobis measure of depth is calculated using the EXCELL program. For Y_i, $(i = 1, 2, ..., 80)$, the values of $MD(F_m; X_i)$ and $R_{MD}(F_m; X_i)$ are given in Appendix 1. Using (16), a r control chart is constructed using the 80 sample points, and are given in Figure 1. The value of LCL is equal to 0.05. From Figure 1, it can be seen that the r control chart revails a shift in the distribution mean and an increase in the scale as the last 40 sample points are out of LCL.

A Q control chart is constructed for $t = 4$ and $t = 10$. The values of $Q_{MD}(F_m, G_t)$ obtained using (21) for $t = 4$ and for $t = 10$ are given in Appendix 2a and Appendix 2b, respectively. Figure 2 and Figure 3 show the Q control charts constructed for these sample points. From Figure 2, it is seen that 10 of the last 40 sample points are beyond the lower control limit for $t = 4$, and similarly it is seen that the last 4 sample points are out-of-control for $t = 10$.

Figure 1. r control chart $(n = 80)$

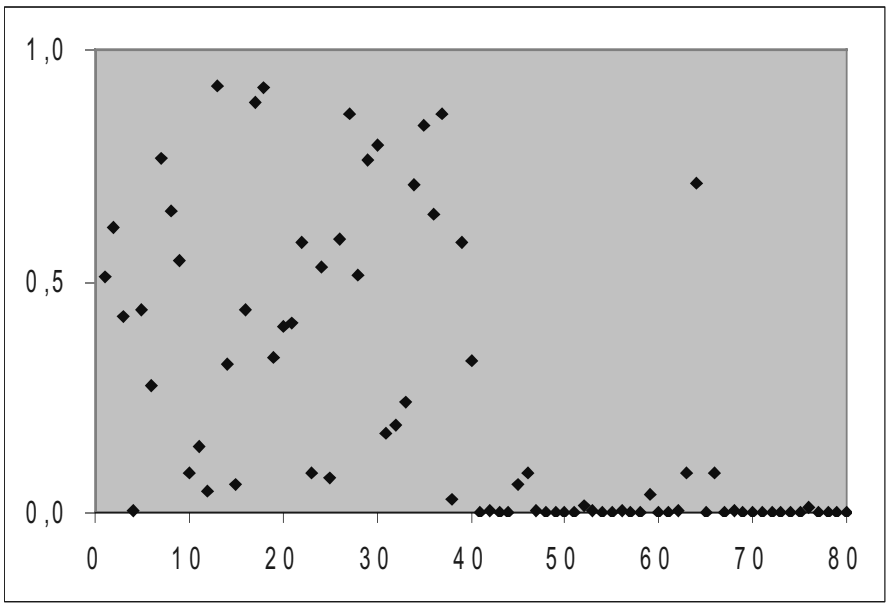

Figure 2. Q control chart ($t = 4, k = 20$)

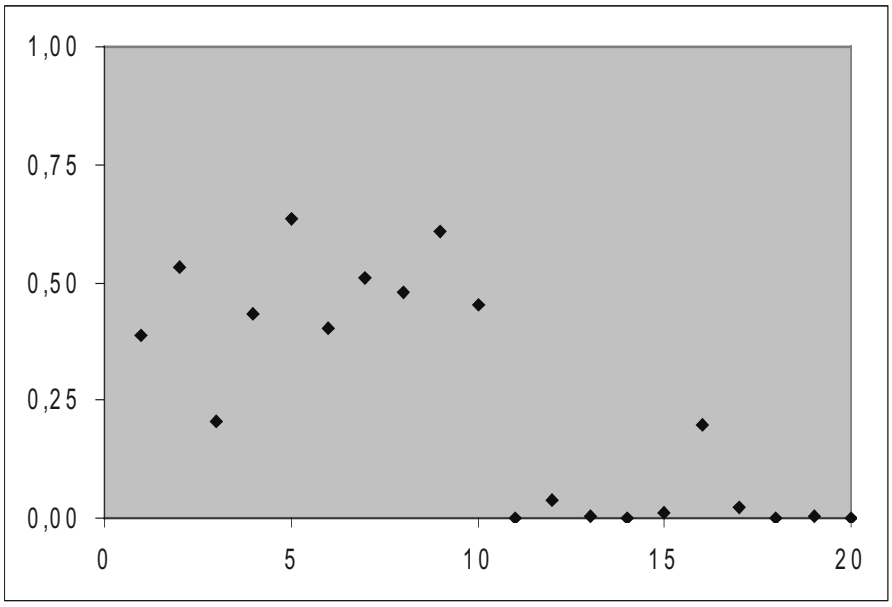

Figure 3. Q control chart ($t = 10, k = 8$)

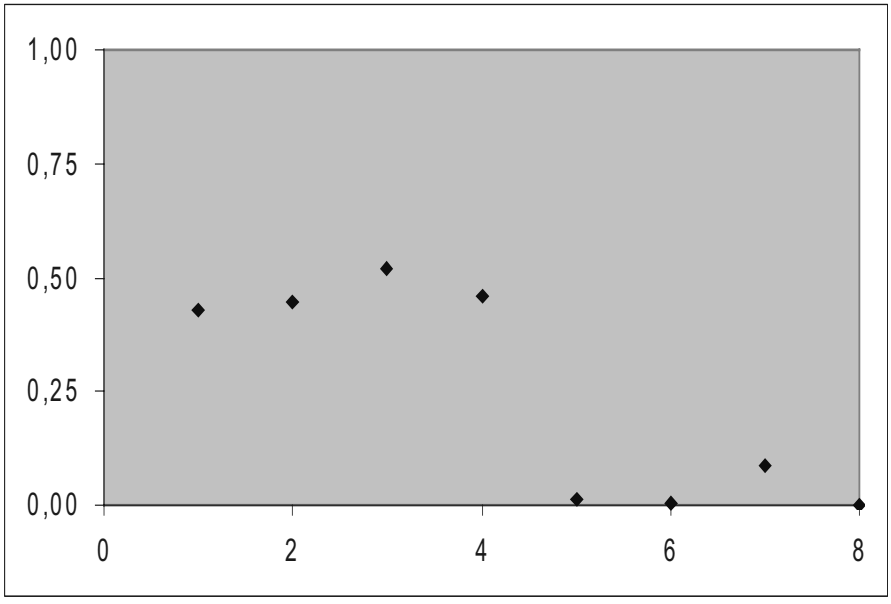

6. Concluding Remarks

r and Q control charts, mainly nonparametric, are constructed using the data depth concept and are used for monitoring the process of multivariate quality measurements, and can be interpreted just as easily as the well-known univariate X, $\overline{X}$ and CUSUM charts. In addition they detect simultaneously the location shift and scale increase of the process [4]. Unlike χ^2 and Hotelling's T^2 charts, one of the advantages of these charts is that a normality assumption is not required.

It might be thought that r and Q control charts constructed using the Mahalanobis depth are similar to a Hotelling T^2 chart, because both of them represent quadratic distance of a point from its mean. However, while constructing r and Q control charts, the Mahalanobis depth serves only as a tool to obtain the ranks of observations. The charts are constructed with respect to the ranks of Mahalanobis depths, not with respect to Mahalanobis depth itself. Also, to decide control limits in Hotelling's T^2, the sample distribution of Hotelling T^2 statistics is needed. For r and Q control charts based on Mahalanobis depth, this is not required as the statistics are converted to ranks. Therefore, the plotting of charts based on Mahalanobis depth is different from that based on Hotelling's T^2 and for an elliptical distributions r and Q control charts based on Mahalanobis depth can be said to be more efficient

References

[1] Alt, F. and Smith, N. *Multivariate process control*, Handbook of Statistics **7**, (P. R. Krishnaiah and C. R. Rao, Amsterdam, 333–351, 1988.

[2] Lýu, R. and Sýngh, K. *A quality index based on data depth and multivariate rank tests*, Journal of The American Statistical Association **88**, 252–260, 1993.

[3] Liu, R. *On a notion of data depth based on random simplicities*, The Annals of Statistics **18**, 405–414, 1990.

[4] Liu, R. *Control charts for multivariate processes*, Journal of the American Statistical Association **90**, 1380–1387, 1995.

[5] Montgomery,D. C. *Introduction to statistical quality control*, (John Wiley & Sons Inc., USA, 1996).

[6] Zuo, Y. and Serfling, R. *Structural properties and convergence results for contours of sample statistical depth functions*, Annals of Statistics, 1–20, 2000.

7. Appendix 1

The values of $MD(F_m;Y_i)$ and $R_{MD}(F_m;Y_i)$ for the last 40 sample points generated from distribution F and for the 40 sample points generated from distribution G

Y_i	$MD(F_m;Y_i)$	$R_{MD}(F_m;Y_i)$	Y_i	$MD(F_m;Y_i)$	$R_{MD}(F_m;Y_i)$
1	0,6265	0,5080	41	0,0822	0,0000
2	0,6945	0,6140	42	0,1292	0,0020
3	0,5649	0,4220	43	0,1025	0,0000
4	0,1556	0,0020	44	0,0660	0,0000
5	0,5801	0,4360	45	0,2684	0,0620
6	0,4383	0,2740	46	0,2885	0,0840
7	0,8158	0,7660	47	0,1213	0,0020
8	0,7316	0,6500	48	0,0506	0,0000
9	0,6500	0,5460	49	0,0671	0,0000
10	0,2844	0,0840	50	0,0172	0,0000
11	0,3439	0,1440	51	0,0828	0,0000
12	0,2527	0,0480	52	0,2007	0,0160
13	0,9355	0,9220	53	0,1406	0,0020
14	0,4718	0,3200	54	0,0106	0,0000
15	0,2701	0,0620	55	0,0396	0,0000
16	0,5790	0,4360	56	0,1729	0,0040
17	0,9088	0,8860	57	0,0557	0,0000
18	0,9331	0,9180	58	0,0404	0,0000
19	0,4874	0,3360	59	0,2460	0,0400
20	0,5430	0,4020	60	0,0598	0,0000
21	0,5530	0,4080	61	0,0970	0,0000
22	0,6695	0,5840	62	0,1549	0,0020
23	0,2982	0,0860	63	0,2841	0,0840
24	0,6426	0,5320	64	0,7861	0,7120
25	0,2766	0,0760	65	0,0255	0,0000
26	0,6797	0,5920	66	0,2930	0,0840
27	0,8883	0,8620	67	0,0250	0,0000
28	0,6291	0,5120	68	0,1058	0,0020
29	0,8109	0,7600	69	0,0791	0,0000
30	0,8326	0,7920	70	0,0479	0,0000
31	0,3610	0,1720	71	0,0860	0,0000
32	0,3766	0,1880	72	0,0996	0,0000
33	0,4111	0,2400	73	0,0762	0,0000
34	0,7803	0,7080	74	0,0559	0,0000
35	0,8633	0,8360	75	0,0845	0,0000
36	0,7307	0,6440	76	0,1920	0,0120
37	0,8883	0,8620	77	0,0325	0,0000
38	0,2242	0,0300	78	0,0541	0,0000
39	0,6697	0,5840	79	0,0526	0,0000
40	0,4763	0,3280	80	0,0386	0,0000

8. Appendix 2

a. The values of $Q_{MD}(F_m, G_t)$ for $t = 4$

Subgroups (k)	$Q_{MD}(F_m, G_t)$ for $t = 4$
1	0,3865
2	0,5315
3	0,2055
4	0,4350
5	0,6355
6	0,4025
7	0,5105
8	0,4780
9	0,6070
10	0,4510
11	0,0005
12	0,0370
13	0,0040
14	0,0015
15	0,0100
16	0,1995
17	0,0215
18	0,0000
19	0,0030
20	0,0000

b. The values of $Q_{MD}(F_m, G_t)$ for $t = 10$

Subgroups (k)	$Q_{MD}(F_m, G_t)$ for $t = 10$
1	0,4302
2	0,4474
3	0,5204
4	0,4592
5	0,0150
6	0,0062
7	0,0884
8	0,0012

Hacettepe Journal of Mathematics and Statistics
Volume 33 (2004), 69 – 76

DETERMINING THE CONDITIONAL PROBABILITIES IN BAYESIAN NETWORKS

Hülya Olmuş* and S. Oral Erbaş*

Received 22 : 07 : 2003 : Accepted 04 : 01 : 2005

Abstract

Bayesian networks are used to illustrate how the probability of having a disease can be updated given the results from clinical tests. The problem of diagnosis, that is of determining whether a certain disease is present, D, or absent, D', based on the result of a medical test, is discussed. Using statistical methods for medical diagnosis, information about the disease and symptoms are collected and the databases are used to diagnose new patients. How can we evaluate the diagnostic probability represented by $\Pr(D \setminus \text{evidence})$, where evidence is the result of a clinical test or tests on a new patient? The object of this article is to answer this question. Using the HUGIN software, diagnostic probabilities are analyzed using the Bayesian approach.

Keywords: Bayesian networks, Medical diagnosis, Conditional probability.

1. Introduction

Bayesian networks were introduced in the 1980's as a formalism for representing and reasoning with models of problems involving uncertainty, adopting probability theory as a basic framework [12]. Over the last decade, the Bayesian network has become a popular representation for encoding uncertain expert knowledge in expert systems [7]. The field of Bayesian networks has grown enormously over the last few years, with theoretical and computational developments in many areas. Bayesian networks are also known as belief networks, causal probabilistic networks, causal nets, graphical probability networks, and probabilistic influence diagrams.

Bayesian networks have proved useful in practical applications, such as medical diagnosis and diagnostic systems. The probability based expert systems for medical diagnosis that emerged during the 60's and 70's could be characterized by the following points: The sets of possible diseases a system could diagnose were mutually exclusive and collectively exhaustive, the evidence was assumed conditionally independent given any hypothesis,

*Gazi University, Department of Statistics, Teknikokullar, Beşevler, Ankara, Turkey.

and only one disease was assumed to exist in any patient. These assumptions were made in order to keep to a manageable size the problem of acquiring and calculating probabilities [10].

A Bayesian network is used to model a domain containing uncertainty in some manner. It is a graphical model for probabilistic relationships among a set of variables and is composed of directed acyclic graphs (DAGs) in which the nodes represent the random variables of interest, and the links represent informational or causal dependencies among the variables [16]. Here, each node contains the states of the random variable and it represents a conditional probability table. The conditional probability table of a node contains probabilities of the node being in a specific state given the states of its parents [2, 5, 9, 11, 13, 15, 20, 21]. Furthermore, edges reflect cause-effect relations within the domain. These effects are normally not completely deterministic (e.g. disease $\rightarrow$ symptom). The strength of an effect is modelled as a probability.

Bayesian networks help us answer questions such as: What is the probability that a random variable will be in a given state if we have observed the values of some other random variables. They can also suggest what could be the best choice for acquiring new evidence. Conditional probabilities are important for building Bayesian networks. But Bayesian networks are also built to facilitate the calculation of conditional probabilities, namely the conditional probabilities for variables of interest given the data (also called evidence) at hand [5].

The quantities of interest in a medical diagnostic procedure are the probabilities of having or not having a disease, i.e. the diagnostic probabilities [17, 18]. These quantities may change their values according to the diagnostic value of the observed evidence. Evidence is produced by responses (called indicants) to clinical questions (tests, signs or symptoms). The data structure is complicated by a number of factors. Studies of acquisition for this problem occur in the literature [6, 12].

The implementation of a Bayesian network is an excellent approach to creating a medical diagnostic system that realistically models the multiple symptoms and indicators (rather than just one particular test) that affect the conditional probability that a person has a particular disease which may be causing the symptoms and positive test results. Because each node in a Bayesian network can have multiple parent and child nodes, and thus multiple ancestor and descendant nodes, evaluating Bayesian networks is more complex than performing a single calculation with Bayes' theorem.

Inference in a Bayesian network means computing the conditional probability for some variables, given information (evidence) concerning other variables. This is easy when all available evidence is for variables that are ancestors of the variable(s) of interest. But when evidence is available on a descendant of the variable(s) of interest, we have to perform inference against the direction of the edges. To this end, we employ Bayes' Theorem:

$$\Pr(A\backslash B) = \frac{\Pr(B\backslash A)\Pr(A)}{\Pr(B)}.$$

2. The HUGIN System

During the early stages of the development of probabilistic expert system, several obstacles were encountered due to difficulties in defining the joint probability distribution of the variables. With the introduction of probabilistic network models, these obstacles have largely been overcome, and probabilistic expert systems have made a spectacular comeback during the last two decades or so. These network models, which include Markov and Bayesian networks, are based on a graphical representation of the relationships among

the variables. This representation leads to efficient propagation algorithms that are used to draw conclusions. An Example of such an expert system shell is the HUGIN expert system [4]. The HUGIN system is a tool enabling the construction of model-based decision support systems in domains characterized by inherent uncertainty. The models supported are DAGs and their extension, influence diagrams. The HUGIN system allows us to define both discrete nodes and to some extent continuous nodes in our models [8]. The HUGIN system can be used to construct models as components in an application in the area of decision support and expert systems. When we have constructed a network, we can use it for entering evidence in some of the nodes where the state is known, and then retrieve the new probabilities corresponding to this evidence calculated in other nodes.

In recent years, diagnostic assistants have been built around Bayesian networks. These networks are a form of graphical probabilistic model that explicates independencies between system components and diagnostic observations in a directed graph. The structure of the graph allows the joint probability distribution over the system components and diagnostic observations to be expressed in a compact form [19]. The use of such a model along with graph-theoretic algorithms for probabilistic inference makes it possible to compute the probability of a component defect given the outcomes of diagnostic observations. There are several commercial and research tools designed for BN model authoring and testing. Among the most popular of these tools is the HUGIN package.

After constructing a Bayesian network that models, as in the example presented in the figure, the states of affairs and their probabilistic causal relationships, one would want to be able to determine, given observed values for any number of nodes in the network, the conditional probabilities of the remaining, unknown nodes. The utility of Bayesian networks lies in being able to make this calculation, which is called *evaluating* or *solving* the network. An algorithm for evaluating Bayesian networks can determine probabilities of causes given observed effects (e.g., the probability that a dam has failed given the observation that there is flooding) or probabilities of effects given observed causes (e.g., the probability that there is flooding given a low barometer reading). In order to maximize efficiency and minimize execution time, algorithms that give exact solutions of Bayesian networks must first simplify the network itself before proceeding with the evaluation process. There is no one algorithm for obtaining exact solutions that is efficient for all Bayesian networks; the choice of an exact algorithm depends on the topological characteristics of the particular Bayesian network that is to be evaluated. There are, however, several approximation schemes which yield reasonably accurate solutions and require less execution time than the exact algorithms. HUGIN is a software package that implements algorithms for evaluating Bayesian networks [3]. Algorithms that achieve exact solutions are derived from Bayes's theorem. Bayes's theorem can be used to make a simple calculation of the conditional probability of a hypothesis given its evidence.

3. A Menopause Example

In this example, the patients who applied to Gazi University Gynecology and Obstetrics Menopause Clinic during the period August–October 1998 are studied [1]. A patient consults with a specialist who is going to start a search to discover whether the patient has the postmenopausal condition, D, or its absence, D'. The physician observes an indicant (E^+= normal bone density or E^-= abnormal bone density), which is new evidence associated with the patient. In a search for information about this new indicant of the postmenopausal condition D, doctors in a certain clinic select 100 patients known to be in postmenopause and another 100 patients known to be in premenopause. Here D is the event that a patient has the postmenopausal condition, while D' is the event

that a patient has the premenopausal condition D'. To each patient they applied a bone mineral densitometry (BMD) test, obtaining a response E^+ for evidence of normal bone density, or E^- for evidence of abnormal bone density [14, 17, 18].

In constructing the graph for the Bayesian network, human experts mostly use "causal" relationships between variables as a guideline. The situation can be modelled by the Bayesian network in Figure 1. In Figure 1, we have the graphical representation of the Bayesian network. However, this is only what we call the qualitative representation of the Bayesian network. We need to specify the quantitative representation. The quantitative representation of a Bayesian network is the set of conditional probability tables of the nodes.

Figure 1. Bayesian network for the menopause example.

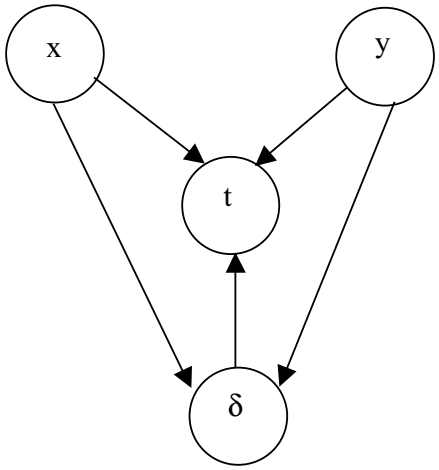

The Bayesian network consist of four nodes: x, y, t and δ which can all be in one of two states. Node x can be is the state corresponding to "normal bone density" or "abnormal bone density" as a result of a BMD test among all former patients with D and node y can be in the state corresponding to "normal bone density" or "abnormal bone density" as a result of a BMD test among all former patients with D'. The state of a new patient is

$$\delta = \begin{cases} 1 & \text{if the patient has postmenopausal condition } D \\ 0 & \text{if the patient has the premenopausal condition } D'. \end{cases}$$

The result of the test for a new patient is

$$t = \begin{cases} 1 & \text{if the BMD test gives normal bone density, i.e. } E^+ \\ 0 & \text{if the BMD test gives abnormal bone density, i.e. } E^-. \end{cases}$$

Here, the conditional probabilities are $\Pr(x), \Pr(y), \Pr(t \backslash x, y, \delta)$ and $\Pr(\delta \setminus x, y)$. Note that all four tables show the probability of a node being in a specific state depending on the states of its parent nodes, but x and y do not have any parent nodes.

The Bayesian network diagram that permits us to evaluate the diagnostic probabilities for all possible values of δ, x, y is presented in Figure 1.

The diagnostic probabilities, the object of the analysis, are $\Pr\{\delta = 1 \backslash t = 1\}$ and $\Pr\{\delta = 1 \backslash t = 2\}$. If a new woman patient's BMD test response is known to be "normal bone density" or "abnormal bone density", what is the probability that this woman is in

a postmenopausal or premenopausal condition? The answer to our problem is given by the probability functions attached to node t.

In this example, the model is defined using binary variables. In the following figures, empty boxes show observable variables whereas the values shown by full boxes are probability values. Also, the value "100" in the figures indicate that the selected level of variable is known. In the figures "1" indicates "normal bone density", whereas "2" indicates "abnormal bone density".

The menopause Bayesian network has been constructed using the HUGIN software. Here the probability that $\delta = 1$ is the prior probability. This prior probability was taken as 0.15 using expert belief. In other words, $\Pr(\delta = 1) = 0.15$.

In Figure 2, the model is shown with initial probabilities. For example, the "normal bone density" and "abnormal bone density" response probabilities for 100 postmenopausal women were 0.4750 and 0.5250, respectively. In other words, $\Pr(x = 1) = 0.4750$ and $\Pr(x = 2) = 0.5250$. On the other hand the "normal bone density" and "abnormal bone density" response probabilities for 100 premenopausal women were 0.40 and 0.60 respectively. In other words, $\Pr(y = 1) = 0.40$ and $\Pr(y = 2) = 0.60$. However, the probability of a new woman patient being postmenopausal is 0.3967, the probability of a woman not being postmenopausal is 0.6033. In other words, $\Pr(\delta = 1) = 0.3967$ and $\Pr(\delta = 2) = 0.6033$. The "normal bone density" and "abnormal bone density" response probability to the BMD test for a new patient are 0.4238 and 0.5762 respectively. In other words, $\Pr(t = 1) = 0.4238$ and $\Pr(t = 2) = 0.5762$.

Figure 2. Marginal Probabilities

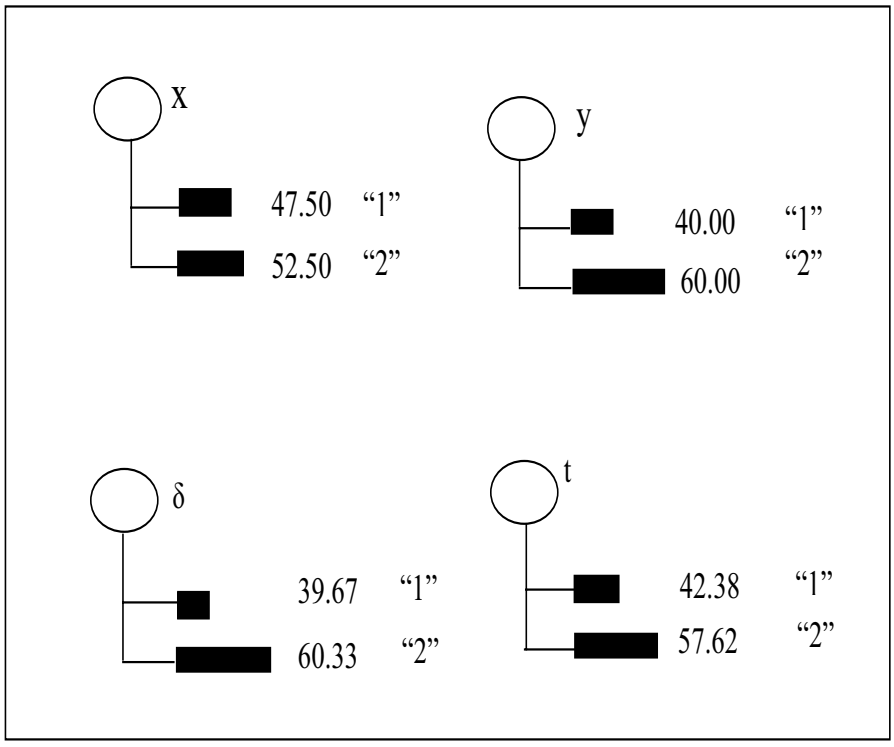

Now, one might want to know the probability of any other combination of states under the assumption that the evidence entered holds. Here, we want to calculate the probability of any other combination of states given the evidence provided by the result of the test for the new patient.

If the result of the test for the new patient is "normal bone density", then the evidence is entered and a sum-propagation is performed. In other words, this gives probabilities $\Pr(\delta = \text{“1”} \setminus t = \text{“1”})$, $\Pr(\delta = \text{“2”} \setminus t = \text{“1‘”})$. The result is shown in Figure 3. For example, if the response to the BMD test for new for woman patient is "normal bone density", the "normal bone density" and "abnormal bone density" response probabilities are 0.5743 and 0.4257 for the 100 postmenopausal women respectively. In other words, $\Pr(x = \text{“1”} \setminus t = \text{“1”}) = 0.5743$ and $\Pr(x = \text{“2”} \setminus t = \text{“1”}) = 0.4257$. Similarly if the new woman patient's BMD test response is known as to be "normal bone density", the "normal bone density" and "abnormal bone density" response probabilities are 0.6534 and 0.3466 for the 100 premenopausal women respectively. In other words, $\Pr(y = \text{“1”} \setminus t = \text{“1”}) = 0.6534$ and $\Pr(x = \text{“2”} \setminus t = \text{“1”}) = 0.3466$. Conversely if the new woman patient's BMD test result is known to be negative, the probability of being postmenopausal or premenopausal for this patient are 0.7309 and 0.2691 respectively. In other words, $\Pr(\delta = \text{“1”} \setminus t = \text{“1”}) = 0.2691$ and $\Pr(\delta = \text{“2”} \setminus t = \text{“1”}) = 0.7309$.

Figure 3. The conditional probabilities of other nodes if the new patient is known to have "normal bone density" as a result of the BMD test.

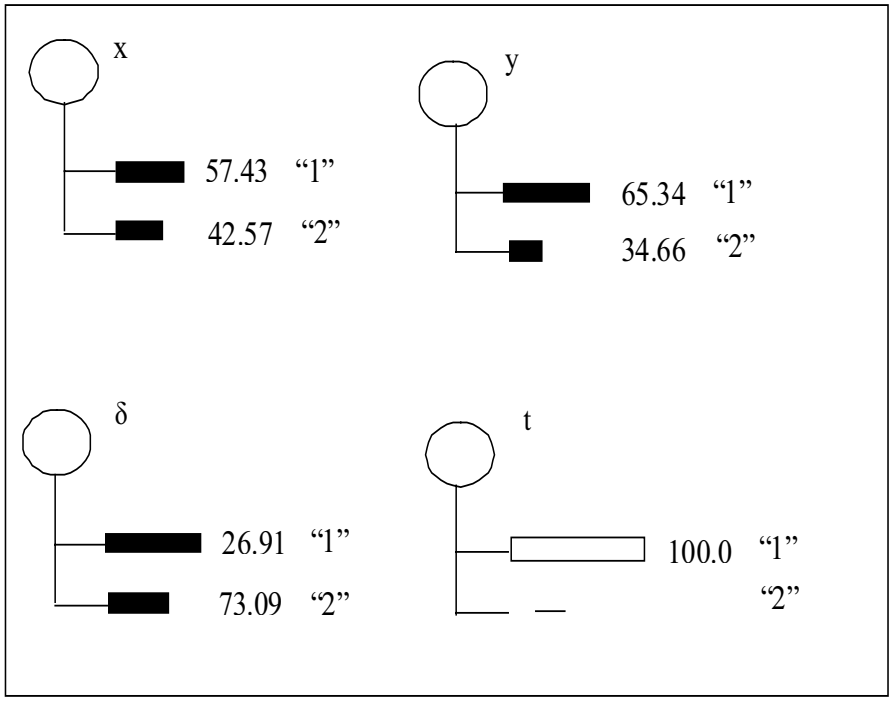

If the result of the test for the new patient is "abnormal bone density", then the evidence is entered and sum-propagation is performed. The result is shown in Figure 4. In other words, this produces the probabilities $\Pr(\delta = \text{“1”} \setminus t = \text{“2”})$ and $\Pr(\delta = \text{“2”} \setminus t = \text{“2”})$. The result is shown in Figure 4.

Figure 4. The conditional probabilities of other nodes if the new patient is known to have "abnormal bone density" as a result of the BMD test.

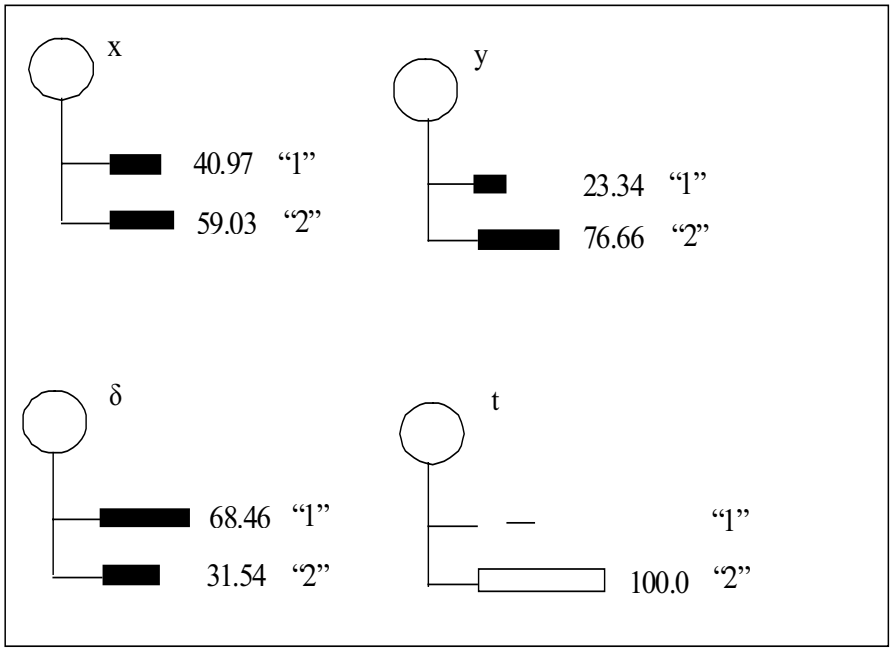

For example, if a new woman patient's BMD test response is known to be "abnormal bone density", the "normal bone density" and "abnormal bone density" response probabilities are 0.4097 and 0.5903 for the 100 postmenopausal women respectively. In other words, $\Pr(x = \text{“1”} \setminus t = \text{“2”}) = 0.4097$ and $\Pr(x = \text{“2”} \setminus t = \text{“2”}) = 0.5903$. Conversely if a new woman patient's BMD test response is known to be "abnormal bone density", the probability of being postmenopausal or premenopausal for this patient are 0.4756 and 0.5254 respectively. In other words, $\Pr(\delta = \text{“1”} \setminus t = \text{“1”}) = 0.6846$ and $\Pr(\delta = \text{“2”} \setminus t = \text{“1”}) = 0.3154$.

4. Conclusion

Bayesian networks are becoming an increasingly important area in applications to medical diagnosis. Here, the cause-effect relation among variables is explained and thus the relations between the variables are modelled.

The analysis of this medical problem has several important applications, including updating the probabilities for data in expert systems. In this study, depending on the results of a clinical test, the probability of a new woman patient being in menopause or not is examined. Also, the conditional probabilities of other nodes are obtained if the new patient is known to have "normal bone density" or "abnormal bone density" as a result of a BMD test.

In this application, the marginal probability of a new patient, who comes to the clinic, being in menopause is 0.3967. If she is known to have "normal bone density", an increase is not observed in the probability of this woman being in menopause. But if she is known to have "abnormal bone density", an increase is observed in the probability of this woman being in menopause.

Osteoporosis is one at the diseases causing bone resorption after the menopause. But it can be seen at an earlier age in young persons infected by the bone disease, and other metabolic disfunctions beside osteoporosis and the menopause. Osteoporosis may not be seen in every women during the menopause. As a conclusion of this study, menopause probability was seen to be higher than normal for those who were diagnosed as having bone resorption by the BMD test. However, it is not possible to correlate bone resorption with the menopause alone. Bone resorption can result from pregnancy, smoking, using alcohol, malnutrition and some hormonal and genetic disturbances. In this study, by using the HUGIN software, the correlation between the menopause and osteoporosis was evaluated by neglecting all other parameters.

References

[1] Ataoğlu, F. *Menapoz dönemindeki kadınların hormon replasman tedavisine (HRT) başlanmadan önceki ve tedavi sonrasındaki serum lipid, alkalen fosfataz ve kalsiyum değerleri*, (Gazi Üniversitesi Sağlık Bilimleri Enstitüsü Biyokimya Anabilim Dalı, Yayınlanmamış Yüksek Lisans Tezi, Ankara, 1999).

[2] Buntine, W. *A guide to the literature on learning probabilistic networks from data*, IEEE Transactions on Knowledge and Data Engineering **8** (2), 195–210, 1996.

[3] Charniak, E. *Bayesian networks without tears*, AI Magazine **12** (4), 50–63, 1991.

[4] Castillo, E., Gutierrez J. M. and Hadi A. S. *Expert systems and probabilistic network models*, (Springer-Verlag, New York, 1997).

[5] Cowell, R. G. *Intrduction to inference in Bayesian networks*, in Learning in Graphical Models, 9–26, 1999.

[6] Dawid, A. P. *Properties of diagnostic data distributions*, Biometrics **32**, 647–658, 1976.

[7] Heckerman, D. *A tutorial on learning with Bayesian networks*, Technical Report MSR-TR-95-06i, Microsoft RESEARCH, 301–354, 1995.

[8] HUGIN EXPERT A/S. *Hugin Help Pages*, URL: [http://www.hugin.dk] Date: 23.05.2000, 1998.

[9] Jensen, F. V. *An introduction to Bayesian Networks*, (UCL Press Ltd., London, 1996).

[10] Jensen, F. V., Olesen, K. G. and Andersen, S. K. *An algebra of Bayesian belief universes for knowledge-based systems*, Networks **20**, 637–659, 1990.

[11] Liarokapis, D. *An introduction to belief networks*, htttp://www.cs.umb.edu/ dimitris, 1999.

[12] Lucas, P. *DAGs in Medicine: a Model-based Approach to Medical Decision Graphs*, (Department of Computing Science, University of Aberdeen, Scotland, UK, 1999).

[13] Niedermayer, D. *An introduction to bayesian networks and their contemporary applications*, (http://www.gpfn.sk.ca/ daryle/papers/bayesian
_networks/bayes html, 1998).

[14] Oliver, R. M. and Smith, J. Q. *Influence Diagrams, Belief Nets and Decision Analysis*, (John Wiley & Sons, New York, 1990).

[15] Pearl, J. *Causality: Models, Reasoning and Inference*, (Cambridge University Press, England, 2000).

[16] Pearl, J. *Bayesian Networks*, (UCLA Cognitive Systems Laboratory, Technical Report (R-246), revision I, 1997).

[17] Pereira, C. A de B. *Medical diagnosis using influence diagrams*, Networks **20**, 565–577, 1990.

[18] Pereira, C. A de B. and Pericchi L. R. *Analysis of diagnosability*, Applied Statistics **39**, No 2, 189–204, 1990.

[19] Przytula, K. W., Dash, D. and Thompson, D. *Evaluation of Bayesian Networks Used for Diagnostics*, (IEEE Aerospace Conference, Big Sky, Montana, 2003).

[20] Spiegelhalter, D. J. and Lauritzen, S. L. *Sequetial updating of conditional probabilities on directed graphical structures*, Networks **20**, 579–605, 1990.

[21] Stephenson, T. A. *An introduction to Bayesian network theory and usage*, (IDIAP Research Report 00-03, 2000).

Hacettepe Journal of Mathematics and Statistics
Volume 33 (2004), 77 – 90

A STATISTICAL MODEL OF OCCUPATIONAL MOBILITY - A SALARY BASED MEASURE

Asis Kumar Chattopadhyay* and Shahjahan Khan†

Received 22 : 08 : 2003 : Accepted 26 : 05 : 2004

Abstract

Mobility models are very useful in explaining the movements of people over socio-economic and job categories. Occupational mobility deals with the movements of individuals over job categories during their employment periods. Since the time interval between successive job changes is a random variable, different occupational mobility models have been developed by scientists using modified Markov and semi-Markov processes. This phenomenon can be modelled by considering the underlying factors such as job satisfaction, salary, distance of the work place, family requirements and others. Unlike most of the previous works in this area, the present study suggests a new measure of occupational mobility based on the distribution of wages. Here a general occupational mobility model has been developed to study the pattern of mobility during the service life of employees. First the probability distribution of the number of job changes in the entire employment life of individuals has been obtained considering the inter-job offer times (within an interval) and the associated wages as random variables. Then a measure of occupational mobility based on this distribution has been developed. The results are obtained under both frequentist and Bayesian frameworks. As an application of the proposed model the results in this paper have been illustrated by using data from a recent survey among the staff members of the University of Southern Queensland, Australia.

Keywords: Occupational mobility; Distribution of wages and job offers; Measure of job changes; Distribution of order statistics; Geometric and Gamma distributions; Survey data.

2000 AMS Classification: Primary 62 P 25, 62-07, Secondary 60 E 05.

*Department of Statistics, Calcutta University, India.
†Department of Mathematics & Computing, University of Southern Queensland, Australia.

1. Introduction

In recent years there has been growing interest in the study of manpower planning. Occupational mobility plays a central role in manpower planning. In broader terms, it refers to the movement of employees between jobs. As a consequence of globalization and the expansion of the job market in the non-traditional sectors, the phenomenon of changing jobs has gained greater attention of the researchers and planners.

Unlike social mobility (cf. Prais, [18]), there is no fixed time interval between successive moves in occupational mobility. Hodge [16] studied occupational mobility as a probability process. Stewman [20] discussed occupational mobility using a Markov model. A comprehensive summary of the theoretical developments and practical applications of occupational mobility have been provided by Stewman [21]. Ginsberg [7–12] has made several attempts to describe occupational mobility patterns in terms of semi-Markov processes.

Bartholomew [2] suggested measures of occupational mobility based on the matrix of transition probabilities and the stochastic process $[m(t)]$, where $m(t)$ is the random number of time points at which individuals decide to change their existing employment during the interval $(0, t)$. Mukherjee and Chattopadhyay [16] developed a measure by considering successive changes in occupation of an individual as constituting a renewal process. Later, Mukherjee and Chattopadhyay [17] proposed a measure based on the reward structure. Chattopadhyay and Baidya [3] considered salary based occupational categories to study social mobility. Khan and Chattopadhyay [14] developed a predictive measure of occupational mobility based on the number of job offers. None of the measures available in the literature has taken into account the explicit role of the reward (remuneration) associated with job offer that directly influences the pattern of job changes.

In this study we propose a new measure of occupational mobility based on the number of job changes and the associated wages. The distribution of the total number of job changes during an individual's entire service life up to the point of study has been derived by considering times between consecutive job offers (within an interval) and the corresponding wages to be independent random variables. The proposed measure of occupational mobility based on the number of job offers and wage distribution has been suggested primarily in the general setup and then it's value has been derived for special situations where some specific assumptions regarding the number of job offers and wage distributions has been made, both under frequentist and Bayesian frameworks.

A survey has been conducted among the staff members of the University of Southern Queensland, Australia to collect data on occupational mobility. The proposed model has been fitted to the survey data to explain the occupational mobility pattern among the employees of the University. For this particular application of the occupational mobility model the number of job offers has been found to best fit the geometric distribution, and the wages best fit a gamma distribution.

The occupational mobility model has been defined and discussed in section 2. The distribution of the number of job changes is obtained in section 3. Section 4 derives a measure of occupational mobility under the general distributional setup. Some special cases for particular choices of number of job offers and wages distributions have been discussed in sections 5 and 6, under frequentist and Bayesian frameworks, respectively. Section 7 is devoted to the analysis of the survey data, and its fitting to the proposed model and measure.

2. The Model

Let the service life of an individual be comprised of k intervals of equal fixed width, t. The individual gets at least one job offer within each such interval, the worth of an offer being determined by the associated salary (reward). The individual (assumed to be in service already) decides to leave the present job or not, at the end of each interval. One moves to a new job for the first time at the end of an interval in which the maximum of the remunerations associated with different job offers (within that interval) exceeds a fixed amount. This is the minimum wage at which the individual is willing to enter the job market for the first time.

Subsequently, one changes the current job at the end of a particular interval only when the maximum of the wages associated with the offers received during that interval exceeds the wage of the current job. A change of job in this paper means that an individual may move from one occupation to another or within the same occupation.

Let the individual get N_i new job offers in the i^{th} interval, and let X_{ij} be the salary corresponding to the j^{th} job offer in the i^{th} interval, for $j = 1, 2, \ldots, n_i$, and $i = 1, 2, \ldots, k$. Note that to reflect the real life situation it is necessary to assume that n_i is strictly greater than zero since no one can enter into the job market without a job offer. Both X_{ij} and N_i are assumed to be independently and identically distributed with pdf $g(x)$, $0 < x < \infty$, and pmf $h(y)$, $y = 1, 2, \ldots, \infty$ respectively. Define

$$Z_i = \max(X_{i1}, X_{i2}, \ldots, X_{in_i}). \tag{2.1}$$

Here Z_i is the maximum wage of all job offers during the i^{th} interval. Since Z_i is the largest order statistic, for a given n_i, the pdf of the conditional distribution of Z_i is

$$f(z_i|n_i) = n_i[G(x_{ij})]^{n_i-1}g(z_i),$$

where $G(\cdot)$ is the cdf of the distribution of X_{ij}. The pdf of the joint distribution of Z_i and N_i becomes

$$f(z_i, n_i) = n_i[G(x_{ij}]^{n_i-1}g(z_i)h(n_i).$$

Hence the marginal distribution of Z_i is given by

$$f(z_i) = \sum_{n_i=1}^{\infty} n_i[G(z_i)]^{n_i-1}g(z_i)h(n_i), \tag{2.2}$$

where $g(\cdot)$ and $h(\cdot)$ have the same specifications as before.

Let $F_{Z_i}(z)$ denote the the corresponding cdf. Let z_0 be the minimum wage for which the individual accepts the first job offer at the i^{ih} interval. Then we can define

$$F_{Z_i}(z_0) = P[Z_i < z_0] \tag{2.3}$$

and its complement

$$\overline{F}_{Z_i}(z_0) = 1 - F_{Z_i}(z_0) = P[Z_i > z_0]. \tag{2.4}$$

3. Distribution of the number of job changes

In this section we derive the distribution of the number of job changes during the service life of an individual. Define $N(k)$ = total number of job changes within the service life of the individual and $p_r^{(k)}$ = the probability of r job changes in the entire service life of the individual. Then

$$p_r^{(k)} = P[N(k) = r]. \tag{3.1}$$

3.1. Theorem. *Under the above definition of* $F_{Z_i}(z_0)$ *and* $p_r^{(k)}$*, we have*

$$p_r^{(k)} = \begin{cases} F^k & \text{if } r = 0, \\ F^{k-1}\bar{F}[\sum_{m=0}^{k-r} \binom{r+m-1}{m}(2F)^{-(r+m-1)}] & \text{if } 1 \le r \le k \end{cases} \tag{3.2}$$

where, for notational convenience, we write $F = F_{Z_i}(z_0)$ *and* $\bar{F} = 1 - F_{Z_i}(z_0)$.

Proof. (Outline) Note that $P[Z_i > Z_j] = P[Z_i < Z_j] = 0.5$ for $i, j = 1, 2, \ldots, k,$, $i \neq j$; and

$$P[Z_i > \max(Z_1, Z_2, \ldots, Z_{i-1})] = P[Z_i < \max(Z_1, Z_2, \ldots, Z_{i-1}] = 0.5 \tag{3.3}$$

Now define S_i as the event that there is a job change in the i^{th} time interval which depends only on the maximum wages of the i^{th} and $(i-1)^{th}$ time intervals, for $i = 1, 2, \ldots, k$ and T_i as the event that there is a job change in the i^{th} interval which depends on the maximum wages of all intervals up to the i^{th} including z_0, the initial minimum acceptable wage, for $i = 2, 3, \ldots, k$, that is

$$S_i = [z_i > z_{i-1}], \text{ for } i = 1, 2, \ldots, k \text{ and}$$
$$T_i = [z_i > \max(z_0, z_1, \ldots, z_{i-1})], \text{ for } i = 2, 3, \ldots, k.$$

Then $p_r^{(k)}$ can be obtained by adding together the probabilities of the $(k - r + 1)$ events E_0, $E_1 \ldots, E_{k-r}$, where

E_0 = there is no change in the first $(k - r)$ intervals and r changes in the last r intervals.

E_1 = there is no change in the first $(k - r - 1)$ intervals, one change at the $(k - r)^{th}$ interval and $(r - 1)$ changes among the last r intervals.

E_2 = there is no change in the first $(k-r-2)$ intervals, one change at the $(k-r-1)^{th}$ interval and $(r - 1)$ changes among the last $(r + 1)$ intervals.

. . . . . .

E_{k-r} = there is a change at the first interval and $(r - 1)$ changes among the last $(k - 1)$ intervals.

Let S^c denote the complement of the event S. Then from the fundamental rule of probability we have

$$\begin{aligned} P(E_0) &= P[S_1^c S_2^c \cdots S_{k-r}^c T_{k-r+1} S_{k-r+1} \cdots S_k] \\ &= F^{k-r}\bar{F}(0.5)^{r-1} \end{aligned} \tag{3.4}$$

Similarly,

$$P(E_1) = F^{k-r-1}\bar{F}\binom{r}{1}(0.5)^r$$

$$P(E_2) = F^{k-r-2}\bar{F}\binom{r+1}{2}(0.5)^{r+1}$$

. . . . . .

$$P(E_{k-r}) = \overline{F}\binom{r + (k-r-1)}{k-r}(0.5)^{r+(k-r-1)} \tag{3.5}$$

Hence the proof is completed by adding the above probabilities. □

3.2. Illustration. Consider the situation when $k = 3$ and $r = 2$.

$$\begin{aligned} p_2^{(3)} &= P(S_1S_2S_3^c) + P(S_1S_2^cT_3) + P(S_1^cT_2S_3) \\ &= P(Z_1 > z_0)P(Z_2 > Z_1)P(Z_3 < Z_2) \\ &\quad + P(Z_1 > z_0)P(Z_2 < Z_1)P(Z_3 > Z_1) + P(Z_1 < z_0)P(Z_2 > z_0)P(Z_3 > Z_2) \\ &= \overline{F}(0.5)(0.5) + \overline{F}(0.5)(0.5) + F\overline{F}(0.5) \\ &= (0.5)\overline{F}(1+F) \end{aligned} \tag{3.6}$$

When $r = 0$,

$$\begin{aligned} p_0^{(3)} &= P(S_1^cS_2^cS_3^c) \\ &= P(Z_1 < z_0)P(Z_2 < z_0)P(Z_3 < z_0) = F^3 \end{aligned} \tag{3.7}$$

3.3. Theorem. *Under the above setup, $p_r^{(k)}$ is a probability distribution, i.e.*

$$\sum_{r=0}^{k} p_r^{(k)} = 1 \tag{3.8}$$

Proof. Write $s = r + m - 1$. Then

$$\begin{aligned} \sum_{r=0}^{k} p_r^{(k)} &= F^k + F^{k-1}\overline{F}\left[\sum_{r=1}^{k}\sum_{m=0}^{k-r}\binom{r+m-1}{m}(0.5F)^{(r+m-1)}\right] \\ &= F^k + F^{k-1}\overline{F}\left[\sum_{s=0}^{k-1}(0.5F)^s\sum_{m=0}^{s}\binom{s}{m}\right] = F^k + F^{k-1}\overline{F}\left[\sum_{s=0}^{k-1}(0.5F)^s 2^s\right] \\ &= F^k + F^{k-1}\overline{F}\left[\sum_{s=0}^{k-1}(1/F)^s\right] = F^k + 1 - F^k = 1. \end{aligned} \tag{3.9}$$

□

4. A Measure of Occupational Mobility

In this section we obtain a measure of occupational mobility using $p_r^{(k)}$ as defined in section 3. From the previous specifications the moments of the number of job changes are reasonable choices as measures of occupational mobility. For practical reasons, the first raw moment has better intuitive appeal in interpreting the phenomenon of job changes than any other moment. Therefore, we suggest, the expectation of the number of job changes can be considered as a measure of occupational mobility. This should of course be normalized with respect to k. Then we have

$$\begin{aligned} \mathrm{E}[N(k)] &= \sum_{r=0}^{k} r p_r^{(k)} \\ &= F^{k-1}\overline{F}\sum_{r=1}^{k}\sum_{m=0}^{k-r} r C_m^{(r+m-1)}(0.5F)^{r+m-1} \\ &= [(k+1)\overline{F} - \overline{F}F^k - F(1-F^k)]/2\overline{F}. \end{aligned} \tag{4.1}$$

In the computation of $\mathrm{E}[N(k)]$ various binomial and geometric series are involved. After normalization with respect to k, the measure becomes $\mathrm{E}[N(k)/k]$.

In a similar way it can be shown that,

$$\mathrm{E}[\{N(K)\}^2] = (0.25)F^{k-1}\overline{F}\sum_{s=0}^{k-1}(1/F)^s(s^2+5s+4). \tag{4.2}$$

Hence the variance of $N(k)$, $\mathrm{Var}[N(k)]$, is readily available from (4.1) and (4.2). As a measure of spread of the above measure of occupational mobility one uses the estimated value of $\mathrm{Var}[N(k)]/k^2$. Computing procedures for $\mathrm{E}[N(k)]$, and $\mathrm{Var}[N(k)]$ are given in section 7.

5. Some special cases

Case 1: To compute the measure of mobility, in this section, we consider specific distributions for the number of job offers and for the wages. Consider the situation where the distribution of wages is exponential and the distribution of the number of job offers is truncated Poisson with the following pdf and pmf respectively,

$$g(x) = \theta \mathrm{e}^{-\theta x}, \quad 0 < x < \infty \tag{5.1}$$

and

$$h(y) = [1/(1 - \mathrm{e}^{-\lambda t})]\mathrm{e}^{-\lambda t}(\lambda t)^y/y!, \quad y = 1, 2, \ldots, \infty. \tag{5.2}$$

Note that $y = 0$ is not a valid value of the number of job offers since by assumption the study includes only those individuals who received at least one job offer. Then from (2.2) the pdf of the distribution of Z_i is

$$f(z_i) = [1/(1 - \mathrm{e}^{-\lambda t})]\lambda t\theta \mathrm{e}^{-(\theta z_i + \lambda t)}\mathrm{e}^{\lambda t}(1 - \mathrm{e}^{-\theta z_i}), \quad 0 < z_i < \infty, \tag{5.3}$$

and the corresponding cdf is

$$F_{Z_i}(z) = [1/(1 - \mathrm{e}^{-\lambda t})](\mathrm{e}^{-\lambda t\mathrm{e}^{-\theta z}} - \mathrm{e}^{-\lambda t}). \tag{5.4}$$

Hence from (3.2) and (3.3) we have

$$p_r^{(k)} = \begin{cases} ((\mathrm{e}^{-\lambda t\mathrm{e}^{-\theta z_0}} - \mathrm{e}^{-\lambda t})/(1 - \mathrm{e}^{-\lambda t}))^k & \text{if } r = 0, \\ \left[\frac{(1-\mathrm{e}^{\lambda t\mathrm{e}^{-\theta z_0}})(\mathrm{e}^{-\lambda t\mathrm{e}^{-\theta z_0}} - \mathrm{e}^{-\lambda t})^{k-1}}{(1-\mathrm{e}^{-\lambda t})^k}\right] & \\ \times \left[\sum_{m=0}^{k-r} \binom{r+m-1}{m} \left(\frac{(1-\mathrm{e}^{-\lambda t})}{2(\mathrm{e}^{-\lambda t\mathrm{e}^{-\theta z_0}} - \mathrm{e}^{-\lambda t})}\right)^{r+m-1}\right] & \text{if } 1 \le r \le k. \end{cases} \tag{5.5}$$

Now, from (5.4), (4.1) becomes

$$\mathrm{E}[N(k)] = \left[(k+1) - (k+2)\frac{\mathrm{e}^{-\lambda t\mathrm{e}^{-\theta z_0}} - \mathrm{e}^{-\lambda t}}{(1 - \mathrm{e}^{-\lambda t})} + \frac{(\mathrm{e}^{-\lambda t\mathrm{e}^{-\theta z_0}} - \mathrm{e}^{-\lambda t})}{(1 - \mathrm{e}^{-\lambda t})} \times \eta_1\right] \times \eta_2, \tag{5.6}$$

where

$$\eta_1 = \frac{2(\mathrm{e}^{-\lambda t\mathrm{e}^{-\theta z_0}} - \mathrm{e}^{-\lambda t})}{(1 - \mathrm{e}^{-\lambda t})} - 1, \quad \eta_2 = \frac{1 - \mathrm{e}^{-\lambda t}}{2(1 - \mathrm{e}^{-\lambda t\mathrm{e}^{-\theta z_0}})}. \tag{5.7}$$

Given the values of the parameters λ and θ one can compute the value of the above measure of occupational mobility for different choices of t. The parameters can be estimated from the sample data. For details refer to Cohen [4].

Case 2: Here we take the distribution of wages as exponential and the number of job changes as truncated Binomial. For the above choices we have

$$g(x) = \theta \mathrm{e}^{-\theta x}, \quad 0 < x < \infty, \tag{5.8}$$

and

$$h(y) = (1/(1 - q^{kt}))\binom{kt}{y} p^y q^{kt-y}, \quad y = 1, 2, \ldots, kt, \tag{5.9}$$

where $q = 1 - p$.

Then from (2.2) the pdf of the distribution of Z_i is given by

$$f(z_i) = [(\theta q^{kt-1})/(1-q^{kt})]\mathrm{e}^{-\theta z_i} kt(p/q) \sum_{n_{1i}=0}^{kt-1} \binom{kt-1}{n_{1i}} [(p/q)(1-\mathrm{e}^{-\theta z_i})]^{n_{1i}}, \tag{5.10}$$

where $n_{1i} = n_i - 1$ and the corresponding cdf is given by

$$F(z) = [(\theta kt q^{kt})/(1-q^{kt})] \sum_{n_{1i}=0}^{kt-1} (p/q)^{n_{1i}+1} \int_0^z \mathrm{e}^{-\theta z}(1-\mathrm{e}^{-\theta z})^{n_{1i}} dz. \tag{5.11}$$

Hence following the same procedure as in case 1, $E[N(k)/k]$ can be computed for given values of the parameters θ and p.

6. Special cases under the Bayesian framework

The occupational mobility measure for the above special cases of the distributions of job offers and wages are obtained here under the Bayesian framework.

Case 1: Consider the special case 1 of section 5 with

$$g(x) = \theta \mathrm{e}^{-\theta x}, \quad 0 < x < \infty, \quad \theta > 0. \tag{6.1}$$

Taking the conjugate prior associated with the Poisson distribution, λ has the following pdf,

$$p(\lambda) = (1/\beta^{\alpha}\Gamma\alpha)\mathrm{e}^{-\lambda/\beta}\lambda^{\alpha-1}, \quad \alpha > 0,\ \beta > 0, \quad 0 < \lambda < \infty. \tag{6.2}$$

For a fixed value of λ, the joint pmf of the distribution of N_i on the basis of a sample of size m is given by,

$$h(y|\lambda) = [1/(1-\mathrm{e}^{-\lambda t})^m]\mathrm{e}^{-m(\lambda t)}(\lambda t)^{\sum_{i=1}^m y_i}/\Pi_{i=1}^m (y_i!) \tag{6.3}$$

and hence the Bayes estimator of λ is obtained as,

$$\begin{aligned} \lambda^B &= \frac{1}{t} \times \frac{\int \lambda h(y|\lambda)p(\lambda)d\lambda}{(\int h(y|\lambda)p(\lambda)d\lambda)} \\ &= \frac{1}{t} \frac{[\Gamma(\sum y_i + \alpha + 1)/(m+\frac{1}{\beta})^{\sum y_i+\alpha+1}] + \Omega_1}{[\{\Gamma(\sum y_i + \alpha)/(m+\frac{1}{\beta})^{\sum y_i+\alpha}\} + \Omega_2]}, \end{aligned} \tag{6.4}$$

where

$$\Omega_1 = \sum_{j=1}^{\infty} \left[(1/j!)m(m+1)\ldots(m+j-1) \left(\frac{\Gamma(\sum y_i + \alpha + 1)}{(m+\frac{1}{\beta}+j)^{\sum y_i+\alpha+1}} \right) \right],$$

$$\Omega_2 = \sum_{j=1}^{\infty} \left[(1/j!)m(m+1)\ldots(m+j-1) \left(\frac{\Gamma(\sum y_i + \alpha)}{(m+\frac{1}{\beta}+j)^{\sum y_i+\alpha}} \right) \right].$$

Note that λ^B can be estimated from the sample values of y_i for some known values of the prior parameters α and β.

Hence $E[N(k)]$ in (5.6) can be estimated by replacing λ with λ^B. If needed, starting with initial values of α and β (say α_0 and β_0) one can generate a sample from the gamma distribution with parameters α_0 and β_0 and on the basis of the simulated sample α and β can be estimated.

Case 2: Considering the special case 2 of section 5 we have

$$g(x) = \theta \mathrm{e}^{-\theta x}, \quad 0 < x < \infty \quad \theta > 0. \tag{6.5}$$

Assuming that p is a random variable, using the conjugate prior associated with the Binomial distribution, p has the following pdf

$$p^*(p) = [1/B(a,b)]p^{a-1}(1-p)^{b-1}, \quad 0 < p < 1,\ a > 0,\ b > 0. \tag{6.6}$$

Given p, the joint pmf of the distribution of N_i for a sample of size m is given by

$$h(y_i|p) = [1/(1-(1-p)^{kt})^m] \prod_{i=1}^{m} \binom{kt}{y_i} p^{\sum y_i}(1-p)^{mkt-\sum y_i}, \tag{6.7}$$

where $y_i = 1, 2, \ldots, kt$. The Bayes estimator of p is found to be

$$p^B = \frac{B(a+\sum y_i+1, b+mkt-\sum y_i)+\Psi_1}{B(a+\sum y_i, b+mkt-\sum y_i)+\Psi_2}, \tag{6.8}$$

where

$$\Psi_1 = \sum_{j=1}^{\infty} \frac{m(m+1)\ldots(m+j-1)B(a+\sum y_i+1, b+kt(m+j)-\sum y_i)}{j!}$$

$$\Psi_2 = \sum_{j=1}^{\infty} \frac{m(m+1)\ldots(m+j-1)B(a+\sum y_i, b+kt(m+j)-\sum y_i)}{j!}.$$

Note that p^B can be estimated from the sample values of y_i for some given values of the prior parameters a and b. Hence $E[N(k)]$ can be estimated by replacing p with p^B in (5.11). If needed, one can generate a sample from the Beta distribution with initial values a_0 and b_0 as parameters and on the basis of that simulated sample a and b can be estimated.

7. Modelling Survey Data

With a view to applying the proposed measure of occupational mobility, a survey among the employees of the University of Southern Queensland (USQ), Australia was conducted. The main objective of the survey was to gather data on the number of job offers received by the individual employees during the entire employment period, including the offer(s) of the current employer. In addition, wages associated with each of the job offers for the employees were collected. The data on the number of job offers and the associated wages have been classified according to the staff category, academic and non-academic, as well as gender, male and female. Separate analysis of the data have been provided based on the above four categories and the values of the proposed measure of occupational mobility have been obtained for all those cases. An overall analysis of the data from all the respondents across the categories has been also been provided.

The sample consisted of 221 employees of the USQ. This comprises of 83 academic and 138 non-academic staff. Among these respondents there were 93 males and 128 females. In the survey we limited the maximum number of offers for any individual to 20 and the range of wages has been equally divided into 6 intervals. In the computation of the measure of occupational mobility and all associate functions as well as fitting of different distributions we have used the MATLAB and SPSS packages. Some Pascal programming has also been used for the fitting of the distribution.

7.1. The Survey. The general distribution of the survey data with respect to the number of job offers and associated wages is provided in this subsection. Table 1 below represents the means and standard deviations of the number of job offers of the respondents by various categories.

Table 1. Summary Statistics of the Number of Job Offers by Gender and Staff Category

	Academic			Non-Academic			Total		
	Count	Mean	Std.	Count	Mean	Std.	Count	Mean	Std.
Male	58	5.40	4.26	35	6.20	4.31	93	5.70	4.27
Female	25	6.20	4.07	103	5.60	4.24	128	5.72	4.20
Total	83	5.64	4.20	138	5.75	4.25	221	5.71	4.22

The average number of job offers received by the employees in the sample is 5.71. The corresponding figure for the academics is 5.64 and that of the non-academics is 5.75. Thus the average number of job offers for non-academics is slightly higher than the academics. The female respondents have a higher average number of job offers than their male counterparts, although the difference is negligible. However, a clear dominance of the females with respect to the average number of job offers over the males is observed

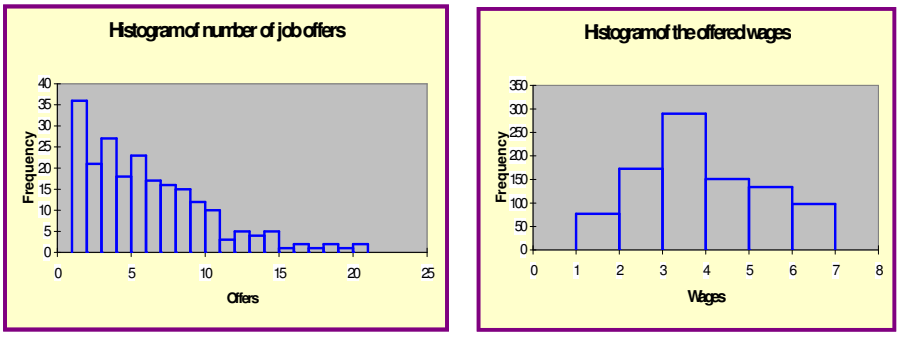

The distributions of the number of job offers and the wages are given in Figure 1. The first graph in Figure 1 shows that the distribution of the number of job offers is highly skewed to the right. From the shape of the distribution it appears that the geometric distribution would be an appropriate model for the data.

The second graph gives the observed distribution of the wages of all employees.

7.2. Fitting of Distributions. First we have fitted the geometric distribution with pmf

$$h(y) = p(1-p)^{y-1}, \quad y = 1, 2, 3, \ldots, \infty \tag{7.1}$$

to the number of job offers for all respondents as well as by all the categories. Here the estimate of the parameter p is $\hat{p} = \frac{1}{\bar{y}}$ where $\bar{y}$ is the sample mean of the observed number of job offers.

From Table 2 it is evident that the data fit very well with the geometric distribution for all respondents as well over all the categories.

Table 2. Table of Expected and Observed Frequency Distributions of Job Offers by Gender and Staff Category

	Academics		Non-Acads.		Male		Female		Total	
Offers	Exp.	Obs.	Exp.	Obs.	Exp.	Obs.	Exp.	Obs.	Exp.	Obs.
1	15	12	25	24	16	15	22	21	36	39
2	12	9	20	12	13	8	18	13	21	32
3	10	11	17	16	11	14	15	13	27	26
4	8	6	14	12	9	7	13	11	18	22
5	7	11	11	12	8	9	10	14	23	18
6	6	5	9	12	6	8	9	9	17	15
7	5	7	8	9	5	6	7	10	16	12
8	4	6	6	9	4	6	6	9	15	10
9	3	3	5	9	3	5	5	7	12	8
10	3	4	4	6	3	3	4	7	10	7
11	2	2	3	1	2	1	3	2	3	6
12	2	1	3	4	2	3	3	2	5	5
13	1	0	2	4	2	2	2	2	4	4
14	1	2	2	3	1	2	2	3	5	3
15	1	0	2	1	1	0	2	1	1	3
16	1	2	1	0	1	2	1	0	2	2
17	1	0	1	1	1	0	1	1	1	2
18	1	1	1	1	1	1	1	1	2	1
19	0	0	1	1	1	0	1	1	1	1
20	0	1	1	1	0	1	1	1	2	1

Then we have fitted the gamma distribution with pdf

$$g(x) = \frac{1}{\beta^{\alpha}\Gamma(\alpha)} \mathrm{e}^{-\frac{x}{\beta}} x^{\alpha-1}, \quad 0 < x < \infty,\ \alpha > 0,\ \beta > 0 \tag{7.2}$$

to the wages for all respondents as well as by all the categories. Salem and Mount [19], and McDonald and Jensen [15] used gamma distribution to model the distribution of income. The estimates of the parameters α and β are $\hat{\alpha} = [\frac{\bar{x}}{s_x}]^2$ and $\hat{\beta} = [\frac{{s_x}^2}{\bar{x}}]$ respectively where $\bar{x}$ is the sample mean of the observed wages and s_x is the corresponding standard deviation. For further details see Cohen and Whitten [5]. Angle [1] used the two parameter gamma distribution to model the income distributions of blacks and the whites.

From Table 3 it is observed that the data fit more or less well with the gamma distribution for all respondents as well as over all the categories.

Table 3. Table of Expected and Observed Frequency Distributions of Wages by Gender and Staff Category

	Academics		Non-Acads		Male		Female		Total	
Wages	Exp.	Obs.	Exp.	Obs.	Exp.	Obs.	Exp.	Obs.	Exp.	Obs.
0	0	0	0	0	0	0	0	0	0	0
1	2	27	11	48	1	25	10	50	10	77
2	38	41	123	127	21	25	114	146	130	173
3	89	67	198	223	85	94	180	193	262	290
4	94	62	139	89	119	88	124	63	244	151
5	64	80	63	52	95	98	55	34	153	134
6	34	70	22	25	53	79	19	17	75	98

Figure 2 displays the observed and fitted distributions of the number of job offers and wages of all respondents.

Figure 2. Graphs of Observed and Fitted Distributions of Job Offers and

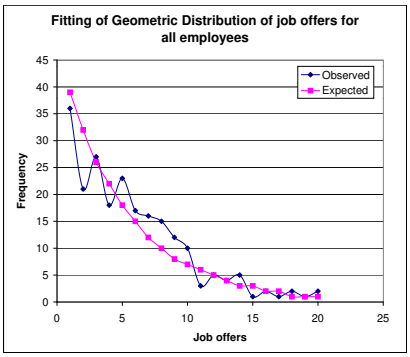

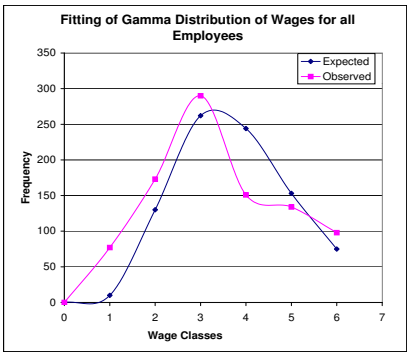

Looking at the observed and the fitted distributions of the number of job offers in the first graph it is evident that the geometric distribution fits the data very well. The same feature of the distributions of job offers for different categories of respondents is observed from Figure 3.

Figure 3. Graphs of Observed and Fitted Distributions of Job Offers by

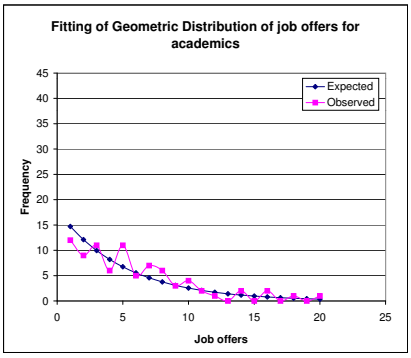

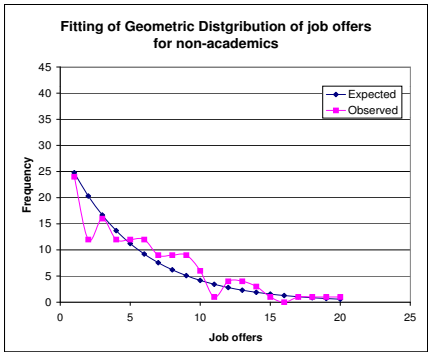

The graphs of the observed and fitted distributions of job offers by gender are given in Figure 4.

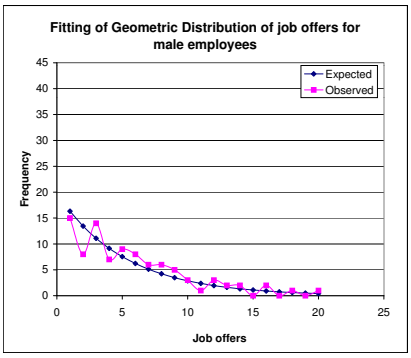

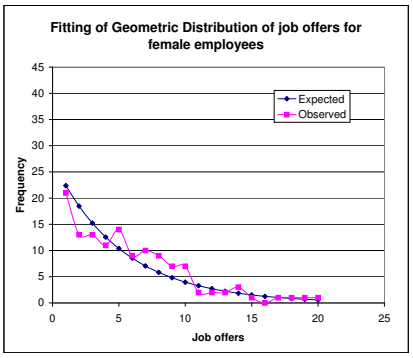

In all the above mentioned graphs the geometric distribution provide a better fit than any other distribution for the number of job offers. The distributions of the observed and the expected values of the wages are given in Figure 5.

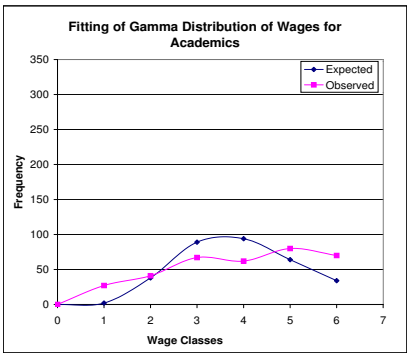

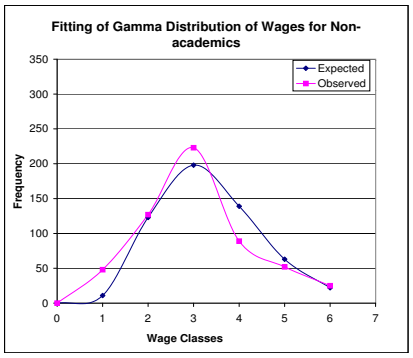

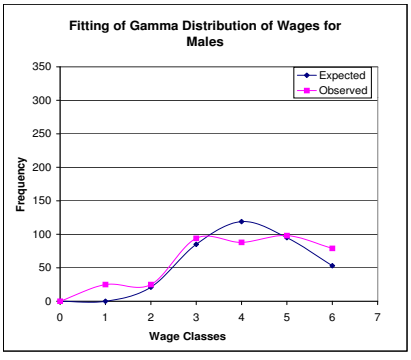

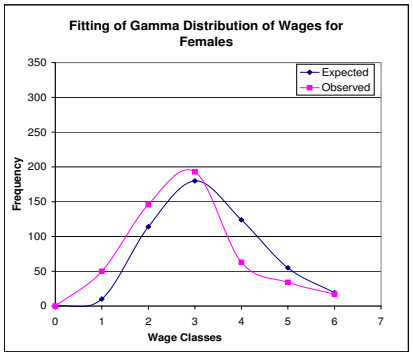

It is observed that the gamma distribution fits very well to the observed data for the non-academics and the female employees. Although for the other categories of respondents

the fitting is not as good. Figure 1 displays that the observed data for the wages show some irregular pattern at some points. Hence the fitting of the gamma distribution is not so good for some parts in the right side of the distribution when all respondents are considered. Nonetheless empirically the gamma distribution provides a better fit than all other relevant distributions.

7.3. Computation of the Measure. Here we derive the expression for the measure of the occupational mobility under the above specifications of distribution of the number of job offers and wages. We also compute the values of the measure as well as the variance of the number of job changes during the employment period for all respondents. The same is also obtained for different categories of respondents to compare the mobility of employees over categories.

From (2.2), assuming α to be an integer (cf. Evan et al. [6], for instance), the pdf of the distribution of the maximum wage is

$$f(z_i) = \frac{1}{\beta^\alpha \Gamma(\alpha)} p e^{-\frac{z_i}{\beta}} z_i^{\alpha-1} \left[(1-p) \left(1 - \mathrm{e}^{-\frac{z_i}{\beta}} \sum_{r=0}^{\alpha-1} \frac{1}{r!} \left\{ \frac{z_i}{\beta} \right\}^r \right) \right]^{n_i - 1} \tag{7.1}$$

and the corresponding cdf is given by

$$F(z_0) = p \sum_{k=1}^{\infty} k(1-p)^{k-1} \tau_k(\alpha,\ \beta,\ \ z_0), \tag{7.2}$$

where

$$\tau_k(\alpha,\ \beta,\ \ z_0) = \int_0^{z_0} \frac{1}{\beta^\alpha \Gamma(\alpha)} \mathrm{e}^{-\frac{z_i}{\beta}} z_i^{\alpha-1} \left(1 - \mathrm{e}^{-\frac{z_i}{\beta}} \sum_{r=0}^{\alpha-1} \frac{1}{r!} \left\{ \frac{z_i}{\beta} \right\}^r \right)^{k-1} dz_i. \tag{7.3}$$

Table 4. Table of the Empirical Distribution Function, the Expectation, Variance of Job Changes and the Measure of Mobility by Different Categories

Variable	$\hat{\alpha}$	$\hat{\beta}$	$\hat{p}$	$F(z_0)$	$E[N(k)]$	$Var[N(k)]$	$E[\frac{N(k)}{k}]$
Academic	6.54	0.61	0.1773	0.00060	10.49969	4.73451	0.52498
Non-Acad.	6.38	0.48	0.1795	0.00200	10.49883	4.75000	0.52494
Male	8.23	0.50	0.1754	0.00020	10.49992	4.75000	0.52500
Female	6.00	0.48	0.1748	0.00400	10.49809	4.75000	0.52490
Overall	5.70	0.60	0.1751	0.00200	10.49896	4.75000	0.52495

Table 4 describes the expectation and variance of the number of job changes for all respondents as well as for the different categories, and the values of the proposed measure. From the expected values it appears that for any particular individual, on the average, the number of job offers with wage associated with a new job offer exceeding the maximum wage earned from a previous offer is a little over 10. The computed values of the measure for the survey data enable us to infer that an employee is more mobile (than expected in the job market) during his occupational life depending on whether the observed value of the measure (computed on the basis of the employee's job changes) exceeds the above computed value of the measure. This is valid under the assumption that the job changes occur only on the basis of wage consideration and for specific values of t and k. The same conclusion can be extended over all the categories considered in the study. The measure reveals the fact that the expected number of job changes is about the same for all employees regardless of gender and staff category.

Acknowledgement The authors offer sincere gratitude to the Department of Mathematics and Computing, Faculty of Sciences, University of Southern Queensland, Australia for its financial support to cover the cost of the visit of the first author and providing excellent computing facilities during the visit. Special thanks go to all the participating staff of the USQ for responding to the survey.

References

[1] Angle, J. *The inequality process and the distribution of income to blacks and whites*, Journal of Mathematical Sociology **17** (1), 77–98, 1992.
[2] Bartholomew, D. J. *Stochastic Models for Social Processes*, (Wiley, New York, 1982).
[3] Chattopadhyay, A. K.,and Baidya, K. *Social mobility among residents of Calcutta*, Demography India **28**, 215–224, 1999.
[4] Cohen, A. C. *Truncated and Censored Samples*, (Mercell Dekker, New York, 1991).
[5] Cohen, A. C. and Whitten, B. J. *Parameter Estimation in Reliability and Life Span Models*, (Mercell Dekker, New York, 1988).
[6] Evans, M., Hestings, N., and Peacock, B. *Statistical Distributions*, (Wiley, New York, 1993).
[7] Ginsberg, R. B. *Semi-Markov processes and mobility*, Journal of Mathematical Sociology **1**, 233–262, 1971.
[8] Ginsberg, R. B. *Critique of probabilistic models: application of semi-Markov model to migration*, Journal of Mathematical Sociology **2**, 63–82, 1972.
[9] Ginsberg, R. B. *Incorporating causal structure and exogeneus information with probabilistic models: with special reference to gravity, migration and Markov chains*, Journal of Mathematical Sociology **2**, 83–103, 1972.
[10] Ginsberg, R. B. *The relationship between timing of moves and choice of destination in stochastic models of migration*, Environment and Planning **10**, 667–679, 1978.
[11] Ginsberg, R. B. *Stochastic Models of Migration: Sweden 1961–1975*, (North Holland, New York, 1979).
[12] Ginsberg, R. B.(1979b), *Tests of stochastic models of timing in mobility histories:comparison of information derived from different observation plans*, Environment and Planning **11**, 1387–1404, 1979.
[13] Hodge, R. W. *Occupational mobility as a probability process*, Demography **3**, 19–34, 1966.
[14] Khan, S. and Chattopadhyay, A. K. *Predictive analysis of occupational mobility*, Journal of Applied Statistical Science **12** (1), 11–22, 2003.
[15] McDonald, J. and Jensen, B. *An analysis of some properties of alternative measures of income inequality based on the gamma distribution*, Journal of the American Statistical Association **47**, 856–860, 1979.
[16] Mukherjee, S. P. and Chattopadhyay, A. K. *Renewal theoretic measurement of occupational mobility*, Calcutta Statistical Association Bulletin **34**, 207–213, 1985.
[17] Mukherjee, S. P. and Chattopadhyay, A. K. *Measurement of occupational mobility using semi Markov models*, Communications in Statistics, Theory and Methods **18** (5), 1961–1978, 1989.
[18] Prais, S. J. *Measuring social mobility*, Journal Royal Statistical Soc. **118A**, 56–66, 1955.
[19] Salem, A. B. Z. and Mount, T. D. *A convenient descriptive model of income distribution: The gamma density*, Econometrica **42**, 1115–1127, 1974.
[20] Stewman, S. *Two Markov models of system occupational mobility: Underlying conceptualization and empirical tests*, American Sociological Review **40**, 298–321, 1975.
[21] Stewman, S. *Markov models of occupational mobility: theoretical development and empirical support (part 1)*, Journal of Mathematical Sociology **4** (2), 203–245, 1976.

Hacettepe Journal of Mathematics and Statistics
Volume 33 (2004), 91 – 96

DETERMINATION OF COMPROMISE INTEGER STRATA SAMPLE SIZES USING GOAL PROGRAMMING

Mustafa Semiz*

Received 15 : 09 : 2003 : Accepted 03 : 11 : 2004

Abstract

This article deals with the determination of compromise integer strata sample sizes using goal programming in multivariate stratified sampling. Firstly, the problem of determining optimum integer strata sample sizes is formulated for the univariate case, and then based on these individual optimal solutions, individual goal variances are calculated. A new compromise criteria is defined for the goal programming approach based on predetermined or calculated goal variances. It is shown that the proposed approach provides relatively more efficient and feasible compromise integer strata sample sizes for multivariate surveys.

Keywords: Stratified sampling, Compromise allocation, Goal programming, Relative efficiency.

1. Introduction

Several alternative compromise criteria and methods have been suggested in order to determine strata sample sizes for multivariate surveys by authors such as Neyman [6], Cochran [2], Chatterjee [1], Kokan and Khan [5], Sukhatme, Sukhatme, Sukhatme, and Asok [8], Jahan, Khan, and Ahsan [3], Khan, Ahsan, and Jahan [4], etc. Determining the compromise strata sample sizes in multivariate stratified sampling has been commonly called compromise allocation. If the total sample size is known and this sample size is divided among stratum, it is called an allocation procedure. However, this study is intended to determine strata sample sizes directly, and the proposed goal programming approach does not involve any allocation techniques. The problem of determining compromise strata sample sizes may be defined as a goal programming problem, since it consists of multiple objectives. In this study, the compromise criteria is the sum of the

*Selçuk University, Faculty of Art and Sciences, Department of Statistics, Konya, Turkey.
E-mail : msemiz@selcuk.edu.tr

proportional increase in variances resulting from absolute deviations from the individual desired variances over all k characteristics. The criterion is formulated as

$$\text{minimize} \sum_{j=1}^{k} \frac{\left|V_{\text{comp}}(\bar{y}_j) - V_d(\bar{y}_j)\right|}{V_d(\bar{y}_j)}, \tag{1.1}$$

where $V_{\text{comp}}(\bar{y}_j)$ is the variance of the sample mean of the jth characteristic under optimum compromise integer strata sample sizes (n_h^*), and $V_d(\bar{y}_j)$ is the desired variance of the sample mean of the jth characteristic under optimum individual strata sample sizes (n_{jh}) in the hth strata. The desired individual variance $V_d(\bar{y}_j)$ can be either predetermined or calculated. If one has no idea how to predetermine $V_d(\bar{y}_j)$, the minimum value of the individual variances $V_{\min}(\bar{y}_j)$ can be used instead of the desired variance $V_d(\bar{y}_j)$. In the first step, the desired individual optimal variances should be predetermined or calculated as $V_{\min}(\bar{y}_j)$ for every characteristic.

2. The individual optimal integer strata sample sizes

The most popular way of calculating the individual optimal strata sample sizes for the jth characteristic in the hth strata is to use the equation

$$n_{jh} = \frac{CW_hS_{jh}/\sqrt{c_h}}{\sum_{h=1}^{L} W_hS_{jh}\sqrt{c_h}}, \tag{2.1}$$

as indicated by Cochran [2], where c_h is the cost of a sample taken from the hth strata, W_h is the weight of the size of the hth strata, $(N_h/\sum_h N_h)$ and S_{jh} is the standard deviation of the hth strata for the jth characteristic. The solution of equation (2.1) depends on the total sampling cost function $f = \sum_{h=1}^{L} c_h n_{jh}$ and a fixed budget C. It is known that equation (2.1) provides non-integer solutions, and Khan, Ahsan, and Jahan [4] showed that it sometimes provides unfeasible solutions, too. However, they used these solutions as an initial point of their algorithms for determining the optimum compromise integer strata sample sizes in multivariate surveys.

For the univariate case, the goal is to minimize the jth individual variance, $V(\bar{y}_j)$, subject to $f \le C$, $n_{jh} \le N_h$, where n_{jh} are integers $(h = 1, 2, \ldots, L)$. This problem can also be presented as a non-linear integer programming (NIP) problem, as proposed by Semiz and Esin [7]. This problem for every jth characteristic is formulated by the following model:

$$\begin{aligned} &\text{minimize } V_{\min}(\bar{y}) = \sum_{h=1}^{L} \frac{W_h^2 S_{jh}^2}{n_{jh}} \\ &\text{subject to } f \le C \\ &\qquad 0 \le n_{jh} \le N_h,\ h = 1, 2, \ldots, L, \\ &\qquad n_{jh} \text{ are integers},\ h = 1, 2, \ldots, L. \end{aligned} \tag{2.2}$$

Individual optimum integer values n_{jh} can be determined by solving the problem (2.2) using the *Lingo* package program [9]. The NIP solution of the problem (2.2) has advantages over the solution of equation (2.1) since one can add different constraints to problem (2.2), and obtain optimal integer results.

2.1. Example. The data, exhibited in Table 1, of the example reviewed by Khan, Ahsan, and Jahan [4], is reconsidered here for the comparison of alternative methods.

Table 1. Data for five strata and three characteristics.

	c_h	N_h	W_h	S_{1h}	S_{2h}	S_{3h}	$W_h^2 S_{1h}^2$	$W_h^2 S_{2h}^2$	$W_h^2 S_{3h}^2$
1	3	39,552	0.197	4.6	11.7	332	0.82119844	5.31256401	4277.683216
2	4	38,347	0.191	3.4	9.8	357	0.42172036	3.50363524	4649.466969
3	5	43,969	0.219	3.3	7.0	246	0.52229529	2.35008900	2902.407876
4	6	36,942	0.184	2.8	6.5	173	0.26543104	1.43041600	1013.276224
5	7	41,760	0.208	3.7	9.8	279	0.59228416	4.15507456	3367.713024

The data includes three characteristics:

(i) The number of cows milked per day,
(ii) The number of gallons of milk yielded per day,
(iii) The total annual cash receipts from dairy products.

The fixed budget for this sampling design is $C = 5,000\,\$$. The individual optimum solutions of Cochran's equation (2.1), and the NIP problem defined in (2.2), are illustrated in Table 2.

Table 2. The individual optimal strata sample sizes, cost and variances obtained from the solution of the Cochran (2.1) and NIP (2.2) methods.

	Cochran (2.1)			NIP (2.2)		
h/j	1	2	3	1	2	3
1	336	341	314	335	340	314
2	209	240	283	210	239	284
3	208	176	200	207	175	200
4	135	125	108	135	126	108
5	187	198	182	187	199	182
Total cost (\$)	**5,003**	4,999	4,996	4,999	5,000	5,000
$V_{\min}(\bar{y}_j)$	0.01210	0.07595	72.45055	0.01211	0.07594	72.39270

The NIP (2.2) solutions are feasible solutions which do not violate any constraints at all. However, sometimes Cochran's solutions may violate some of the constraints due to rounding off. In this example, for the first characteristic the sampling cost is over the fixed budget of 5,000 \$. The individual variances are smaller with the NIP (2.2) solutions. These optimum integer individual strata sample sizes determined by NIP can be considered as a starting point for algorithms such as Dynamic programming used by Khan, Ahsan, and Jahan [4], and the related individual minimum variances $V_{\min}(\bar{y}_j)$ are considered as the individual desired variances $V_d(\bar{y}_j)$.

3. Compromise integer solution via goal programming

Goal programming aims to attain predetermined goals for multiple objectives. In multivariate surveys, there are k predetermined goal variances $V_d(\bar{y}_j)$. Therefore, there

are k absolute deviations between the compromise variances $V_{\text{comp}}(\bar{y}_j)$ and the minimum individual, or desired known variances $V_d(\bar{y}_j)$. The absolute positive deviations are formulated as

$$V_{\text{comp}}(\bar{y}_j) = d_j^- - d_j^+ = V_d(\bar{y}_j),\ j = 1, 2, \ldots, k,$$

where

$$\begin{aligned} V_{\text{comp}}(\bar{y}_j) < V_d(\bar{y}_j) &\implies d_j^- > 0,\ d_j^+ = 0, \\ V_{\text{comp}}(\bar{y}_j) > V_d(\bar{y}_j) &\implies d_j^- = 0,\ d_j^+ > 0, \\ V_{\text{comp}}(\bar{y}_j) = V_d(\bar{y}_j) &\implies d_j^- = 0,\ d_j^+ = 0. \end{aligned}$$

For the jth characteristic, if the variances are not equal, one of these positive deviations d_j^+ or d_j^- come into existence. Therefore, the decision criteria is to minimize the sum of the deviations d_j^+ and d_j^-. However, the deviations of different characteristics may have different units. For each characteristic, the deviation d_j^+ or d_j^- becomes unit free by applying the transformation

$$\frac{d_j^+}{V_d(\bar{y}_j)} \text{ or } \frac{d_j^-}{V_d(\bar{y}_j)},\ j = 1, 2, \ldots, k, \tag{3.1}$$

respectively. As seen in Equation (3.1), the jth unit free standardized deviation is equal to the jth proportional increase in variance resulting from the absolute deviation between $V_{\text{comp}}(\bar{y}_j)$ and $V_d(\bar{y}_j)$ in (1.1). Consequently, by using goal programming, the compromise integer strata sample sizes in the multivariate case may be presented as the following nonlinear integer programming problem:

$$\begin{aligned} &\text{minimize} \sum_{j=1}^{k} w_j \frac{d_j^+ + d_j^-}{V_d(\bar{y}_j)} \equiv \text{minimize} \sum_{j=1}^{k} w_j \frac{|V_{\text{comp}}(\bar{y}_j) - V_d(\bar{y}_j)|}{V_d(\bar{y}_j)} \\ &\text{subject to } V_{\text{comp}}(\bar{y}_j) + d_j^- - d_j^+ = V_d(\bar{y}),\ j = 1, 2, \ldots, k, \\ &\qquad f_c \le C, \\ &\qquad 1 \le n_h^* \le N_h,\ h = 1, 2, \ldots, L, \\ &\qquad n_h^* \text{ are integers},\ h = 1, 2, \ldots, L, \end{aligned} \tag{3.2}$$

where $f_c = \sum_{h=1}^{L} c_h n_h^*$ can be of any form. The problem (3.2) may accept many constraints, and w_j can be added as the weight of the jth characteristic according to its importance. Therefore, this approach is much more flexible than the other algorithms. This problem can be solved by the Lingo package program [9].

Taking NIP (2.2) individual optimal solutions as the desired variances, and assuming the importance of all characteristics to be equal ($w_j = 1,\ j = 1, 2, 3$), the solution of the compromise integer problem defined in (3.2) gives the compromise integer strata sample sizes as

$$n_1^* = 329,\ n_2^* = 246,\ n_3^* = 195,\ n_4^* = 123,\ n_5^* = 188,$$

and the compromise variances of characteristics as

$$V_{\text{comp}}(\bar{y}_1) = 0.012197215,\ V_{\text{comp}}(\bar{y}_2) = 0.076172628,\ V_{\text{comp}}(\bar{y}_3) = 72.93787706.$$

4. Comparisons and Conclusions

The mean sum of relative efficiencies of variances is used for the comparison of the proposed goal programming approach (3.2) with other compromise methods. The compared methods are:

i) Minimizing the trace of the covariance matrix, as proposed by Sukhatme, Sukhatme, Sukhatme and Asok [8],
ii) Averaging the individual strata sample sizes over the characteristics calculated using (2.1),
iii) Minimizing the total relative increase in the variances, as proposed by Chatterjee [1],
iv) Minimizing the total relative increase in the variances with integer restrictions, as proposed by Khan, Ahsan, and Jahan [4], and
v) Minimizing the total proportional increase in variances, as proposed by the author (3.2).

Since every characteristic can have different units, in (i), the appropriateness of the sum of the variances should be reevaluated carefully. The compromise strata sample sizes are presented in Table 3 for each method.

Table 3. Compromise Strata Sample Sizes for the Methods Compared.

Methods and compromise integer strata sample sizes	n_1^*	n_2^*	n_3^*	n_4^*	n_5^*
(i) Minimizing the trace	314	283	200	108	182
(ii) Cochran's Average	330	244	195	123	189
(iii) Chatterjee's Method	330	245	195	123	189
(iv) Integer DP	331	246	195	123	187
(v) Proposed integer GP	329	246	195	123	188

The comparison is based on the mean sum of relative efficiencies (MSRE) of each method:

$$\text{MSRE} = \frac{1}{k}\sum_{j=1}^{k}\frac{V_{\text{comp}}(\bar{y}_j)}{V_{\min}(\bar{y}_j)} = \frac{1}{k}\text{SRE}. \tag{4.1}$$

Table 4. Sum of relative efficiencies (SRE) and mean sum of relative efficiencies (MSRE) as compared to the optimal individual variances determined by NIP (2.2).

Methods and compromised variances	$V(\bar{y}_1)$	$V(\bar{y}_2)$	$V(\bar{y}_3)$	SRE	MSRE (4.1)	Cost
Optimal Integer Individual (NIP) (2.2)	0.0121	0.0759	72.3927	3.0000	1.0000	$*$
(i) Minimizing the Trace	0.0124	0.0771	72.4506	3.0414	**1.0138**	4996
(ii) Cochran's Average	0.0122	0.0761	72.9586	3.0187	1.0062	**5002**
(iii) Chatterjee's Method	0.0122	0.0761	72.8808	3.0176	1.0059	**5006**
(iv) Integer DP	0.0122	0.0762	72.9551	3.0200	1.0067	4999
(v) Proposed integer GP (3.2)	0.0122	0.0762	72.9379	3.0197	***1.0066***	***5000***

Method (i) does not directly provide integer strata sample sizes. Solutions of (i) have to be rounded. The mean sum of the relative efficiencies of (i) is greater than for the proposed method (v). Also, the trace concept of the variance terms, which have different units, is still in question.

Methods (ii) and (iii) have lower MSRE values than the proposed method (v). However, these strata sample size solutions require to be rounded off. As seen in Table 4, these

solutions result in a cost over the budget and these methods may not provide feasible solutions.

Method (iv), proposed by Khan, Ahsan, and Jahan [4], is as efficient as the proposed method (v). However, the solutions of (iv) are determined by an algorithm for a fixed problem subject to the fixed cost function ($f_c = \sum_{h=1}^{L} c_h n_h^*$) and for a limited and specified set of constraints. Therefore, method (iv) is not flexible for different multivariate survey problems.

Method (v) is a mathematical programming model which optimizes the goal programming model subject to the constraints, which are the cost function and the integer strata sample sizes. Therefore, Method (v) always provides integer and feasible solutions for the strata sample sizes for compromise situation in multivariate stratified sampling problems. In addition this proposed goal programming method (v) has a flexible structure because it can accept different kinds of restrictions appropriate to different problems. Depending upon the problem structure, constraints may be deleted, added or changed in the new method (3.2). In addition to these advantages, the proposed goal programming solution method (v) has, for this specific example, the best MSRE value among the methods (i), (iv) and (v) that provide feasible solutions. In conclusion, as seen in this example, this goal programming method seems to provide a flexible approach as well as feasible and efficient integer compromise strata sample sizes in multivariate stratified sampling.

References

[1] Chatterjee, S. *A note on optimum allocation*, Scandinavian Actuarial Journal **50**, 40–44, 1967.

[2] Cochran, W. G. *Sampling Techniques*, 2nd Ed. (John Wiley and Sons Inc., New York, 1963).

[3] Jahan, N., Khan, M. G. M. and Ahsan, M. J. *A generalized compromise allocation*, Journal of the Indian Statistical Association **32**, 95–101, 1994.

[4] Khan, M. G. M., Ahsan, M. J. and Jahan, N. *Compromise allocation in multivariate stratified sampling: An integer solution*, Naval Research Logistics **44**, 69–79, 1997.

[5] Kokan, A. R. and Khan, S. *Optimum allocation in multivariate surveys: An analytical solution*, Journal of the Royal Statistical Society, Series B **29**, 115–125, 1967.

[6] Neyman, J. *On the two different aspects of the representative methods: The method of stratified sampling and the method of purposive selection*, Journal of the Royal Statistical Society **97**, 558–606, 1934.

[7] Semiz, M. and Esin, A. A. *Tabaka örnek hacimlerinin doğrusal olmayan tamsayılı programlama ile Belirlenmesi*, İstatistik Sempozyumu-2000, pp. 199–207, (Gazi University, Department of Statistics, Ankara, Turkey, 2000).

[8] Sukhatme, P. V., Sukhatme, B. V., Sukhatme, S. and Asok, C. *Sampling Theory of Surveys with Applications*, (Indian Society of Agricultural Statistics, New Delhi, India, and Iowa State University Press, Ames, IA, 1984).

[9] Winston, W. L. *User's Guide for Lindo and Lingo: Operations Research: Applications and Algorithms, Introduction to Mathematical Programming: Applications and Algorithms*, (Duxbury Press, New York, 1997).

Hacettepe Journal of Mathematics and Statistics
Volume 33 (2004), 97 – 109

STOCHASTIC COVARIATES IN BINARY REGRESSION

Evrim Oral* and Süleyman Günay†

Received 27 : 04 : 2004 : Accepted 23 : 09 : 2004

Abstract

Binary regression has many medical applications. In applying the technique, the tradition is to assume the risk factor X as a non-stochastic variable. In most situations, however, X is stochastic. In this study, we discuss the case when X is stochastic in nature, which is more realistic from a practical point of view than X being non-stochastic. We show that our solutions are much more precise than those obtained by treating X as non-stochastic when, in fact, it is stochastic.

Keywords: Binary regression, Modified Maximum Likelihood Estimator, Robustness, Skew family, Symmetric family.

1. Introduction

A binary regression model typically is

$$\pi(x) = E(Y \mid X = x) = \int_{-\infty}^{z} f(x)\,dx = F(z), \tag{1.1}$$

where $z = \gamma_0 + \gamma_1 x\,(\gamma_1 > 0)$, Y is a stochastic variable that assumes values 1 or 0 and X is a risk factor which in the literature has been treated as non-stochastic. In most situations, however, X is stochastic. Consider, for example, the following data:

(1) The 27 observations on (Y, X) given in Agresti [2, p. 88], where X measures the proliferative activity of cells after a patient receives an injection of tritiated thymidine and the response variable Y represents whether the patient achieves remission or not.

(2) The following 10 observations on (Y, X) given in Hosmer and Lemeshow [5, p.132]

$Y : 0, 1, 0, 0, 0, 0, 0, 1, 0, 1$

$X : 0.225, 0.487, -1.080, -0.870, -0.580, -0.640, 1.614, 0.352, -1.025, 0.929;$

*Department of Statistics, Middle East Technical University, Ankara 06531, Turkey.
†Department of Statistics, Hacettepe University, Ankara 06532, Turkey.

X is generated from normal $N(0,1)$. In the examples above, and many others (Aitkin *et al.*, [3]), X is clearly stochastic but has been treated as a non-stochastic variable. The function $f(x)$ has traditionally been taken to be logistic but Tiku and Vaughan [18] have extended the methodology to non-logistic density functions treating X as non-stochastic. The purpose here is to give solutions in the more realistic situations when X is stochastic and $f(x)$ is logistic or non-logistic. Since maximum likelihood methodology is intractable, modified likelihood methodology is invoked. The latter is known to yield MMLE (modified maximum likelihood estimators) as efficient as the MLE (maximum likelihood estimators). Unlike the MLE, the MMLE are explicit functions of sample observations and are easy to compute; see Vaughan [22] and Tiku and Vaughan [18]. In fact, Vaughan [23, p.228] states five very desirable properties of the MMLE. Moreover, as pointed out in Şenoğlu and Tiku [14, p.363], the MMLE are numerically the same (almost) as the MLE in all situations where authentic iterative MLE are available. See also Vaughan [23, p. 233]. The solutions we give are enormously more precise than those obtained by treating X as a non-stochastic variable when, in fact, it is stochastic.

2. Maximum Likelihood

Let Y be a binary random variable which assumes values $y_i = 1$ or 0 with probabilities θ and $1-\theta$, respectively, and let the corresponding observations on the risk factor X be denoted by $x_i\,(1 \le i \le n)$. The model is

$$F(z_i) = \pi(x_i) = E(Y|X = x_i) = \int_{-\infty}^{z_i} f(u)\,du, \tag{2.1}$$

where $z_i = \gamma_0 + \gamma_1 x_i$ and $f(u)$ is a completely specified density function; Y is presumed to increase with X so that γ_1 is a priori positive. Let $h(x)$ denote the probability density function of the stochastic variable X. The methodology developed here is applicable to any completely specified density f in (2.1) and any location-scale density $h(x)$. We consider, for illustration, two families of densities: (a) skew and (b) symmetric, which are prevalent in practice (Rasch [11]; Spjotvoll and Aastveit [12]; Tiku et al. [19]).

Skew family: Consider the family of Generalized Logistic densities

$$GL(b,\gamma_1) : h(x) = \frac{b\gamma_1 \mathrm{e}^{-(\gamma_0+\gamma_1 x)}}{\left(1+\mathrm{e}^{-(\gamma_0+\gamma_1 x)}\right)^{b+1}},\ -\infty < x < \infty. \tag{2.2}$$

Note that the probability density function of $Z = (X-\mu)/\sigma = \gamma_0 + \gamma_1 X$, ($\gamma_0 = -\mu/\sigma$, $\gamma_1 = 1/\sigma$), is

$$h(z) = \frac{be^{-z}}{\left(1+\mathrm{e}^{-z}\right)^{b+1}},\ -\infty < z < \infty. \tag{2.3}$$

The densities $f(u)$ and $h(z)$ are assumed to have the same functional forms although our methodology easily extends to situations where f and h are different from each other. The latter will perhaps be true if there are more than one risk factor and $z = \gamma_0 + \sum_i \gamma_1 x_i$.

For $b < 1$, (2.3) represents negatively skewed density functions. For $b > 1$, it represents positively skewed density functions. For $b = 1$, it is the well known logistic density. The mean and variance of (2.3) are

$$E(Z) = \psi(b) - (1) \text{ and } V(Z) = \psi'(b) + \psi'(1) \tag{2.4}$$

respectively The values of the psi-function $\psi(b)$ and its derivative $\psi'(b)$ are given in Tiku *et al.* [20, p. 1356]. See Abramowitz and Stegun [1] for analytical and computational aspects of psi-functions.

The likelihood function of the random sample (y_i, x_i), $1 \leq i \leq n$, is

$$L = L_X L_{Y|X} \propto \prod_{i=1}^{n} (\gamma_1 h(z_i)) \left\{ (F(z_i))^{y_i} (1 - F(z_i))^{1-y_i} \right\}. \tag{2.5}$$

This gives

$$\ln L \propto n \ln \gamma_1 + \sum_{i=1}^{n} \{\ln h(z_i) + y_i \ln F(z_i) + (1 - y_i) \ln (1 - F(z_i))\}; \tag{2.6}$$

$z_i = \gamma_0 + \gamma_1 x_i$ and $F(z_i) = \left(1 + e^{-z_i}\right)^{-b}$.

The likelihood equations are expressions in terms of the intractable functions

$$g(z) = e^{-z} / \left(1 + e^{-z}\right), \; g_1(z) = f(z)/F(z) \text{ and } g_2(z) = f(z) / \{1 - F(z)\}. \tag{2.7}$$

They have no explicit solutions and are almost impossible to solve by iterative methods. The MLE are, therefore, elusive. See also Tiku and Vaughan [18] who work with the conditional likelihood function $L_{Y|X}$ as do other authors (Agresti [2]; Hosmer and Lemeshow [5]; Kleinbaum [6]).

To obtain the MMLE, we first express the likelihood equations $\partial \ln L / \partial \gamma_0 = 0$ and $\partial \ln L / \partial \gamma_1 = 0$ in terms of the ordered variates $z_{(i)}$. Since γ_1 is a priori positive,

$$z_{(i)} = \gamma_0 + \gamma_1 x_{(i)}, 1 \leq i \leq n, \tag{2.8}$$

where $x_{(i)}$ are the order statistics of the random sample x_i, $(1 \leq i \leq n)$. Since complete sums are invariant under ordering, e.g. $\sum_{i=1}^{n} z_i = \sum_{i=1}^{n} z_{(i)}$, we have

$$\frac{\partial \ln L}{\partial \gamma_0} = -n + \sum_{i=1}^{n} \left\{ (b+1) g\left(z_{(i)}\right) + w_i g_1\left(z_{(i)}\right) - (1 - w_i) g_2\left(z_{(i)}\right) \right\} = 0 \tag{2.9}$$

and

$$\begin{aligned} \frac{\partial \ln L}{\partial \gamma_1} &= \frac{n}{\gamma_1} - \sum_{i=1}^{n} x_{(i)} + \sum_{i=1}^{n} x_{(i)} \left\{ (b+1) g\left(z_{(i)}\right) + w_i g_1\left(z_{(i)}\right) - (1 - w_i) g_2\left(z_{(i)}\right) \right\} \\ &= 0, \end{aligned} \tag{2.10}$$

where $w_i = y_{[i]}$ is the concomitant of $x_{(i)}$, i.e., $y_{[i]}$ is that observation y_i which is coupled with $x_{(i)}$ when (y_i, x_i) are ordered with respect to x_i, $(1 \leq i \leq n)$. As mentioned earlier, (2.8)-(2.9) are almost impossible to solve.

3. Modified Likelihood

To obtain the modified likelihood equations, we linearize the functions $g(z)$, $g_1(z)$ and $g_2(z)$ by using the first two terms of their Taylor series expansions as follows:

$$\begin{aligned} g\left(z_{(i)}\right) &\cong g\left(t^*_{(i)}\right) + \left(z_{(i)} - t^*_{(i)}\right) \left\{ \frac{d}{dz} g(z) \right\}_{z = t^*_{(i)}} \\ &= \alpha_i - \beta_i z_{(i)}, \; 1 \leq i \leq n, \end{aligned} \tag{3.1}$$

where

$$\alpha_i = (1 + e^{\alpha_i})^{-1} + \beta_i a_i \text{ and } \beta_i = e^{a_i} / (1 + e^{a_i})^2, \; a_i = t^*_{(i)}; \tag{3.2}$$

a_i is determined by the equation

$$\int_{-\infty}^{a_i} h(z)\, dz = \frac{i}{n+1}, \; 1 \leq i \leq n. \tag{3.3}$$

Similarly,

$$g_1\left(z_{(i)}\right) \cong \alpha_{1i} - \beta_{1i} z_{(i)} \text{ and } g_2\left(z_{(i)}\right) = \alpha_{2i} + \beta_{2i} z_{(i)}, \; 1 \leq i \leq n, \tag{3.4}$$

where

$$\beta_{1i} = \left\{f^2\left(t_{(i)}\right) - F\left(t_{(i)}\right) f'\left(t_{(i)}\right)\right\} / F^2\left(t_{(i)}\right) \text{ and } \alpha_{1i} = g_1\left(t_{(i)}\right) + \beta_{1i} t_{(i)}, \tag{3.5}$$

and

$$\begin{aligned} \beta_{2i} &= \left\{f^2\left(t_{(i)}\right) + \left(1 - F\left(t_{(i)}\right)\right) f'\left(t_{(i)}\right)\right\} / \left(1 - F\left(t_{(i)}\right)\right)^2, \\ \alpha_{2i} &= g_2\left(t_{(i)}\right) - \beta_{2i} t_{(i)}. \end{aligned} \tag{3.6}$$

Here, $t_{(i)}$ is determined by the equation

$$\int_{-\infty}^{t_{(i)}} f(z)\, dz = \frac{i}{n+1},\ 1 \le i \le n. \tag{3.7}$$

For the Generalized Logistic,

$$t_{(i)} = -\ln\left\{q_i^{-\frac{1}{b}} - 1\right\},\ q_i = i/(n+1). \tag{3.8}$$

Since $f(u)$ and $h(z)$ are assumed to have the same forms, $a_{(i)} = t_{(i)}$ $(1 \le i \le n)$.

Incorporating (3.1) and (3.4) in (2.9)-(2.10) gives the modified likelihood equations which have the following beautiful expressions:

$$\frac{\partial \ln L}{\partial \gamma_0} \cong \frac{\partial ln L^*}{\partial \gamma_0} = -n + \sum_{i=1}^{n} \left\{\delta_i - m_i z_{(i)}\right\} = 0 \tag{3.9}$$

and

$$\frac{\partial \ln L}{\partial \gamma_1} \cong \frac{\partial ln L^*}{\partial \gamma_1} = \frac{n}{\gamma_1} - \sum_{i=1}^{n} x_{(i)} + \sum_{i=1}^{n} x_{(i)} \left\{\delta_i - m_i z_{(i)}\right\} = 0 \tag{3.10}$$

where

$$\delta_i = w_i \alpha_{1i} - (1 - w_i)\, \alpha_{2i} + (b+1)\, \alpha_i \text{ and } m_i = w_i \beta_{1i} + (1 - w_i)\, \beta_{2i} + (b+1)\, \beta_i. \tag{3.11}$$

The solutions of (3.9)-(3.10) are the MMLE $\hat{\gamma_0}$ and $\hat{\gamma_1}$ of γ_0 and γ_1, respectively:

$$\hat{\gamma_0} = \{(\delta - n)/m\} - \hat{\gamma_1} \overline{x}_{(.)} \text{ and } \hat{\gamma_1} = \left\{B + \sqrt{(B^2 + 4nC)}\right\} / 2C \tag{3.12}$$

where

$$\begin{aligned} &\delta = \sum_{i=1}^{n} \delta_i,\ m = \sum_{i=1}^{n} m_i,\ \overline{x}_{(.)} = \frac{1}{m} \sum_{i=1}^{n} m_i x_{(i)}, \\ &B = \sum_{i=1}^{n} (\delta_i - 1) \left(x_{(i)} - \overline{x}_{(.)}\right), \text{ and} \\ &C = \sum_{i=1}^{n} m_i \left(x_{(i)} - \overline{x}_{(.)}\right)^2 = \sum_{i=1}^{n} m_i x_{(i)}^2 - \frac{1}{m} \left(\sum_{i=1}^{n} m_i x_{(i)}\right)^2. \end{aligned} \tag{3.13}$$

Revised estimates: Following Lee *et al.* [7] and Tiku and Vaughan [18, p. 888], in order to sharpen the MMLE, we calculate the coefficients $(\alpha_{1i}, \beta_{1i})$ and $(\alpha_{2i}, \beta_{2i})$ from (3.5)-(3.6) by replacing $t_{(i)}$ by

$$t_i = \hat{\gamma_0} + \hat{\gamma_1} x_{(i)},\ 1 \le i \le n, \tag{3.14}$$

and calculate the revised estimates from (3.12)-(3.13). We may repeat this process a few times until the estimates stabilize to, say, three decimal places. No revision is needed in the coefficients (α_i, β_i) in (3.1); they are computed from (3.2) once and for all. See also Tiku and Suresh [17] and Vaughan [22, 23].

4. Asymptotic Variances and Covariances

It has been rigourously proved by Vaughan and Tiku [24] that the MMLE are asymptotically equivalent to the MLE. Bhattacharyya [4] establishes this result for censored samples. Therefore, the MMLE $\hat{\gamma}_0$ and $\hat{\gamma}_1$ above are asymptotically unbiased and efficient. Their asymptotic variance-covariance matrix $\mathbf{V}$ is given by $\mathbf{I}^{-1}(\gamma_0, \gamma_1)$, where $\mathbf{I}$ is the Fisher information matrix consisting of the following elements:

$$I_{11} = -E\left(\frac{\partial^2 \ln L}{\partial \gamma_0^2}\right) = Q + P_1, \tag{4.1}$$

$$I_{12} = -E\left(\frac{\partial^2 \ln L}{\partial \gamma_0 \partial \gamma_1}\right)$$

$$= \frac{1}{\gamma_1}\left\{-(Q+P_1)\gamma_0 + [\psi(b) - \psi(1)]Q + [\psi(b+1) - \psi(2)]P_1\right\} \tag{4.2}$$

and

$$I_{22} = -E\left(\frac{\partial^2 \ln L}{\partial \gamma_1^2}\right)$$

$$= \frac{1}{\gamma_1^2}((Q+P_1)\gamma_0^2 - 2\gamma_0([\psi(b) - \psi(1)]Q + [\psi(b+1) - \psi(2)]P_1) +$$

$$+ \left([\psi(b) - \psi(1)]^2 + \psi'(b) + \psi'(1)\right)Q +$$

$$+ \left([\psi(b+1) - \psi(2)]^2 + \psi'(b+1) + \psi'(2)\right)P_1 + n), \tag{4.3}$$

where

$$Q_i = \frac{f^2(z_i)}{F(z_i)(1 - F(z_i))},\ Q = \sum_{i=1}^{n} Q_i \text{ and } P_1 = \frac{nb}{b+2}. \tag{4.4}$$

The expressions (4.1)-(4.3) are obtained along the same lines as in Tiku and Vaughan [18, Section 5] and realizing that for a bounded bivariate random function $g(Z, Y)$,

$$E\{g(Z,Y)\} = E_Z\left\{E_{Y/Z}g(Z,Y)\right\}. \tag{4.5}$$

Thus,

$$\mathbf{V} = \begin{bmatrix} I_{11} & I_{12} \\ I_{12} & I_{22} \end{bmatrix}^{-1}. \tag{4.6}$$

In particular, the asymptotic variance of $\hat{\gamma}_1$ is given by

$$\text{var}(\hat{\gamma}_1/\gamma_1) \cong (Q + P_1)/\Delta, \tag{4.7}$$

where

$$\Delta = \left(\left[\psi'(b) - \psi'(1)\right]Q(Q+P_1) + \left[\psi'(b+1) + \psi'(2)\right]P_1(Q+P_1) +\right.$$

$$\left. + ([\psi(b) - \psi(1)] - [\psi(b+1) - \psi(2)])^2 QP_1 + n(Q+P_1)\right.,$$

which is free of γ_0.

An estimate of the variance of $\hat{\gamma}_1$ is obtained by replacing z_i by $\hat{z}_i = \hat{\gamma}_0 + \hat{\gamma}_1 x_i$ in (4.4). The standard error of $\hat{\gamma}_1$ is the square root of this estimated variance and, similarly, for $\hat{\gamma}_0$.

For $b = 1$ (logistic density), (4.7) simplifies and since $\psi'(1) = 1.6449$ and

$$\psi'(2) = 1.6449,\ \text{var}(\hat{\gamma}_1/\gamma_1) \cong 1/(3.2898Q + 1.2898P_1 + n). \tag{4.8}$$

We now give a few examples to illustrate the enormous gain in efficiency of the estimators when the complete likelihood function L is used as against using only the conditional likelihood $L_{Y|X}$.

4.1. Example. Consider the widely reported CHD (coronary heart disease) data on 100 randomly chosen patients (Hosmer and Lemeshow [5]). Here, X represents the age and Y the presence or absence of CHD. The density $f(u)$ in (2.1) has traditionally been taken to be logistic. With logistic $h(x)$, i.e. $GL(1,\gamma_1)$ in (2.2), we have the MMLE and their standard errors reported in Table 1. Only two iterations were needed for the estimates to stabilize to three decimal places. Also reported are the MLE and the MMLE (and their standard errors) based only on the conditional likelihood $L_{Y|X}$, reproduced from Tiku and Vaughan [18, p. 890]. It can be seen that the MMLE based on the complete likelihood (2.5) are enormously more precise, that is, they have considerably smaller standard errors than those based only on the conditional likelihood.

Table 1. Estimates and their Standard Errors for the CHD Data, $n = 100$.

		Coefficient	Estimate	Standard Error
Conditional Likelihood	ML	γ_0	-5.310	1.134
		γ_1	0.111	0.024
	MML	γ_0	-5.309	1.134
		γ_1	0.111	0.024
Complete Likelihood	MML	γ_0	-6.181	0.463
		γ_1	0.136	0.010

It may be noted that the MMLE based on the complete likelihood are not much different numerically from those based only on the conditional likelihood.

4.2. Example. Consider the Agresti [2, p.88] data (27 observations) mentioned earlier. The MLE and the MMLE and their standard errors are given in Table 2. Again, the MMLE based on the complete likelihood function are not very different numerically from those based on the conditional likelihood but are enormously more precise.

Table 2: Estimates and their Standard Errors for Agresti's Data, $n = 27$.

		Coefficient	Estimate	Standard Error
Conditional Likelihood	ML	γ_0	-3.777	$*$
		γ_1	0.145	0.059
	MML	γ_0	-3.777	1.379
		γ_1	0.145	0.059
Complete Likelihood	MML	γ_0	-3.688	0.576
		γ_1	0.175	0.024

$*$: Not given in Agresti [2]

Simulation study: To illustrate further the gain in efficiency which the MMLE (3.12) provide over those based only on the conditional likelihood (Tiku and Vaughan [18]), i.e.,

$$\text{(4.9)} \qquad \hat{\gamma}_{1c} = \sum_{i=1}^{n} \delta_i \left(x_{(i)} - \overline{x}_a\right) / \sum_{i=1}^{n} m_i \left(x_{(i)} - \overline{x}_a\right)^2 \text{ and } \hat{\gamma}_{0c} = (\delta/m) - \hat{\gamma}_{1c}\overline{x}_a,$$

$$\delta = \sum_i \delta_i,\ m = \sum_i m_i,\ \delta_i = \alpha_{1i} w_i - \alpha_{2i}(1 - w_i),$$

$$m_i = \beta_{1i} w_i + \beta_{2i}(1 - w_i) \text{ and } \overline{x}_a = (1/m) \sum_i m_i x_{(i)}.$$

we did an extensive Monte Carlo study as follows:

We generated a random sample $x_1, x_2, \ldots, x_n$ of size n from (2.2) and calculated the MMLE of γ_0 and γ_1 (Tiku and Suresh [17]; Vaughan [22]) from the order statistics

$$x_{(i)} \leq x_{(2)} \leq \cdots \leq x_{(n)}.$$

Denote them by $\hat{\gamma}_{00}$ and $\hat{\gamma}_{10}$. Specifically,

$$\begin{aligned} \hat{\gamma}_{00} &= \frac{1}{m}\sum_{i=1}^{n}\left(\alpha_i - \frac{1}{b+1}\right) - \hat{\gamma}_{10}\overline{x}_{(..)} \text{ and }, \\ \hat{\gamma}_{10} &= \left\{-B_0 + \sqrt{B_0^2 + 4nC_0}\right\}/2C_0, \end{aligned} \tag{4.10}$$

where

$$\begin{aligned} m &= \sum_{i=1}^{n}\beta_i,\ \overline{x}_{(..)} = (1/m)\sum_{i=1}^{n}\beta_i x_{(i)}, \\ B_0 &= (b+1)\sum_{i=1}^{n}\left(\alpha_i - \frac{1}{b+1}\right)\left(x_{(i)} - \overline{x}_{(..)}\right) \text{ and} \\ C_0 &= (b+1)\sum_{i=1}^{n}\beta_i\left(x_{(i)} - \overline{x}_{(..)}\right)^2; \end{aligned} \tag{4.11}$$

the values of α_i and β_i being obtained from (3.2).

We generated the concomitant binary observations $w_i = y_{[i]},\ (1 \leq i \leq n)$, by calculating the probability

$$\hat{P}_i = \left(1 + \mathrm{e}^{-\hat{z}_{(i)}}\right)^{-b},\ \hat{z}_{(i)} = \hat{\gamma}_{00} + \hat{\gamma}_{10}x_{(i)} \tag{4.12}$$

and defining

$$w_i = \begin{cases} 1 & \text{if } U_i \leq \hat{P}_i, \\ 0 & \text{otherwise,} \end{cases} \tag{4.13}$$

where U_i, $(1 \leq i \leq n)$, are independent uniform (0,1) variates.

The observations $\left(w_i, x_{(i)}\right)$, $1 \leq i \leq n$, so generated were substituted in (3.12) and the MMLE $\hat{\gamma}_0$ and $\hat{\gamma}_1$ obtained. The corresponding conditional likelihood MMLE were obtained from the equations (4.9). Both sets of estimates were the result of three iterations. The procedure was repeated $N = [100000/n]$ (integer value) times. The means and variances of the resulting estimates were calculated for $b = 0.5, 1, 2$ and 4. Both were found to be (almost) unbiased. The MMLE $\hat{\gamma}_0$ and $\hat{\gamma}_1$, however, were found to be enormously more efficient than the conditional MMLE for all values of b. For illustration, we reproduce in Table 3 the means and variances of the estimators for $b = 1$. It can be seen that the MMLE based on the complete likelihood are very much more efficient than those based only on the conditional likelihood.

It is interesting to see that the mean and variance of $\hat{\gamma}_1/\gamma_1$ are almost invariant to γ_0 for all n, in agreement with the fact that $\hat{\gamma}_1$ is (almost) unbiased for γ_1 and the equation (4.7) is free of γ_0. Incidentally, the simulated variance of $\hat{\gamma}_1/\gamma_1$ is close to those obtained from (4.7) for large n (> 100)

Table 3. Simulated Means and Variances: (a) Mean and (b) Variance.

			Complete Likelihood				Conditional Likelihood			
			(a)		(b)		(a)		(b)	
γ_0	γ_1	n	$\hat{\gamma}_0$	$\hat{\gamma}_1/\gamma_1$	$\hat{\gamma}_0$	$\hat{\gamma}_1/\gamma_1$	$\hat{\gamma}_{(0)}$	$\hat{\gamma}_{(1)}/\gamma_1$	$\hat{\gamma}_{(0)}$	$\hat{\gamma}_{(1)}/\gamma_1$
0	0.001	50	0.001	1.018	0.075	0.017	0.003	1.112	0.233	0.155
		100	-0.005	1.007	0.035	0.008	-0.011	1.062	0.101	0.070
	0.10	50	0.006	1.023	0.079	0.017	0.001	1.121	0.229	0.168
		100	0.003	1.009	0.039	0.008	-0.000	1.048	0.108	0.061
	1.00	50	-0.005	1.022	0.075	0.017	-0.010	1.132	0.223	0.165
		100	-0.005	1.011	0.037	0.008	-0.011	1.066	0.103	0.069
2	0.001	50	2.029	1.017	0.142	0.017	2.245	1.127	0.892	0.161
		100	2.025	1.011	0.073	0.008	2.124	1.056	0.350	0.063
	0.10	50	2.035	1.016	0.139	0.016	2.239	1.119	0.866	0.159
		100	2.018	1.005	0.070	0.008	2.111	1.048	0.375	0.067
	1.00	50	2.048	1.024	0.136	0.015	2.278	1.139	0.891	0.170
		100	2.021	1.008	0.070	0.008	2.114	1.055	0.352	0.059

4.3. Remark. The assumed values of γ_0 and γ_1 may as well be used in (4.12) to generate w_i from (4.13). That does not change the values in Table 3 in any substantial way.

5. Hypothesis Testing

Since X is a genuine risk factor, its effect on Y will logically be never zero. The real issue, therefore, is whether it has some effect howsoever small. Testing $H_0 : \gamma_1 = \gamma_{10} (> 0)$ is, therefore, of major importance. To test H_0, we propose the statistic

$$W = \hat{\gamma}_1/\gamma_{10}. \tag{5.1}$$

Large values of W lead to the rejection of H_0 in favour of $H_1 : \gamma_1 > \gamma_{10}$. Since $\hat{\gamma}_1$ is asymptotically equivalent to the MLE, the asymptotic null distribution of W is normal with mean 1 and variance given by the right hand side of (4.7). Simulations reveal, however, that it takes a large sample size n (> 100) to attain near-normality of the null distribution of W. To study the null distribution of W for small n, we simulated the coefficients of skewness $\beta_1^* = \mu_3^2/\mu_2^3$ and kurtosis $\beta_2^* = \mu_4/\mu_2^2$ of W. Interestingly, $\mu_3 > 0$ and β_1^* and β_2^* are close to the Type III line in the Pearson plane (Pearson [9]; Tiku [15,16]; Pearson and Tiku [10, Fig.1]), i.e.,

$$|\beta_2^* - (3 + 1.5\beta_1^*)| \leq 0.5. \tag{5.2}$$

For $n = 20$, $\gamma_0 = 2$ and $\gamma_1 = 0.001$, for example, $\beta_1^* = 0.732$ and $\beta_2^* = 4.309$ so that (5.2) equals 0.211; for $n = 100$, $\beta_1^* = 0.139$ and $\beta_2^* = 3.153$, and (5.2) equals 0.056. The Pearson-Tiku 3-moment chi-square approximation is applicable. This works as follows:

Let

$$\chi^2 = (W + c)/d, \tag{5.3}$$

where χ^2 is a chi-square variate with ν degrees of freedom. Determine ν, d and c such that the first three moments on both sides agree. This gives

$$\nu = 8/\beta_1^*,\ d = \sqrt{(\mu_2/2\nu)} \text{ and } c = b\nu - \mu_1'. \tag{5.4}$$

Here μ_1' and μ_2 are the simulated mean and variance of W. Thus, the $100\,(1-\alpha)\,\%$ point of W is given by

$$W_\alpha = d\chi^2_\alpha\,(\nu) - c, \tag{5.5}$$

where $\chi^2_\alpha\,(\nu)$ is the $100\,(1-\alpha)\,\%$ point of a chi-square distribution with ν degrees of freedom. The 3-moment chi-square approximation gives remarkably accurate values. For example, we have the following simulated values of the probability $P\,(W \geq W_\alpha|H_0)$ with its value presumed to be 0.050:

Simulated Values of The Probability

n	$b = 0.5$	1	2	4
20	0.049	0.044	0.046	0.048
50	0.051	0.050	0.049	0.047
100	0.049	0.045	0.051	0.051

5.1. Remark. Since $\hat{\gamma}_1$ is as efficient as the MLE, it will not be easy to improve over the W test so far as its power is concerned.

Since X has been assumed to be non-stochastic, it is now possible to study the robustness of the W test as follows.

Robustness: In practice, a value of the shape parameter b in (2.3) is located with the help of $Q-Q$ plots and/or formal goodness-of-fit tests; see specifically Tiku and Vaughan [18, Appendix B]. In spite of ones best efforts, however, it might not be possible to locate the exact value of b. Moreover, the data might contain outliers or be contaminated. That brings the robustness issue in focus. Assume, for illustration, that the true value in (2.3) is $b = 1$ (logistic distribution) which we will call the population model. As plausible alternatives, we consider the following which we will call sample models; $\sigma = 1/\gamma_1$.

Misspecified model:

Student's t distribution with degrees of freedom

(1) $\upsilon = 9$,
(2) $\upsilon = 19$.

Outlier model:

(3) $(n-r)$ observations come from $GL\,(1,\sigma)$ and r (we do not know which) come from $GL\,(1,4\sigma)$, $r = [0.5 + 0.1n]$.
(4) $(n-r)$ observations come from $GL\,(0.5,\sigma)$ and r come from $GL\,(0.5,4\sigma)$.

Mixture model:

(5) $0.90GL\,(1,\sigma) + 0.10GL\,(1,4\sigma)$,
(6) $0.90GL\,(0.5,\sigma) + 0.10GL\,(0.5,4\sigma)$.

Contamination model:

(7) $(n-r)$ observations come from $GL\,(1,\sigma)$ and r from uniform $U\,(0,1)$.

Models (4) and (6) represent skew distributions. All other models represents symmetric distributions.

To study the robustness of Type I error of the W test above, since the assumed population model is the logistic $GL\,(1,\sigma)$, we take $b = 1$ in all the equations above and use the corresponding W_α in (5.5) for all the alternative models (1)–(7). The simulated Type I errors are given in Table 4. It can be seen that the W test is remarkably robust. This

is typical of the hypothesis testing procedures based on the MMLE since the coefficients β_i have umbrella or half-umbrella ordering; see specifically Şenoğlu and Tiku [13,14].

Table 4. Simulated Values of The Type I Error; $\gamma_0 = 0$, $\gamma_1 = 0.001$.

Model	$n = 50$	60	80	100	Model	$n = 50$	60	80	100
Logistic	0.050	0.052	0.052	0.048	(1)	0.049	0.051	0.048	0.048
(2)	0.049	0.047	0.048	0.051	(3)	0.049	0.049	0.048	0.052
(4)	0.053	0.050	0.050	0.050	(5)	0.051	0.047	0.046	0.050
(6)	0.051	0.049	0.050	0.051	(7)	0.050	0.049	0.050	0.052

The random numbers generated from all the models in the table were standardized to have variance 1. Although we have reported values only for $\gamma_0 = 0$ and $\gamma_1 = 0.001$, the results are essentially the same for other values of γ_0 and γ_1. Similarly, the power of the test is not diminished in any substantial way under plausible deviations from an assumed model. We omit details for conciseness. Thus, the W test has both criterion robustness as well as efficiency robustness.

6. Symmetric family

Consider the situation when X has density

$$h(x) = \frac{\gamma_1}{\sqrt{k}B\left(\frac{1}{2}, p-\frac{1}{2}\right)}\left\{1+\frac{1}{k}\left(\gamma_0+\gamma_1 x\right)^2\right\}^{-p},\ -\infty < x < \infty; \tag{6.1}$$

$k = 2p-3$, $p \geq 2$. The probability density function of $Z = \gamma_0 + \gamma_1 X$ is

$$h(z) = \frac{1}{\sqrt{k}B\left(\frac{1}{2}, p-\frac{1}{2}\right)}\left\{1+\frac{1}{k}z^2\right\}^{-p},\ -\infty < z < \infty. \tag{6.2}$$

Realize that $t = \sqrt{(\nu/k)}Z$ has the Student's t distribution with $\nu = 2p-1$ degrees of freedom.

Given an ordered sample $\left(w_i, x_{(i)}\right)$, $1 \leq i \leq n$, the likelihood equations are ($w_i = y_{[i]}$),

$$\frac{\partial lnL}{\partial \gamma_0} = \sum_{i=1}^{n}\left\{-\frac{2p}{k}g\left(z_{(i)}\right) + w_i g_1\left(z_{(i)}\right) - \left(1-w_i\right)g_2\left(z_{(i)}\right)\right\} = 0 \tag{6.3}$$

and

$$\frac{\partial lnL}{\partial \gamma_1} = \frac{n}{\gamma_1} + \sum_{i=1}^{n} x_{(i)}\left\{-\frac{2p}{k}g\left(z_{(i)}\right) + w_i g_1\left(z_{(i)}\right) - \left(1-w_i\right)g_2\left(z_{(i)}\right)\right\} = 0 \tag{6.4}$$

where

$$g(z) = z/\left\{1+(1/k)z^2\right\},\ g_1(z) = f(z)/F(z) \text{ and } g_2(z) = f(z)/\left\{1-F(z)\right\}. \tag{6.5}$$

Here, $f(u)$ and $h(z)$ are assumed to be the same functions (6.2) and $F(z) = \int_{-\infty}^{z} f(u)\,du$. Again, it is almost impossible to solve the equations (6.3)–(6.4).

Proceeding exactly along the same lines as in Section 2, modified likelihood equations are obtained. The solutions of these equations are the following MMLE:

$$\hat{\gamma}_0 = (\delta/m) - \hat{\gamma}_1 \overline{x}_{(.)} \text{ and } \hat{\gamma}_1 = \left\{B + \sqrt{B^2+4nC}\right\}/2C, \tag{6.6}$$

where

$$
\begin{aligned}
&B=\sum_{i=1}^{n}\delta_i\left(x_{(i)}-\overline{x}_{(.)}\right) \text{ and}\\
&C=\sum_{i=1}^{n}m_i\left(x_{(i)}-\overline{x}_{(.)}\right)^2=\sum_{i=1}^{n}m_ix_{(i)}^2-(1/m)\left(\sum_{i=1}^{n}m_ix_{(i)}\right)^2;\\
&\delta_i=w_i\alpha_{1i}-(1-w_i)\,\alpha_{2i}-(2p/k)\,\alpha_i \text{ and } m_i=w_i\beta_{1i}+(1-w_i)\,\beta_{2i}+(2p/k)\,\beta_i.
\end{aligned}
\tag{6.7}
$$

The coefficients α_i and β_i are given by

$$
\alpha_i=\frac{(2/k)\,a_i^3}{\left\{1+(1/k)\,a_i^2\right\}^2} \text{ and } \beta_i=\frac{1-(1/k)\,a_i^2}{\left\{1+(1/k)\,a_i^2\right\}^2},
\tag{6.8}
$$

where a_i is determined from the equation

$$
F(a_i)=\int_{-\infty}^{a_i}h(z)\,dz=\frac{i}{n+1},\quad 1\le i\le n.
\tag{6.9}
$$

An IMSL subroutine is available to evaluate (6.9) which is essentially the cumulative density function of the Student's t distribution.

The coefficients (α_{1i},β_{1i}) and (α_{2i},β_{2i}) are given in (3.5)–(3.6) with $f(z)$ replaced by the density on the right hand side of (6.2), and $F(z)=\int_{-\infty}^{z}f(u)\,du$.

6.1. Remark. If $\beta_1>0$, then all the coefficients β_i are positive since they increase until the middle value and then decrease in a symmetric fashion (umbrella ordering). If, however, β_1 assumes a negative value (which happens only if p is small and n is large), $\hat{\sigma}$ might cease to be real and positive. In such a situation, α_i and β_i in (6.7) are replaced by $\alpha_i^*=0$ and $\beta_i^*=\left\{1+(1/k)\,a_i^2\right\}$ respectively. This ensures that $\hat{\gamma}_1$ is always real and positive. The asymptotic efficiency of $\hat{\gamma}_0$ and $\hat{\gamma}_1$ is not affected since $\alpha_i+\beta_iz_{(i)}\cong\alpha_i^*+\beta_i^*z_{(i)}$ realizing that $z_{(i)}-t_{(i)}\cong 0$ (asymptotically). See also Tiku et al. [21].

Information matrix: Because of the symmetry of (6.1), the elements of the Fisher information matrix are simpler than those in (4.1)–(4.3) and are given by

$$
\begin{aligned}
&I_{11}=Q+P,\ I_{12}=-\left(\gamma_0/\gamma_1\right)(Q+P) \text{ and}\\
&I_{22}=\left(1/\gamma_1^2\right)\left\{(Q+P)\,\gamma_0^2+(Q+R)\right\}.
\end{aligned}
\tag{6.10}
$$

Here,

$$
P=np\,(p-1/2)\,/\,(p+1)\,(p-3/2) \text{ and } R=2n\,(p-1/2)\,/\,(p+1),\ (p\ge 2),
\tag{6.11}
$$

and Q_i, Q have exactly the same expressions as (4.4).

In particular, for the asymptotic variance

$$
var\left(\hat{\gamma}_1/\gamma_1\right)\cong 1/\left(Q+R\right),
\tag{6.12}
$$

which is free of γ_0.

Efficiency: We simulated the means and variances of the MMLE $\hat{\gamma}_0$ and $\hat{\gamma}_1$ and compared them with the corresponding estimators (Tiku and Vaughan [18]) based only on the conditional likelihood function $L_{Y|X}$. As for the $GL(b,\gamma_1)$ family (2.2), $\hat{\gamma}_0$ and $\hat{\gamma}_1$ were found to be (almost) unbiased and enormously more efficient. The test of $H_0:\gamma_1=\gamma_{10}$ based on the statistic $W=\hat{\gamma}_1/\gamma_{10}$ was found to be remarkably robust to plausible deviations from an assumed value of p in (6.1) and to data anomalies, e.g., outliers and contaminated data. Details are given in Oral [8]. To save space we do not reproduce them here.

Generalization: The methodology above readily extends to the situation when

$$z = \gamma_0 + \sum_{i=1}^{k} \gamma_i x_i$$

and the risk factors X_i $(1 \leq i \leq k)$ are independently distributed with densities $h_i(x)$. The coefficients γ_i are a priori all positive. The MMLE based on the conditional likelihood

$$L_{Y|X_1,X_2,\ldots,X_k}$$

is given in Tiku and Vaughan [18]. It will be of great interest to extend the methodology to correlated risk factors. Extensions to censored (Type I and Type II) data are also of enormous interest from a practical point of view. Another interesting extension is to the situation when Y is multinomial and assumes more than two values.

In conclusion it must be said that it is advantageous to use the complete likelihood function to obtain efficient and robust estimators. Conditional likelihood was perhaps used to make estimation computationally feasible. Modified likelihood methodology makes estimation easy both analytically and computationally. Its use with the complete likelihood function gives estimators which are enormously more efficient than those based only on the conditional likelihood function. Moreover, the method is applicable to any location-scale distribution and no specialized computer software is needed to compute the MMLE.

Acknowledgment. We would like to thank to Professor M. L. Tiku for supervising this research.

References

[1] Abramowitz, M. and Stegun, I. A. *Handbook of Mathematical Functions*, (Dover, New York, 1965).
[2] Agresti, A. *Categorical Data Analysis*, (John Wiley and Sons, New York, 1996).
[3] Aitkin, M., Anderson, D., Francis, B. and Hinde, J. *Statistical Modelling In GLIM*, (Oxford Science, New York, 1989).
[4] Bhattacharyya, G. K. *The asymptotics of maximum likelihood and related estimators based on Type II censored data*, J. American Statistical Association **80**, 398–404, 1985.
[5] Hosmer, D. W. and Lemeshow, S. *Applied Logistic Regression*, (John Wiley and Sons, New York, 1989).
[6] Kleinbaum, D. G. *Logistic Regression*, (Springer, New York, 1994).
[7] Lee, K. R., Kapadia, C. H. and Dwight, B. B. *On estimating the scale parameter of Rayleigh distribution from censored samples*, Statistische Hefte **21**, 14–20, 1980.
[8] Oral, E. *Stochastic and Nonstochastic Covariates in Binary Regression*, Unpublished Ph. D. Thesis, (Hacettepe Univ., Ankara, Turkey., 2002).
[9] Pearson, E. S. *Some problems arising in approximating the probability distributions using moments*, Biometrika **50**, 95–112, 1963.
[10] Pearson, E. S. and Tiku, M. L. *Some notes on the relationship between the distributions of central and non-central F*, Biometrika **57**, 175–179, 1970.
[11] Rasch, D. *Probleme der Angewandten Statistik, Robustheit I: Fz. Für Tierproduktion*, Dummerstorf-Rostock, Heft 4, 1980.
[12] Spjotvoll, E. and Aastveit, A. H. *Comparison of Robust Estimators on Some Data from Field Experiments*, Scand. J. Statist. **7**, 1–13, 1980.
[13] Senoglu, B. and Tiku, M. L. *Analysis of variance in experimental design with nonnormal rrror distributions*, Communications in Statistics-Theory and Methods **30**, 1335–1352, 2001.
[14] Senoglu, B. and Tiku, M. L. *Linear contrasts in experimental design with nonidentical error distributions*, Biometrical J. **44**, 359–374, 2002.
[15] Tiku, M. L. *Laguerre series forms of non-central Chi-square and F distributions*, Biometrika **52**, 415–427, 1965.

[16] Tiku, M. L. *Distribution of the derivative of the likelihood function*, Nature **210**, 766, 1966.
[17] Tiku, M. L. and Suresh, R. P. *A new method of estimation for location and scale parameters*, Journal of Statistical Planning and Inference **30**, 281–292, 1992.
[18] Tiku, M. L. and Vaughan, D. C. *Logistic and nonlogistic density functions in binary regression with nonstochastic covariates*, Biometrical J. 39, 883–898, 1997.
[19] Tiku, M. L., Tan, W. Y. and Balakrishnan, N. *Robust Inference*, (Marcel Dekker, New York, 1986).
[20] Tiku, M. L., Wong, W. K. and Bian, G. *Time series models with asymmetric innovations*, Communications in Statistics-Theory and Methods **28**, 1331–1360, 1999.
[21] Tiku, M. L., Wong, W. K. and Vaughan, D. C. *Time series models in non-normal situations: Symmetric innovations*, J. Time Series Analysis **21**, 571–596, 2000.
[22] Vaughan, D. C. *On the Tiku-Suresh method of estimation*, Communications in Statistics-Theory and Methods **21**, 451–469, 1992.
[23] Vaughan, D. C. *The generalized secant hyperbolic distribution and its properties*, Communications in Statistics-Theory and Methods **31**, 219–238, 2002.
[24] Vaughan, D. C. and Tiku M., L. *Estimation and hypothesis testing for nonnormal bivariate distribution with applications*, Mathematical and Computer Modelling **32**, 53–67, 2000.